



Search for direct stau production in events with two hadronic tau-leptons in root s=13 TeV pp collisions with the ATLAS detector

Aad, G.; Abbott, B.; Abbott, DC; Abud, AA; Abeling, K.; Abhayasinghe, DK; Abidi, S.H.; AbouZeid, Ossama Sherif Alexander; Abraham, NL; Abramowicz, H.; Abreu, H.; Abulaiti, Y.; Alonso Diaz, Alejandro; Camplani, Alessandra; hqz214, hqz214; Dam, Mogens; Galster, Gorm Aske Gram Krohn; Hansen, Peter Henrik; Hansen, Jørn Dines; Hansen, Jørgen Beck; Ignazzi, Rosanna; Monk, James William; Petersen, Troels Christian; Stark, Simon Holm; Wiglesworth, Graig; Xella, Stefania; Bajic, Milena; ATLAS Collaboration

Published in:
Physical Review D

DOI:
[10.1103/PhysRevD.101.032009](https://doi.org/10.1103/PhysRevD.101.032009)

Publication date:
2020

Document version
Publisher's PDF, also known as Version of record

Document license:
[CC BY](#)

Citation for published version (APA):
Aad, G., Abbott, B., Abbott, DC., Abud, AA., Abeling, K., Abhayasinghe, DK., Abidi, S. H., AbouZeid, O. S. A., Abraham, NL., Abramowicz, H., Abreu, H., Abulaiti, Y., Alonso Diaz, A., Camplani, A., hqz214, H., Dam, M., Galster, G. A. G. K., Hansen, P. H., Hansen, J. D., ... ATLAS Collaboration (2020). Search for direct stau production in events with two hadronic tau-leptons in root s=13 TeV pp collisions with the ATLAS detector. *Physical Review D*, 101(3), [032009]. <https://doi.org/10.1103/PhysRevD.101.032009>

Search for direct stau production in events with two hadronic τ -leptons in $\sqrt{s} = 13$ TeV pp collisions with the ATLAS detector

G. Aad *et al.*^{*}
(ATLAS Collaboration)



(Received 18 November 2019; accepted 16 January 2020; published 28 February 2020)

A search for the direct production of the supersymmetric partners of τ -leptons (staus) in final states with two hadronically decaying τ -leptons is presented. The analysis uses a dataset of pp collisions corresponding to an integrated luminosity of 139 fb^{-1} , recorded with the ATLAS detector at the Large Hadron Collider at a center-of-mass energy of 13 TeV. No significant deviation from the expected Standard Model background is observed. Limits are derived in scenarios of direct production of stau pairs with each stau decaying into the stable lightest neutralino and one τ -lepton in simplified models where the two stau mass eigenstates are degenerate. Stau masses from 120 GeV to 390 GeV are excluded at 95% confidence level for a massless lightest neutralino.

DOI: [10.1103/PhysRevD.101.032009](https://doi.org/10.1103/PhysRevD.101.032009)

I. INTRODUCTION

Supersymmetry (SUSY) [1–7] postulates the existence of superpartners, referred to as *sparticles*, whose spin differs by one half unit from each corresponding Standard Model (SM) particle. In models that conserve R -parity [8], sparticles are always produced in pairs, and the lightest supersymmetric particle (LSP) is stable and is a dark-matter candidate [9,10].

In SUSY models, the sector of sparticles with only electroweak interactions contains charginos ($\tilde{\chi}_i^\pm$, $i = 1, 2$ in order of increasing masses), neutralinos ($\tilde{\chi}_j^0$, $j = 1, 2, 3, 4$ in order of increasing masses), charged sleptons ($\tilde{\ell}$), and sneutrinos ($\tilde{\nu}$). Charginos and neutralinos are the mass eigenstates formed from linear superpositions of the superpartners of the charged and neutral Higgs bosons and electroweak gauge bosons. The sleptons are the superpartners of the charged leptons and are referred to as left or right ($\tilde{\ell}_L$ or $\tilde{\ell}_R$) depending on the chirality of their SM partners. The slepton mass eigenstates are a mixture of $\tilde{\ell}_L$ and $\tilde{\ell}_R$, and are labeled as $\tilde{\ell}_k$ ($k = 1, 2$ in order of increasing mass). In this work, the scalar superpartner of the left-handed τ -lepton (the stau-left, $\tilde{\tau}_L$) and right-handed τ -lepton (the stau-right, $\tilde{\tau}_R$) are assumed to be mass degenerate.

Final states with τ -leptons originating from stau decays are of particular interest for SUSY searches. Models with

light staus can lead to a dark-matter relic density consistent with cosmological observations [11] and light sleptons in general could play a role in the coannihilation of neutralinos [12,13]. Sleptons are expected to have masses of order 100 GeV in gauge-mediated [14–16] and anomaly-mediated [17,18] SUSY breaking models.

In some scenarios the direct production rate of sleptons can greatly exceed the production rate of squarks and gluinos at the Large Hadron Collider (LHC). In the simplified models studied in this paper, the lightest neutralino is the LSP and is purely the superpartner of the U(1) gauge field (the bino) and not admixed with the superpartner of the SU(2) gauge field (wino). Further, the two staus are assumed to be mass-degenerate. The stau-left and stau-right decay each with a 100% branching fraction into a binolike neutralino and a τ -lepton. All sparticles other than those explicitly mentioned here are assumed to be inaccessible at the LHC energy. This paper focuses on the direct production of a stau pair, leading to the final state illustrated in Fig. 1.

Signal events are characterized by the presence of exactly two τ -leptons and large missing transverse momentum due to the undetected neutrinos, as a result of the τ -lepton decays, and lightest neutralinos. Final states with exactly two hadronically decaying τ -leptons ($\tau \rightarrow \text{hadrons } \nu_\tau$) are considered.

The search described in this document uses a dataset of $\sqrt{s} = 13$ TeV pp collisions collected with the ATLAS detector from 2015 to 2018 at the LHC. At LEP [19–24], searches set a lower limit of 86.6 GeV at 95% confidence level (C.L.) on the mass of promptly decaying staus. Similar searches were performed previously by the ATLAS and CMS Collaborations using data collected at $\sqrt{s} = 8$ TeV in 2012 at the LHC [25,26], with the ATLAS

^{*}Full author list given at the end of the article.

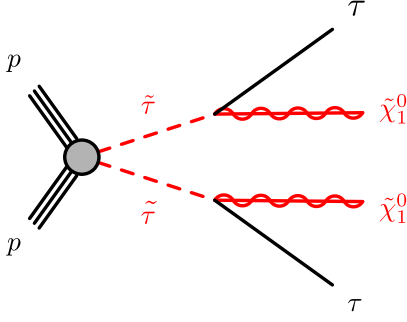


FIG. 1. A diagram illustrating the pair production of staus and subsequent decay into a two- τ -lepton final state with missing transverse momentum from the neutralinos.

result excluding a single $\tilde{\tau}$ mass hypothesis of 109 GeV decaying to a τ -lepton and massless neutralino. CMS has performed a similar search using an integrated luminosity of 77.2 fb^{-1} of $\sqrt{s} = 13 \text{ TeV}$ pp collisions and has excluded degenerate production of $\tilde{\tau}$ pairs with mass up to 150 GeV for a nearly massless neutralino [27].

II. ATLAS DETECTOR

The ATLAS detector [28] is a multipurpose particle physics detector with forward-backward symmetric cylindrical geometry and nearly 4π coverage in solid angle.¹ It features an inner tracking detector (ID) surrounded by a 2 T superconducting solenoid, electromagnetic and hadronic calorimeters, and a muon spectrometer (MS). The ID covers the pseudorapidity region $|\eta| < 2.5$ and consists of a silicon pixel detector, a silicon microstrip detector, and a transition radiation tracker. One significant upgrade for the $\sqrt{s} = 13 \text{ TeV}$ running period is the presence of the insertable B-layer [29,30], an additional pixel layer close to the interaction point which provides high-resolution hits at a small radius to improve the tracking and vertex reconstruction performance. The calorimeters are composed of high-granularity liquid-argon (LAr) electromagnetic calorimeters with lead, copper, or tungsten absorbers (in the pseudorapidity region $|\eta| < 3.2$) and a steel-scintillator hadronic calorimeter (for $|\eta| < 1.7$). The end cap and forward regions are instrumented with LAr calorimeters for both the electromagnetic and hadronic measurements up to $|\eta| = 4.9$. The MS surrounds the calorimeters and consists of three large superconducting air-core toroidal magnets, each with eight coils, a system of

¹ATLAS uses a right-handed coordinate system with its origin at the nominal interaction point (IP) in the center of the detector, and the z -axis along the beam line. The x -axis points from the IP to the center of the LHC ring, and the y -axis points upwards. Cylindrical coordinates (r, ϕ) are used in the transverse plane, ϕ being the azimuthal angle around the z -axis. Observables labeled *transverse* refer to the projection into the x - y plane. The pseudorapidity is defined in terms of the polar angle θ by $\eta = -\ln \tan(\theta/2)$.

precision tracking chambers ($|\eta| < 2.7$), and detectors for triggering ($|\eta| < 2.4$). A two-level trigger system is used to select events for recording [31].

III. DATA AND SIMULATED EVENT SAMPLES

After the application of beam, detector, and data quality requirements, the analyzed dataset corresponds to an integrated luminosity of 139 fb^{-1} of pp collision data recorded from 2015 to 2018 at $\sqrt{s} = 13 \text{ TeV}$. The uncertainty in the combined 2015–2018 integrated luminosity is 1.7% [32], obtained using the LUCID-2 detector [33] for the primary luminosity measurements. The average number of interactions per bunch crossing ($\langle \mu \rangle$) for this dataset ranges from about 10 up to 60, with a mean value of 34.

Monte Carlo (MC) simulated event samples were used to estimate the SUSY signal yields and to aid in evaluating the SM backgrounds. Generated SM events were passed through a detailed detector simulation [34] based on GEANT4 [35]. SUSY MC events were processed with a fast detector simulation that parameterizes the response of the electromagnetic and hadronic calorimeters but uses GEANT4 for the other detectors. All simulated events were overlaid with multiple pp collisions (pileup) simulated with the soft strong-interaction processes of PYTHIA 8.186 [36] using the A3 set of tuned parameters [37] and the NNPDF23LO [38] parton distribution function (PDF) set. The simulated events were reconstructed using the same algorithms as the data, and were reweighted so that the distribution of the expected number of collisions per bunch crossing matched the one in the data.

A. Simulated background samples

Events with $Z/\gamma^* \rightarrow \ell\ell$ ($\ell = e, \mu, \tau$) and $W \rightarrow \ell\nu$ produced with accompanying jets (including jets initiated by heavy flavor quarks) were generated with SHERPA 2.2.1 [39,40]. Matrix elements (ME) were calculated for up to two additional partons at NLO and four additional partons at leading order (LO), using the Comix [41] and OPENLOOPS [42,43] generators and merged with the SHERPA parton shower (PS) [44] using the ME + PS@NLO prescription [40]. The NNPDF3.0NNLO [45] PDF set was used in conjunction with a dedicated PS tuning developed by the SHERPA authors. The W/Z + jets events were normalized using their next-to-next-to-leading-order (NNLO) cross sections [46].

Fully leptonically and semileptonically decaying diboson samples ($VV = WW/WZ/ZZ$) were simulated with the SHERPA 2.2.1 and 2.2.2 [39] generator at NLO. In this setup, multiple matrix elements were matched and merged with the SHERPA parton shower based on Catani–Seymour dipole factorization [44] using the MEPS@NLO prescription [40,47–49]. The virtual QCD corrections for matrix elements at NLO accuracy were provided by the OPENLOOPS library [43]. Samples were generated using

the NNPDF3.0NNLO set, along with the dedicated set of tuned parton-shower parameters developed by the SHERPA authors.

The production of top-quark pairs ($t\bar{t}$) and single top quarks in the Wt and s -channels was performed with POWHEG-BOX v2 [50–53], with the NNPDF2.3LO [54] PDF set at NLO in the ME calculations and the ATLAS underlying-event tune A14 [55]. Electroweak t -channel single-top-quark events were generated using the POWHEG-BOX v2 event generator. The PS, fragmentation, and the underlying event were simulated using PYTHIA 8.186 with the NNPDF2.3LO PDF set and a corresponding set of A14 tuned parameters. The top-quark mass was set to 172.5 GeV. The $t\bar{t}$ sample is normalised to the cross section prediction at next-to-next-to-leading order (NNLO) in QCD including the resummation of next-to-next-to-leading logarithmic (NNLL) soft-gluon terms calculated using TOP++2.0 [56–62]. The cross section for single-top-quark was computed for the Wt -channel at NLO in QCD with NNLL soft gluon corrections [63,64], and to NLO in QCD for the t - and s -channels [63,64]. Top-quark pair production with an additional W or Z boson was calculated using MADGRAPH5_aMC@NLO 2.2.2 [65] at NLO in the ME calculations, while fragmentation and hadronization were simulated with PYTHIA 8.186. The underlying-event tune A14 was used with the NNPDF2.3LO PDF set, and the cross sections were normalized using NLO predictions [66,67].

Small contributions from Higgs boson events produced by gluon-gluon fusion and vector-boson fusion were modeled using POWHEG-BOX v2 with the NNPDF3.0NNLO PDF and showered using PYTHIA 8.186. Contributions from the associated production of a Higgs boson with a vector boson and from a Higgs boson in association with two top quarks were simulated using PYTHIA 8.186 and MADGRAPH5_aMC@NLO, respectively. All Higgs boson samples were normalized to cross sections from Ref. [68].

For all samples showered with PYTHIA 8, EVTGEN 1.2.0 [69] was used to simulate the decays of bottom and charmed hadrons.

B. Simulated signal samples

Simulated signal samples were generated using MADGRAPH5_aMC@NLO 2.6.2 interfaced to PYTHIA 8.186 with the A14 tune for the PS modeling, hadronization, and underlying event. The ME calculation was performed at tree level and includes the emission of up to two additional partons. The NNPDF2.3LO PDF set was used. The ME–PS matching used the CKKW-L [70] prescription, with a matching scale set to one quarter of the mass of the pair of produced particles. Signal cross sections were calculated to next-to-leading order in the strong coupling constant, adding the resummation of soft gluon emission at next-to-leading-logarithm accuracy (NLO + NLL) using the PDF4LHC15mc PDF set [71]. The nominal cross section and its uncertainty were taken from an envelope

of cross section predictions using different PDF sets and factorization and renormalization scales, as described in Refs. [71–75].

The masses of all charginos and neutralinos apart from the $\tilde{\chi}_1^0$, were set to 2.5 TeV, thus leaving a single kinematically allowed decay: $\tilde{\tau} \rightarrow \tilde{\chi}_1^0 \tau$. The stau-left and stau-right were combined and have the same mass, which was varied between 100 and 440 GeV and no mixing was assumed between the gauge and mass eigenstates. The mass of the binolike $\tilde{\chi}_1^0$ was varied in the range 1–200 GeV.

Reference points with $\tilde{\tau}$ masses of 120 GeV, 280 GeV, and a $\tilde{\chi}_1^0$ mass of 1 GeV are used throughout this paper to illustrate typical features of the SUSY models to which this analysis is sensitive. The theoretical cross section used at NLO + NLL was 140 (50) fb with $\tilde{\tau}_L \tilde{\tau}_L$ ($\tilde{\tau}_R \tilde{\tau}_R$) of 120 GeV, and 5.8 (2.2) fb with $\tilde{\tau}_L \tilde{\tau}_L$ ($\tilde{\tau}_R \tilde{\tau}_R$) of 280 GeV.

IV. EVENT RECONSTRUCTION

Events with at least one reconstructed primary vertex [76] are selected. A primary vertex must have at least two associated charged-particle tracks with transverse momentum $p_T > 500$ MeV and be consistent with the collision region. In events with multiple primary vertices, the one with the largest $\sum p_T^2$ of the associated tracks is chosen.

Jets are reconstructed from three-dimensional calorimeter energy clusters [77] using the anti- k_t algorithm [78,79] with a radius parameter of 0.4. Jet energies are corrected for detector inhomogeneities, the noncompensating response of the calorimeter, and the impact of pileup, using factors derived from test beam and pp collision data, and from a detailed GEANT4 detector simulation [80]. The impact of pileup is accounted for using a technique, based on jet areas, that provides an event-by-event and jet-by-jet correction [81]. Jets that are likely to have originated from pileup are not considered in this analysis [82]. The efficiency of this pileup-rejection selection is approximately 92%. Jets are required to have $p_T > 20$ GeV and $|\eta| < 2.8$. Events containing jets that are likely to have arisen from detector noise or cosmic rays are removed.

Jets containing b -hadrons (b -jets) are identified using the MV2c10 algorithm [83], based on a multivariate discriminant making use of track impact parameters and reconstructed secondary vertices [84]. Candidate b -jets are required to have $p_T > 20$ GeV and $|\eta| < 2.5$. A working point with an average b -tagging efficiency of 77% for simulated $t\bar{t}$ events is used. This working point corresponds to a c -jet and light-jet rejection of 4.9 and 110, respectively [85,86].

Electron candidates are reconstructed by matching clusters in the electromagnetic calorimeter with charged-particle tracks in the inner detector. Electrons are required to have $p_T > 17$ GeV and $|\eta| < 2.47$, and to satisfy the “loose” working point according to a likelihood-based identification [87]. Muon candidates are reconstructed from

MS tracks matching ID tracks. Muons are required to have $p_T > 14$ GeV and $|\eta| < 2.7$ and fulfill the “medium” quality criteria of Ref. [88]. Events containing a muon candidate with a poorly measured charge-to-momentum ratio ($\sigma(q/p)/|q/p| > 0.4$) are rejected.

Electrons and muons are required to satisfy isolation criteria to reduce the number of jets misidentified as charged leptons. The scalar sum of the p_T of tracks inside a variable-size cone around the lepton (excluding its own track), must be less than 15% of the lepton p_T . The track isolation cone size² for electrons (muons) ΔR is given by the minimum of $\Delta R = 10 \text{ GeV}/p_T$ and $\Delta R = 0.2$ (0.3). In addition, for electrons (muons) the sum of the transverse energy of the calorimeter energy clusters in a cone of $\Delta R = 0.2$ around the lepton, excluding the energy from the lepton itself, must be less than 20% (30%) of the lepton p_T . For electrons with $p_T > 200$ GeV these isolation requirements are not applied, and instead an upper limit of $\max(0.015 \times p_T[\text{GeV}], 3.5 \text{ GeV})$ is placed on the transverse energy of the calorimeter energy clusters in a cone of $\Delta R = 0.2$ around the electron.

The efficiencies for electrons and muons to satisfy the reconstruction, identification, and isolation criteria are measured in samples of leptonic Z and J/ψ decays, and corrections are applied to the simulated samples to reproduce the efficiencies in data.

The reconstruction of hadronically decaying τ -leptons is based on information from tracking in the ID and three-dimensional clusters of energy in the electromagnetic and hadronic calorimeters. The τ -lepton reconstruction algorithm is seeded by jets reconstructed as described above but with $p_T > 10$ GeV and $|\eta| < 2.5$. The reconstructed energies of the hadronically decaying τ -lepton candidates are corrected to the τ -lepton energy scale, which is calibrated using simulation and *in situ* measurements using $Z \rightarrow \tau\tau$ decays [89]. The τ -neutrino from the hadronic τ -lepton decay is not taken into account in the reconstruction and calibration of the τ -lepton energy and momentum. Hadronic τ -lepton decay candidates are required to have one or three associated charged-particle tracks (prongs) and the total electric charge of those tracks must be ± 1 times the electron charge. To improve the discrimination between hadronically decaying τ -leptons and jets a multivariate algorithm is used [89]. The τ -lepton identification algorithm is based on a boosted decision tree (BDT) method. The BDT algorithm uses various track and cluster variables as input to discriminate between τ -leptons and jets. For 1-prong (3-prong) τ -lepton candidates, the signal efficiencies are 75% (60%) and 60% (45%) for the “medium” and “tight” working points, respectively. In the following, τ -lepton candidates are required to satisfy the “medium” identification criteria for jet discrimination (medium

τ -lepton candidates), unless otherwise stated. For electron discrimination, an additional BDT is trained to discriminate τ -leptons from electrons and a selection is applied on the output of the discriminant. This requirement has about 95% efficiency for selecting τ -leptons, and a background electron rejection factor from 10 to 50 depending on the η . The τ -lepton candidates are required to have $p_T > 20$ GeV and $|\eta| < 2.5$, excluding the transition region between the barrel and end cap calorimeters ($1.37 < |\eta| < 1.52$).

The simulation is corrected for differences between the efficiencies of τ identification in data and simulation at both trigger and reconstruction level. For hadronically decaying τ -leptons originating from prompt gauge-boson decays, the corrections are calculated with a *tag-and-probe* method in a sample of $Z \rightarrow \tau\tau$ events where one τ -lepton decays hadronically and the other leptonically into a muon and two neutrinos [90]. Small differences between data and simulation for electron, muon, jet identification, and trigger efficiencies are corrected with scale factors derived in control regions. For the trigger corrections, dedicated regions enriched in $t\bar{t}$, Z , and W events are used.

The measurement of the missing transverse momentum vector, $\mathbf{p}_T^{\text{miss}}$, and its magnitude, E_T^{miss} , is based on the negative vectorial sum of the \mathbf{p}_T of all identified jets, τ -lepton candidates, electrons, muons, photons [87], and an additional soft term. The soft term is constructed from all high-quality tracks that are associated with the primary vertex but not with any identified particle or jet. In this way, the missing transverse momentum is adjusted for the best calibration of the jets and the other identified particles, while maintaining pileup independence in the soft term [91].

Possible double counting of reconstructed objects is resolved in the following order. The τ -lepton candidates close to electron or muon candidates ($\Delta R < 0.2$) are removed, as are electrons that share a track with a muon. For electrons close to a jet ($\Delta R < 0.4$), the electron is removed, except when $\Delta R < 0.2$ and the jet is not b -tagged, in which case the jet is removed. For a muon close to a jet ($\Delta R < 0.4$), the muon is removed unless the jet has less than three tracks associated with it and is within $\Delta R < 0.2$. In the latter case, the jet is removed. Any remaining jet within $\Delta R = 0.2$ of a τ -lepton candidate is removed.

V. EVENT SELECTION

The events are required to have exactly two medium τ -lepton candidates with opposite-sign electric charge (OS) and to have passed either an *asymmetric di- τ* trigger or a combined *di- τ + E_T^{miss}* trigger [92]. In events selected by the *di- τ + E_T^{miss}* trigger, the offline reconstructed E_T^{miss} must be larger than 150 GeV, to achieve full trigger efficiency. In 2015–2017 data the efficiency of the asymmetric *di- τ* (*di- τ + E_T^{miss}*) trigger is 75–80% for events with the leading τ -lepton candidate $p_T > 95$ (50) GeV and the subleading

² $\Delta R = \sqrt{(\Delta y)^2 + (\Delta \phi)^2}$, where y is the rapidity and ϕ the azimuthal angle.

τ -lepton candidate $p_T > 60(40)$ GeV. The efficiency is evaluated for events with correctly identified τ -leptons and the p_T thresholds are quoted at reconstruction level. As the luminosity increased in later years, the trigger selection was tightened; in 2018 the same efficiency was reached for the leading τ -lepton candidate $p_T > 95(75)$ GeV and the subleading τ -lepton candidate $p_T > 75(40)$ GeV for the asymmetric di- τ ($\text{di-}\tau + E_T^{\text{miss}}$) trigger. Events with an additional third medium τ -lepton or light lepton are rejected.

The reconstructed invariant mass of the visible decay products of the two leading τ -lepton candidates, $m(\tau_1, \tau_2)$, must be larger than 120 GeV to remove τ -leptons originating from decays of low-mass resonances and to suppress contributions from Z + jets and Higgs boson events (Z/H -veto).

In order to further discriminate between SUSY signal events and SM background processes, additional requirements are applied to define the signal region (SR) selections. To reject events from SM processes containing a top quark, selected events must not contain any b -tagged jets (b -jet veto). A lower bound on the *transverse mass* m_{T2} [93,94] is imposed to reduce contributions from $t\bar{t}$ and WW events. The m_{T2} variable is defined as:

$$m_{T2} = \min_{\mathbf{q}_T} [\max(m_{T,\tau_1}(\mathbf{p}_{T,\tau_1}, \mathbf{q}_T), m_{T,\tau_2}(\mathbf{p}_{T,\tau_2}, \mathbf{p}_T^{\text{miss}} - \mathbf{q}_T))],$$

where \mathbf{p}_{T,τ_1} and \mathbf{p}_{T,τ_2} are the transverse momenta of the two τ -lepton candidates, and the transverse momentum vector of one of the invisible particles, \mathbf{q}_T , is chosen to minimize the larger of the two transverse masses m_{T,τ_1} and m_{T,τ_2} . The latter masses are defined by

$$m_T(\mathbf{p}_T, \mathbf{q}_T) = \sqrt{2(p_T q_T - \mathbf{p}_T \cdot \mathbf{q}_T)}.$$

For $t\bar{t}$ and WW events, in which two W bosons decay leptonically and $\mathbf{p}_T^{\text{miss}}$ is the sum of the transverse momenta of the two neutrinos, the m_{T2} distribution has a kinematic endpoint at the W boson mass. For large mass differences between the staus and the lightest neutralino, the m_{T2} distribution for signal events extends significantly beyond this endpoint.

The SRs were optimized for stau discovery by varying the kinematic selection criteria. Events are selected by the asymmetric di- τ trigger to cover the low stau mass region (SR-lowMass) and by the $\text{di-}\tau + E_T^{\text{miss}}$ trigger to cover the high stau mass region (SR-highMass), as shown in Table I. Values of $E_T^{\text{miss}} < 150$ GeV ($E_T^{\text{miss}} > 150$ GeV) are required for SR-lowMass (SR-highMass) to keep the two SRs orthogonal. Both (at least one) of the τ -lepton candidates must satisfy the tight identification criteria for jet discrimination ('tight' τ -lepton candidate) for SR-lowMass (SR-highMass). Values of $E_T^{\text{miss}} > 75$ GeV are required for SR-lowMass to increase signal sensitivity.

TABLE I. Summary of selection requirements for the signal regions.

SR-lowMass	SR-highMass
2 tight τ (OS)	2 medium τ (OS), ≥ 1 tight τ
asymmetric di- τ trigger	di- $\tau + E_T^{\text{miss}}$ trigger
$75 < E_T^{\text{miss}} < 150$ GeV	$E_T^{\text{miss}} > 150$ GeV
τp_T cut described in Sec. V	
light lepton veto and 3rd medium τ veto	
b -jet veto	
Z/H veto ($m(\tau_1, \tau_2) > 120$ GeV)	
$ \Delta\phi(\tau_1, \tau_2) > 0.8$	
$\Delta R(\tau_1, \tau_2) < 3.2$	
$m_{T2} > 70$ GeV	

In addition, the two τ -lepton candidates are required to satisfy $\Delta R(\tau_1, \tau_2) < 3.2$, $|\Delta\phi(\tau_1, \tau_2)| > 0.8$ and $m_{T2} > 70$ GeV to further suppress contributions from SM backgrounds. The product of acceptance and efficiency is around 0.04% (0.03%) and 0.53% (1.22%) for the reference points with $\tilde{\tau}$ masses of 120 GeV and 280 GeV, respectively, and a $\tilde{\chi}_1^0$ mass of 1 GeV in SR-lowMass (SR-highMass).

VI. STANDARD MODEL BACKGROUND ESTIMATION

The main SM processes contributing to the selected final states are multijet, W + jets and diboson production. Background events may contain a combination of "real" τ -leptons, defined as correctly identified prompt τ -leptons, or "fake" τ -leptons, which can originate from a misidentified quark or gluon jet, an electron, or a muon.

In multijet events in the SRs, nearly all τ -lepton candidates are misidentified jets. The multijet contribution in the SRs is estimated from data, as described in Sec. VI A. The contribution arising from heavy-flavor multijet events containing a real τ -lepton from the heavy-flavor quark decay is included in the multijet estimation. The contribution of W + jets events, which contain one real τ -lepton from the W boson decay and one or more misidentified jets, is estimated from MC simulation and normalized to data in a dedicated control region (CR), as described in Sec. VI B.

Diboson production contributes mainly events containing real τ -leptons originating from WW and ZZ decaying into a $\tau\tau\nu\nu$ final state. Additional SM backgrounds arise from Z + jets production, or events that contain a top quark or a top-quark pair in association with jets or additional W or Z bosons (collectively referred to as *top*-quark background in the following). The contribution from real τ -leptons exceeds 90% in Z + jets and diboson production, and ranges from 45% to 75% in backgrounds containing top quarks according to the MC simulation. The contribution of fake τ -leptons from heavy-flavor decays in jets is found to be negligible in MC simulation. To estimate

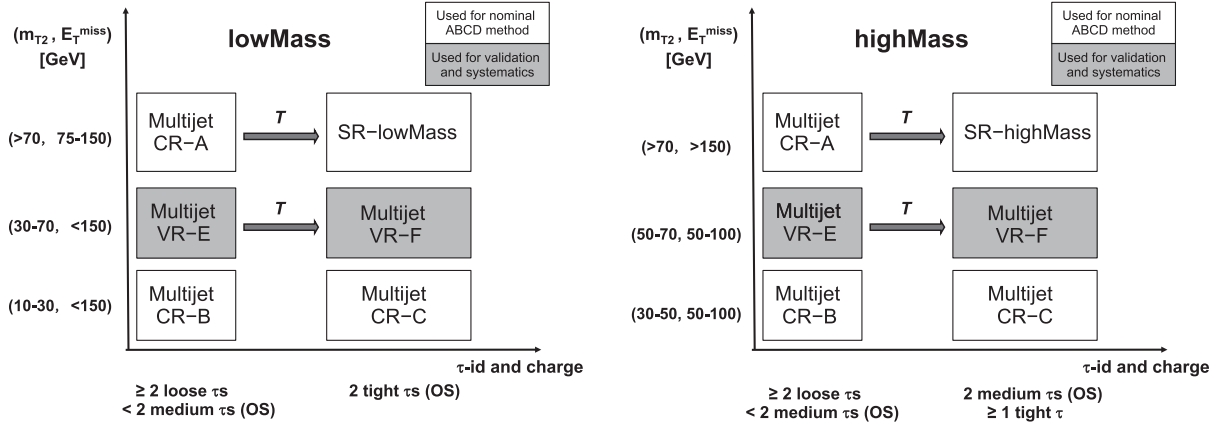


FIG. 2. Illustration of the ABCD method for the multijet background determination for SR-lowMass (left) and SR-highMass (right). The control regions A, B, C, and signal region D for the ABCD method described in the text (labeled as CR-A, CR-B, CR-C and SR-lowMass/SR-highMass) are drawn as white boxes. Shown shaded and labeled VR are the regions E and F, which are used to validate the ABCD method and to estimate the systematic uncertainty. The transfer factor T used in the ABCD method is the ratio of number of multijet events in the regions C and B.

the irreducible background, which includes diboson, Z + jets and top-quark events, only MC simulated samples are used and validated in dedicated validation regions (VRs), as described in Sec. VIC.

A simultaneous fit of the event yields in the control regions, based on the profile likelihood method, is performed to normalize the multijet and W + jets background estimates and propagate systematic uncertainties, as described in Sec. VIII. The sources of systematic uncertainty in the background estimates are described in Sec. VII. Results showing the level of agreement in the validation regions after the fit are labeled “postfit” and results shown in the control regions prior to the fit are labeled “prefit.”

A. Multijet background estimation

One of the dominant backgrounds in the SRs originates from jets misidentified as τ -leptons in multijet production. It accounts for 44% (30%) of the total SM contribution in SR-lowMass (SR-highMass). This contribution is estimated from data using the so-called *ABCD method*. All regions used for the ABCD method are schematically drawn in Fig. 2. Four exclusive regions, labeled as A, B, C, and D, are defined in a two-dimensional plane as a function of two (or more) discriminating variables that are largely uncorrelated. The ratio of events in the regions C and B is then equal to that in the regions D and A. The number of multijet events in region D, N_D , can therefore be calculated from the multijet events in region A, N_A , multiplied by the transfer factor $T = N_C/N_B$, where N_C (N_B) is the number of multijet events in region C (B). The region D corresponds to the SR defined in Sec. V, whereas the regions A, B, and C are control regions defined accordingly. In the following, the regions A, B, C, D are labeled as CR-A, CR-B, CR-C and SR-lowMass

(or SR-highMass), respectively. The ABCD method only provides a first-order estimate of multijet background, the normalization and uncertainty being then modified by a combined fit to CR-A (lowMass) and CR-A (highMass) described in Sec. VIII, in which the transfer factor is used as an input and fixed. The above two-fold method has the advantages of taking the possibility of contamination from signal in multijet CR-A into account in the signal exclusion fit described in Sec. X, as well as considering the correlation of systematic uncertainties among control regions and among background processes.

The definition of the regions used in the ABCD method for the multijet estimation is given in Table II; only those requirements that differ between the CRs/VRs and the SRs are listed. In all of the regions, the di- $\tau + E_T^{\text{miss}}$ or asymmetric di- τ triggers described in Sec. V are used. CR-A and CR-B include the events with two “loose” τ -leptons, either same sign (SS) or OS, and veto the events with two medium OS τ -leptons to remain orthogonal to the SR and reduce the potential contamination by signal events. CR-C and CR-B have events with lower m_{T2} and E_T^{miss} ; no $\Delta R(\tau_1, \tau_2)$ requirement is applied. Furthermore, two sets of VRs, VR-E and VR-F, are defined corresponding to each SR. The validation regions are used to validate the extrapolation of the ABCD estimation to the SRs and to estimate the systematic uncertainty from the residual correlation between the τ -lepton identification and charge requirements and the kinematic variable m_{T2} .

The number of multijet events in each control region and validation region is estimated from data after subtraction of other SM contributions estimated from MC simulation. In CR-B and VR-E, respectively, around 96% and 90% (75% and 79%) of the events are from multijet production in the lowMass (highMass) region. For CR-A and CR-C, respectively, the multijet purity is 74% and 57% (58% and 53%)

TABLE II. Definition of the regions used in the ABCD method for the multijet estimation in the SRs. Only those requirements that differ between the CRs/VRs and the SRs are listed.

CR-A (lowMass)	SR-lowMass
≥ 2 loose τ	2 tight τ (OS)
< 2 medium τ (OS)	...
$\Delta R(\tau_1, \tau_2) < 3.2$	$\Delta R(\tau_1, \tau_2) < 3.2$
$75 < E_T^{\text{miss}} < 150$ GeV	$75 < E_T^{\text{miss}} < 150$ GeV
$m_{T2} > 70$ GeV	$m_{T2} > 70$ GeV
VR-E (lowMass)	VR-F (lowMass)
≥ 2 loose τ	2 tight τ (OS)
< 2 medium τ (OS)	...
$\Delta R(\tau_1, \tau_2) < 3.2$	$\Delta R(\tau_1, \tau_2) < 3.2$
$E_T^{\text{miss}} < 150$ GeV	$E_T^{\text{miss}} < 150$ GeV
$30 < m_{T2} < 70$ GeV	$30 < m_{T2} < 70$ GeV
CR-B (lowMass)	CR-C (lowMass)
≥ 2 loose τ	2 tight τ (OS)
< 2 medium τ (OS)	...
no $\Delta R(\tau_1, \tau_2)$ cut	no $\Delta R(\tau_1, \tau_2)$ cut
$E_T^{\text{miss}} < 150$ GeV	$E_T^{\text{miss}} < 150$ GeV
$10 < m_{T2} < 30$ GeV	$10 < m_{T2} < 30$ GeV
CR-A (highMass)	SR-highMass
≥ 2 loose τ	2 medium τ (OS)
< 2 medium τ (OS)	≥ 1 tight τ
$E_T^{\text{miss}} > 150$ GeV	$E_T^{\text{miss}} > 150$ GeV
$\Delta R(\tau_1, \tau_2) < 3.2$	$\Delta R(\tau_1, \tau_2) < 3.2$
$m_{T2} > 70$ GeV	$m_{T2} > 70$ GeV
VR-E (highMass)	VR-F (highMass)
≥ 2 loose τ	2 medium τ (OS)
< 2 medium τ (OS)	≥ 1 tight τ
$50 < E_T^{\text{miss}} < 100$ GeV	$50 < E_T^{\text{miss}} < 100$ GeV
$\Delta R(\tau_1, \tau_2) < 3.2$	$\Delta R(\tau_1, \tau_2) < 3.2$
$50 < m_{T2} < 70$ GeV	$50 < m_{T2} < 70$ GeV
CR-B (highMass)	CR-C (highMass)
≥ 2 loose τ	2 medium τ (OS)
< 2 medium τ (OS)	≥ 1 tight τ
no $\Delta R(\tau_1, \tau_2)$ cut	no $\Delta R(\tau_1, \tau_2)$ cut
$50 < E_T^{\text{miss}} < 100$ GeV	$50 < E_T^{\text{miss}} < 100$ GeV
$30 < m_{T2} < 50$ GeV	$30 < m_{T2} < 50$ GeV

in the lowMass (highMass) regions. In VR-F the multijet purity is 51%.

Good agreement between data and the estimated SM background is found for the m_{T2} and E_T^{miss} distributions in the validation regions, as shown in Fig. 3.

The contamination from signal in multijet CR-A is defined as the ratio of the number of signal events to the sum of the number of signal events and SM background processes. It ranges from 0.4% (1.2%) to 9.4% (21.4%) for SR-lowMass (SR-highMass) and is taken into account in the fit.

The multijet background estimation is also validated using a different method, the *fake-factor method*. Fake factors (FF) are derived in a region enriched in multijet events consisting of events with two τ -lepton candidates with the same electric charge. Both τ -lepton candidates are used to compute the fake factor as the ratio to the number of leading or subleading τ -lepton candidates satisfying all of the nominal signal identification criteria over the number of τ -lepton candidates failing the requirement on the jet-veto BDT, and are parametrized by the p_T , η and N_{prong} of the τ -lepton candidates. An observed dependence on the BDT output score of the second τ -lepton candidate in the event is also taken into account. The expected number of multijet events entering a selection is computed by applying the fake factors to the yields in a set of sideband regions where either the leading, subleading or both τ -lepton candidates fail the identification requirements. The predicted multijet event yields from the ABCD method and the FF method in both SRs and the multijet VRs agree within the statistical and systematic uncertainties.

B. W + jets background estimation

The production of W + jets events with at least one misidentified τ -lepton accounts for about 25% of the expected SM background in the two SRs. A dedicated control region (WCR) is used to normalize the W + jets MC estimate to data and another region is used to validate the W + jets estimate (W validation region, WVR). To suppress contamination by multijet events, the WCR is enriched in events where the W boson decays leptonically into a muon and a neutrino. Events are selected with a single-muon trigger using the lowest unrescaled p_T thresholds available. Events containing exactly one muon and one candidate τ -lepton with opposite electric charge are selected. The muon is required to have $p_T > 50$ GeV. The τ -lepton candidate must satisfy the medium τ -lepton identification criteria and is required to have $p_T > 60$ GeV.

The contribution from events with top quarks is suppressed by rejecting events containing b -tagged jets, and rejecting events which are kinematically compatible with $t\bar{t}$ production (top-tagged) through the use of the *transverse mass* variable m_{CT} [95]. The definitions of the WCR and WVR are given in Table III. The transverse mass of the $\mu + E_T^{\text{miss}}$ system, $m_{T,\mu}$ is used to reduce the contribution from Z + jets, top-quark, and diboson events. To further suppress multijet and Z + jets events, E_T^{miss} and $\Delta R(\tau, \mu)$ cuts are applied. The invariant mass of the muon and τ -lepton, $m(\mu, \tau)$, and $m_{T,\tau} + m_{T,\mu}$ are used to improve the W + jets purity. Events in the WCR (WVR) are selected by requiring low (high) m_{T2} .

The multijet contribution in the WCR (WVR) is estimated using the so-called *OS-SS* method by counting the number of events in data satisfying the same requirements as for the WCR (WVR) but with the electric charge of the two leptons having the same sign. Events from SM

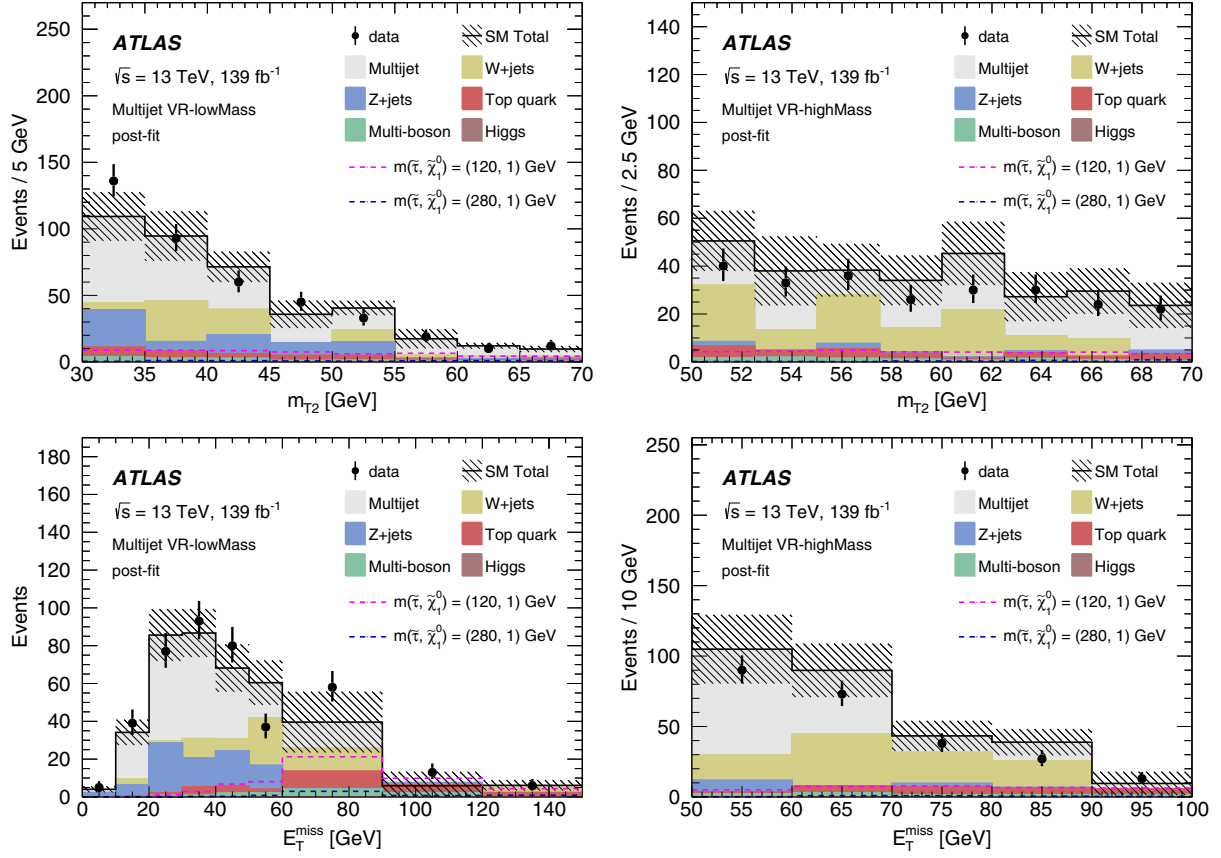


FIG. 3. The m_{T2} (top) and E_T^{miss} (bottom) postfit distributions in the multijet background validation region VR-F (lowMass) at left and VR-F (highMass) at right. The stacked histograms show the contribution of each relevant SM process. The multijet shape is taken from VR-E in the ABCD method and the normalization is determined by the transfer factor T and rescaled by a correction factor determined by the background-only fit to data, described in Sec. VIII. The hatched bands represent the combined statistical and systematic uncertainties in the sum of the SM backgrounds shown. For illustration, the distributions from the SUSY reference points (defined in Sec. III) are also shown as dashed lines.

processes other than multijet production are subtracted from the data counts in the SS region using MC simulation. The OS–SS method relies on the fact that in the multijet background the ratio of SS to OS events is close to unity, while it is around one-seventh for $W + \text{jets}$ production. The latter is dominated by gu/gd -initiated processes that often give rise to a jet originating from a quark, the charge of which is anticorrelated with the W boson charge. Based on studies with simulated samples, a systematic uncertainty of 100% is assigned to the multijet estimate in the WCR.

The purity of the $W + \text{jets}$ selection is around 79% (69%) in the WCR (WVR). The prefit m_{T2} distribution in the WCR is shown in Fig. 4, and good agreement, both for the normalization and shape, between data and SM predictions is observed. The contamination from signal in the WCR and WVR is negligible.

C. Irreducible background estimation

Irreducible SM backgrounds arise mainly from $t\bar{t}$, single top quark, $t\bar{t} + V$, $Z + \text{jets}$, and multiboson (diboson (WW , WZ and ZZ), triboson (VVV)) and Higgs boson. They are

estimated with MC simulation. Other SM backgrounds are found to be negligible.

The total contribution from $t\bar{t}$, single top quarks, $t\bar{t} + V$ and $Z + \text{jets}$ amounts to about 8% and 20% of the total background in SR-lowMass and SR-highMass, respectively. The diboson background accounts for 23–25% of the

TABLE III. Summary of selection requirements for the W control (WCR) and validation (WVR) regions.

WCR	WVR
	1 medium τ and 1 isolated μ (OS)
	single-muon trigger
	$p_T(\tau) > 60 \text{ GeV}$, $p_T(\mu) > 50 \text{ GeV}$
	$E_T^{\text{miss}} > 60 \text{ GeV}$
	b -jet veto and top-tagged events veto
	$m(\mu, \tau) > 70 \text{ GeV}$
	$1 < \Delta R(\mu, \tau) < 3.5$
	$50 < m_{T,\mu} < 150 \text{ GeV}$
	$m_{T,\mu} + m_{T,\tau} > 250 \text{ GeV}$
$30 < m_{T2} < 70 \text{ GeV}$	$m_{T2} > 70 \text{ GeV}$

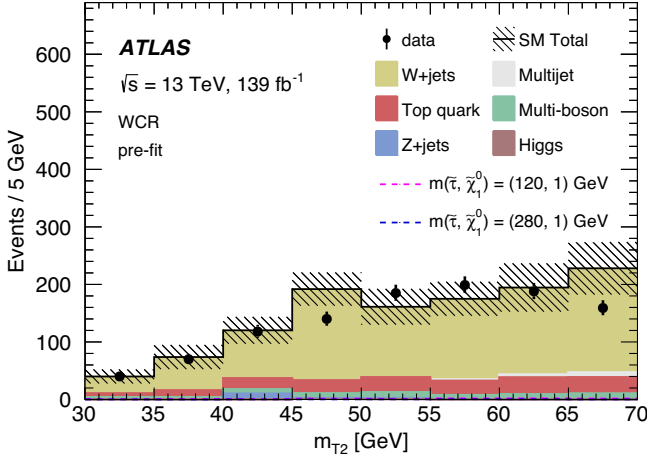


FIG. 4. The prefit m_{T2} distribution in the WCR. The SM backgrounds other than multijet production are estimated from MC simulation. The multijet contribution is estimated from data using the OS-SS method. The hatched bands represent the combined statistical and systematic uncertainties of the total SM background. For illustration, the distributions from the SUSY reference points defined in Sec. III are also shown as dashed lines.

total SM contribution in the SRs and mainly arises from $WW \rightarrow \tau\nu\tau\nu$ and $ZZ \rightarrow \tau\nu\nu$ events, in which more than 96% of the contribution is from events with two real τ -leptons according to the MC simulation.

The MC estimates are validated in regions enriched in Z + jets, top-quark, and multiboson events. For these validation regions, events are required to pass either the combined di- $\tau + E_T^{\text{miss}}$ trigger or the asymmetric di- τ trigger with the same offline threshold as described in Table IV. Events are required to have at least two τ -lepton candidates satisfying the medium τ -lepton identification criteria with opposite electric charge, and at least one τ -lepton candidate must satisfy the “tight” τ -lepton identification criteria in order to be close to the SRs. In the top-quark validation regions (TVR), to increase the contribution from top-quark events, events must satisfy the requirement $\Delta R(\tau_1, \tau_2) > 1.2$ and contain at least one

b -tagged jet with $p_T > 20$ GeV. In order to be close to the SRs, $m_{T2} > 60$ GeV is required. In the Z + jets and multiboson validation regions (ZVR, VVVR), in order to suppress top-quark backgrounds, events containing b -tagged jets are vetoed. To further enhance the purity of Z + jets events, $\Delta R(\tau_1, \tau_2)$, $m(\tau_1, \tau_2)$ and m_{T2} requirements are applied. Further, $m(\tau_1, \tau_2)$, $m_{T, \tau 1} + m_{T, \tau 2}$ and m_{T2} cuts are applied in order to enhance multiboson purity. The ZVRs, TVRs and VVVRs requirements are summarized in Table IV.

The data event yields and the SM predictions in the W + jets (WVR), top quark (TVR), Z + jets (ZVR) and multiboson (VVVR) validation regions are shown in Fig. 5. The data and SM prediction in each validation region agree within the uncertainties. The purity of the selection in Z + jets and $t\bar{t}$ (multiboson) events is 83%–96% (47%–71%) in the respective validation regions.

VII. SYSTEMATIC UNCERTAINTIES

Systematic uncertainties have an impact on the estimates of the background and signal event yields in the control and signal regions. Uncertainties arising from experimental and theoretical sources are estimated.

The main sources of experimental systematic uncertainty in the SM background estimates include τ -lepton and jet energy scale and resolution, τ -lepton identification, pileup, and uncertainties related to the modeling of E_T^{miss} in the simulation. The uncertainties in the energy and momentum scale of each of the objects entering the E_T^{miss} calculation are estimated, as well as the uncertainties in the soft-term resolution and scale. A pileup reweighting procedure is applied to simulation to match the distribution of the number of reconstructed vertices observed in data [96]. The corresponding uncertainty is derived by a reweighting in which $\langle \mu \rangle$ is varied by $\pm 4\%$. The main contributions to experimental systematic uncertainties in the SRs are from the τ -lepton identification and energy scale [89], and jet energy scale and resolution. Systematic uncertainties associated with the τ -lepton triggers are also included

TABLE IV. Summary of selection requirements for top quark (TVR), Z + jets (ZVR) and multiboson (VVVR) validation regions.

Selections	TVR -lowMass	ZVR -lowMass	VVVR -lowMass	TVR -highMass	ZVR -highMass	VVVR -highMass
	$\geq 1b$ -jet	b -jet veto	≥ 2 medium τ (OS), ≥ 1 tight τ	$\geq 1b$ -jet	b -jet veto	
$m(\tau_1, \tau_2)$...	< 70 GeV	< 110 GeV	...	< 60 GeV	< 110 GeV
$\Delta R(\tau_1, \tau_2)$	> 1.2	< 1	...	> 1.2	< 1	...
$m_{T,\tau_1} + m_{T,\tau_2}$	> 250 GeV	> 200 GeV
m_{T2}	> 60 GeV	< 60 GeV	> 60 GeV	> 60 GeV	< 60 GeV	> 60 GeV
Trigger	asymmetric di- τ trigger $60 < E_{\text{T}}^{\text{miss}} < 150$ GeV			di- $\tau + E_{\text{T}}^{\text{miss}}$ trigger $E_{\text{T}}^{\text{miss}} > 150$ GeV		
	τp_{T} and $E_{\text{T}}^{\text{miss}}$ cuts described in Sec. V					

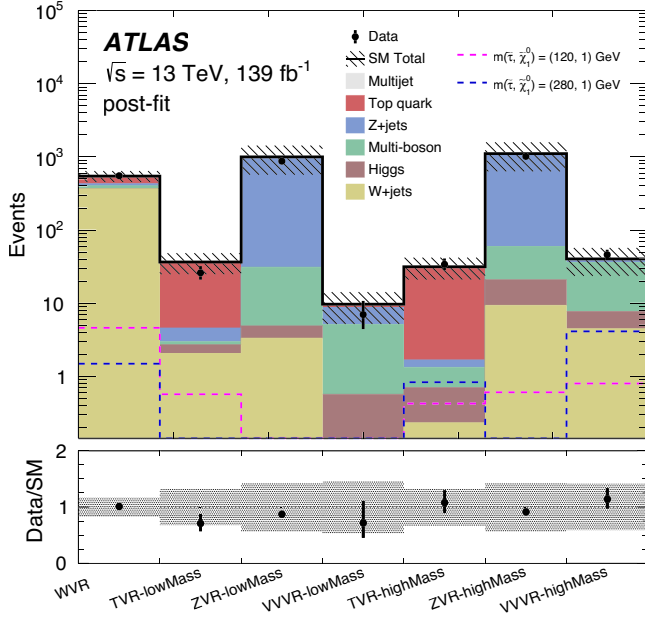


FIG. 5. The postfit yields in the WVR, TVRs, ZVRs and VVVRs. The SM backgrounds other than multijet production are estimated from MC simulation. The multijet contribution is negligible and is estimated from data using the ABCD method, using CRs obtained with the same technique used for the SRs, and described in Sec. VI A. The hatched bands represent the combined statistical and systematic uncertainties of the total SM background. The background-only fit to data is used, described in Sec. VIII. For illustration, the distributions from the SUSY reference points (defined in Sec. III) are also shown as dashed lines. The lower panel shows the ratio of data to the SM background estimate.

with the τ -lepton identification. Other contributions are less than 3%.

Theoretical uncertainties affecting the SHERPA MC event generator predictions, for the $W + \text{jets}$, $Z + \text{jets}$ and multi-boson samples, are estimated by varying the PDF sets following the PDF4LHC recommendations [97] as well as the seven variations of the QCD renormalization and factorization scales in the matrix element by factors of 2 and 0.5 avoiding variations in opposite direction [98]. For $t\bar{t}$ production, uncertainties in the parton shower simulation, modeling of initial- and final-state radiation, and associated with the choice of event generator are considered. The theory uncertainties are implemented as a separate nuisance parameter for each scale variation and process; they are not constrained. The theory uncertainty in $W + \text{jets}$ (multi-boson) production is mainly due to the QCD renormalization scale variation, which amounts to 2%–3% (5%–6%) compared to the total background yield.

The following sources of uncertainty are considered for the ABCD method used to determine the multijet background: the correlation among the τ -lepton identification, the charge requirement, and the kinematic variable m_{T2} , the limited number of events in the CRs, and the subtraction of

TABLE V. The postfit relative systematic uncertainty (%) in the background estimate (signal reference points) in the SR-lowMass and SR-highMass regions from the leading sources at top (bottom). Uncertainties from different sources in the background estimate may be correlated, and do not necessarily add in quadrature to the total uncertainty.

Source of systematic uncertainty on background prediction	SR-lowMass [%]	SR-highMass [%]
Statistical uncertainty of MC samples	11	21
τ -lepton identification and energy scale	19	10
Normalization uncertainties of the multijet background	12	8
Multijet estimation	4	10
Jet energy scale and resolution	5	8
Diboson theory uncertainty	5	6
$W + \text{jets}$ theory uncertainty	2	3
E_T^{miss} soft-term resolution and scale	2	2
Total	28	32

Source of systematic uncertainty on signal prediction	SR-lowMass [%]	SR-highMass [%]
$m(\tilde{\tau}, \tilde{\chi}_1^0)$ [GeV]	(120, 1)	(280, 1)
τ -lepton identification and energy scale	29	14
Statistical uncertainty of MC samples	6	10
Jet energy scale and resolution	3	2
Signal cross section uncertainty	2	2
E_T^{miss} soft-term resolution and scale	3	< 1
Total	31	17

other SM backgrounds. The systematic uncertainty in the correlation is estimated by comparing the transfer factor from CR-B to CR-C to that of VR-E to VR-F. The combined experimental systematic uncertainty and theory uncertainty in the nonmultijet background subtraction in the control regions is estimated by considering the systematic uncertainty of the MC estimates of the nonmultijet background in these regions. These uncertainties are negligible due to high multijet purity in the CRs. The statistical uncertainty of the event yields in the control regions is propagated to the signal regions as a systematic uncertainty.

The systematic uncertainties of the background estimates in the SRs are summarized in Table V. The dominant uncertainties in the SRs are the statistical uncertainty of the MC predictions (11%–21%), τ -lepton identification and energy scale (10%–19%), and multijet background normalization (8%–12%).

The total uncertainty in the signal yields for the SUSY reference points defined in Sec. III is about 17%–31%. The dominant uncertainties in the SRs are from τ -lepton

TABLE VI. Observed and expected numbers of events in the control and signal regions. The expected event yields of SM processes are given after the background-only fit described in Sec. VIII. The entries marked as “–” are negligible. The uncertainties correspond to the sum in quadrature of statistical and systematic uncertainties. The correlation of systematic uncertainties among control regions and among background processes is fully taken into account.

SM process	Multijet CR-A -lowMass	Multijet CR-A -highMass	WCR	SR -lowMass	SR -highMass
Diboson	1.4 ± 0.6	1.9 ± 1.0	63 ± 21	1.4 ± 0.8	2.6 ± 1.4
$W + \text{jets}$	13 ± 4	4^{+7}_{-4}	850 ± 70	1.5 ± 0.7	2.5 ± 1.8
Top quark	2.7 ± 0.9	3.3 ± 1.6	170 ± 40	$0.04^{+0.80}_{-0.04}$	2.0 ± 0.6
$Z + \text{jets}$	$0.25^{+1.43}_{-0.25}$	1.5 ± 0.8	13 ± 7	$0.4^{+0.5}_{-0.4}$	$0.05^{+0.13}_{-0.05}$
Multijet	55 ± 10	16 ± 6	–	2.6 ± 0.7	3.1 ± 1.4
SM total	72 ± 8	27 ± 5	1099 ± 33	6.0 ± 1.7	10.2 ± 3.3
Observed	72	27	1099	10	7

identification and the τ -lepton energy scale (14%–29%) and the statistical uncertainty of the signal MC predictions (6%–10%). The cross section uncertainty is taken into account as the main source of the signal modeling theoretical uncertainty; and it varies from 2% to 3% for the SUSY models considered.

VIII. STATISTICAL ANALYSIS

The statistical interpretation of the results is performed using the profile likelihood method implemented in the HistFitter framework [99]. The likelihood function is a product of the probability density functions for every region contributing to the fit. The number of events in a given CR or SR is described using a Poisson distribution, the mean of which is the sum of the expected contributions from all background and signal sources. The systematic uncertainties in the expected event yields are included as

nuisance parameters and are assumed to follow a Gaussian distribution with a width determined by the size of the uncertainty. Correlations between control and signal regions, and among background processes are taken into account through common nuisance parameters. The fit parameters are determined by maximizing the product of the Poisson probability functions and the Gaussian probability constraints for the nuisance parameters.

Three types of fits are performed for the combined SR-lowMass and SR-highMass regions.

- (i) The *background-only* fit uses as input the number of observed events and expected SM contributions in the multijet CR-A and WCR as well as the transfer factors, which relate the number of multijet or $W + \text{jets}$ events in the control regions to the number in the signal regions. The free parameters in the fit are the normalizations of the $W + \text{jets}$ and

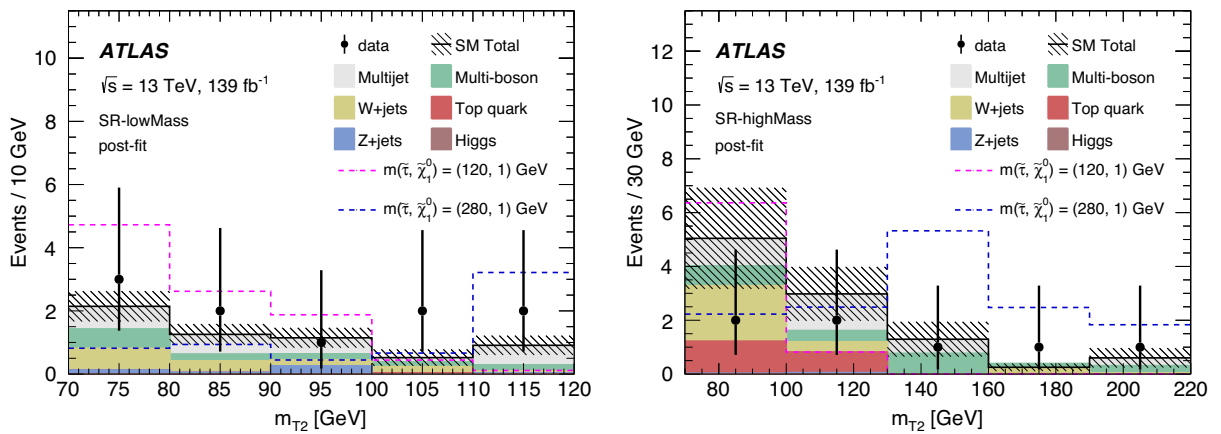


FIG. 6. The postfit m_{T2} distribution for SR-lowMass (left) and SR-highMass (right). The stacked histograms show the expected SM backgrounds. The multijet contribution is estimated from data using the ABCD method. The contributions of multijet and $W + \text{jets}$ events are scaled with the corresponding normalization factors derived from the background-only fit described in Sec. VIII. The hatched bands represent the sum in quadrature of systematic and statistical uncertainties of the total SM background. For illustration, the distributions from the SUSY reference points (defined in Sec. III) are also shown as dashed lines. The last bin includes the overflow events.

TABLE VII. Expected event yields for the SUSY reference points (defined in Sec. III) are shown along with the one-sided p_0 -values, and the observed and expected 95% C.L. upper limits on the visible non-SM cross section (σ_{vis}^{95}) are given. Values of $p_0 > 0.5$ are truncated at $p_0 = 0.5$.

	SR-lowMass	SR-highMass
$m(\tilde{\tau}, \tilde{\chi}_1^0) = (120, 1)$ GeV	9.8 ± 3.0	7.2 ± 2.2
$m(\tilde{\tau}, \tilde{\chi}_1^0) = (280, 1)$ GeV	6.1 ± 1.5	14.4 ± 2.5
p_0	0.11	0.50
Expected σ_{vis}^{95} [fb]	$0.055^{+0.025}_{-0.014}$	$0.065^{+0.025}_{-0.019}$
Observed σ_{vis}^{95} [fb]	0.08	0.05

multijet contributions. The signal is assumed to be absent in this fit.

- (ii) A *model-independent limit* fit combines the data event yield in a given SR with the SM background estimate and its uncertainties to test whether any non-SM signal contributes to the SR. The significance of a possible excess of observed events over the SM prediction is quantified by the one-sided probability, $p(\text{signal} = 0)$ denoted by p_0 , of the background alone to fluctuate to the observed number of events or higher using the asymptotic formula described in Ref. [100]. The background yields and uncertainties are taken from the background-only fit results. The presence of a non-SM signal would manifest itself as a small p_0 value.
- (iii) In the *model-dependent limit* fit the SUSY signal is allowed to populate both the signal regions and the control regions, and it is scaled by a freely floating signal normalization factor. The background normalization factors are also determined simultaneously in the fit. A SUSY model with a specific set of sparticle masses is rejected if 95% C.L. upper limit on the signal normalization factor obtained in this fit is smaller than unity.

IX. RESULTS

The observed number of events in each control, and signal region and the expected contributions from SM processes are given in Table VI. The contributions of multijet and $W + \text{jets}$ events are scaled with the normalization factors obtained from the background-only fit described in Sec. VIII. The multijet normalization in the SR is 1.03 times the prediction from the ABCD method and has an uncertainty of around 28%, due to the small number of observed events in the multijet CR-A. The $W + \text{jets}$ normalization is 0.91 ± 0.12 . The m_{T2} distributions are shown in Fig. 6 for data, expected SM backgrounds, and the SUSY reference points defined in Sec. III. In both signal regions, observations and background predictions are found to be compatible within uncertainties.

Individual model-independent fits of the SR-lowMass and SR-highMass are used to derive the one-sided p_0 -values. In addition, the observed and expected 95% C.L. upper limits on the visible non-SM cross section (σ_{vis}^{95}) are derived using the same model-independent fits. The σ_{vis}^{95} is defined as the product of acceptance, reconstruction efficiency and production cross section, obtained normalizing the limit on the non-SM yield in the SR by the integrated luminosity of the data sample. These results are shown in Table VII. All limits are calculated using the CL_s prescription [101].

X. INTERPRETATION

In the absence of a significant excess over the expected SM background, the observed and expected numbers of events in the signal regions are used to set exclusion limits at 95% C.L. using the model-dependent limit fit. The exclusion limits for the combined SR-lowMass and SR-highMass for the simplified models described in Sec. III are shown in Fig. 7. The solid (dashed) lines show the observed (expected) exclusion contours. The band

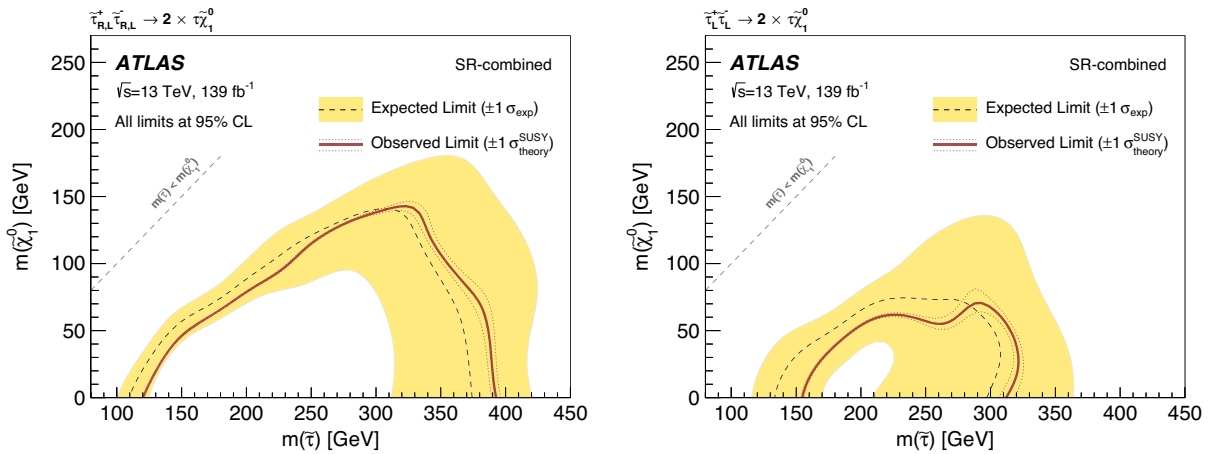


FIG. 7. The 95% C.L. exclusion contours for the combined fit of SR-lowMass and SR-highMass for simplified models with (a) combined $\tilde{\tau}_{\text{R,L}}^+ \tilde{\tau}_{\text{R,L}}^-$ production and (b) $\tilde{\tau}_L^+ \tilde{\tau}_L^-$ only production. The text provides details of exclusion curves and uncertainty bands.

around the expected limit shows the $\pm 1\sigma$ variations, including all uncertainties except theoretical uncertainties in the signal cross section. The dotted lines around the observed limit indicate the sensitivity to $\pm 1\sigma$ variations of the theoretical uncertainties in the signal cross section.

Stau masses from 120 GeV to 390 GeV are excluded for a massless lightest neutralino in the scenario of combined stau-left and stau-right $\tilde{\tau}_{R,L}^+ \tilde{\tau}_{R,L}^-$ production. For stau-left pair production only, $\tilde{\tau}_L^+ \tilde{\tau}_L^-$, the exclusion region extends from 155 GeV to 310 GeV. While the stau-left pairs have a higher production cross section, the stau-right pairs have a higher efficiency times acceptance due to kinematic differences in the resulting decay products.

These limits extend significantly beyond previous results [25,27,102,103] in the high $\tilde{\tau}$ mass region.

Uncertainties in each background from scale variations are fully correlated across regions and bins, and uncorrelated between processes. In some cases this may result in uncertainties canceling out, while the higher-order corrections may not cancel out. A different fit with scale variations uncorrelated in all bins results in a less than 1% change in the limits on the excluded cross section near the edge of exclusion for combined left and right $\tilde{\tau} \tilde{\tau}$ production.

XI. CONCLUSION

Searches for stau-pair production in events with at least two hadronically decaying τ -leptons and missing transverse momentum were performed using 139 fb^{-1} of pp collision data at $\sqrt{s} = 13 \text{ TeV}$ recorded with the ATLAS detector at the LHC. Agreement between data and SM predictions is observed in two optimized signal regions. The results are used to set limits on the visible cross section for events beyond the Standard Model in each signal region.

Exclusion limits are placed on parameters of simplified electroweak supersymmetry models in scenarios of stau-pair production. Stau masses from 120 GeV to 390 GeV are excluded for a massless lightest neutralino in the scenario of direct production of stau pairs, with each stau decaying into the lightest neutralino and one τ -lepton. These limits extend significantly beyond previous results by the ATLAS and CMS experiments in the high $\tilde{\tau}$ mass region.

ACKNOWLEDGMENTS

We thank CERN for the very successful operation of the LHC, as well as the support staff from our institutions without whom ATLAS could not be operated efficiently. We acknowledge the support of ANPCyT, Argentina; YerPhI, Armenia; ARC, Australia; BMWFW and FWF, Austria; ANAS, Azerbaijan; SSTC, Belarus; CNPq and FAPESP, Brazil; NSERC, NRC and CFI, Canada; CERN; CONICYT, Chile; CAS, MOST and NSFC, China; COLCIENCIAS, Colombia; MSMT CR, MPO CR and VSC CR, Czech Republic; DNRF and DNSRC, Denmark; IN2P3-CNRS, CEA-DRF/IRFU, France; SRNSFG, Georgia; BMBF, HGF, and MPG, Germany; GSRT, Greece; RGC, Hong Kong SAR, China; ISF and Benoziyo Center, Israel; INFN, Italy; MEXT and JSPS, Japan; CNRST, Morocco; NWO, Netherlands; RCN, Norway; MNiSW and NCN, Poland; FCT, Portugal; MNE/IFA, Romania; MES of Russia and NRC KI, Russian Federation; JINR; MESTD, Serbia; MSSR, Slovakia; ARRS and MIZŠ, Slovenia; DST/NRF, South Africa; MINECO, Spain; SRC and Wallenberg Foundation, Sweden; SERI, SNSF and Cantons of Bern and Geneva, Switzerland; MOST, Taiwan; TAEK, Turkey; STFC, United Kingdom; DOE and NSF, United States of America. In addition, individual groups and members have received support from BCKDF, CANARIE, CRC and Compute Canada, Canada; COST, ERC, ERDF, Horizon 2020, and Marie Skłodowska-Curie Actions, European Union; Investissements d'Avenir Labex and Idex, ANR, France; DFG and AvH Foundation, Germany; Herakleitos, Thales and Aristeia programmes co-financed by EU-ESF and the Greek NSRF, Greece; BSF-NSF and GIF, Israel; CERCA Programme Generalitat de Catalunya, Spain; The Royal Society and Leverhulme Trust, United Kingdom. The crucial computing support from all WLCG partners is acknowledged gratefully, in particular from CERN, the ATLAS Tier-1 facilities at TRIUMF (Canada), NDGF (Denmark, Norway, Sweden), CC-IN2P3 (France), KIT/GridKA (Germany), INFN-CNAF (Italy), NL-T1 (Netherlands), PIC (Spain), ASGC (Taiwan), RAL (UK) and BNL (USA), the Tier-2 facilities worldwide and large non-WLCG resource providers. Major contributors of computing resources are listed in Ref. [104]. Unfortunately, our colleague Jihyun Jeong passed away shortly before the completion of this work.

[1] Y. Golfand and E. Likhtman, Extension of the algebra of poincare group generators and violation of p invariance, Pis'ma Zh. Eksp. Teor. Fiz. **13**, 452 (1971) [JETP Lett. **13**, 323 (1971)].

[2] D. V. Volkov and V. P. Akulov, Is the neutrino a goldstone particle? Phys. Lett. **46B**, 109 (1973).

[3] J. Wess and B. Zumino, Supergauge transformations in four dimensions, Nucl. Phys. **B70**, 39 (1974).

- [4] J. Wess and B. Zumino, Supergauge invariant extension of quantum electrodynamics, *Nucl. Phys.* **B78**, 1 (1974).
- [5] S. Ferrara and B. Zumino, Supergauge invariant Yang-Mills theories, *Nucl. Phys.* **B79**, 413 (1974).
- [6] A. Salam and J. A. Strathdee, Supersymmetry and non-Abelian gauges, *Phys. Lett. B* **51**, 353 (1974).
- [7] S. P. Martin, A supersymmetry primer, *Adv. Ser. Dir. High Energy Phys.* **18**, 1 (1998).
- [8] G. R. Farrar and P. Fayet, Phenomenology of the production, decay, and detection of new hadronic states associated with supersymmetry, *Phys. Lett. B* **76**, 575 (1978).
- [9] H. Goldberg, Constraint on the Photino Mass from Cosmology, *Phys. Rev. Lett.* **50**, 1419 (1983); Erratum, *Phys. Rev. Lett.* **103**, 099905 (2009).
- [10] J. R. Ellis, J. S. Hagelin, D. V. Nanopoulos, K. A. Olive, and M. Srednicki, Supersymmetric relics from the big bang, *Nucl. Phys.* **B238**, 453 (1984).
- [11] D. Albornoz Vásquez, G. Bélanger, and C. Boehm, Revisiting light neutralino scenarios in the MSSM, *Phys. Rev. D* **84**, 095015 (2011).
- [12] G. Belanger, F. Boudjema, A. Cottrant, A. Pukhov, and A. Semenov, WMAP constraints on SUGRA models with non-universal gaugino masses and prospects for direct detection, *Nucl. Phys.* **B706**, 411 (2005).
- [13] S. King, J. Roberts, and D. Roy, Natural dark matter in SUSY GUTs with non-universal gaugino masses, *J. High Energy Phys.* **10** (2007) 106.
- [14] M. Dine and W. Fischler, A phenomenological model of particle physics based on supersymmetry, *Phys. Lett.* **110B**, 227 (1982).
- [15] L. Alvarez-Gaume, M. Claudson, and M. B. Wise, Low-energy supersymmetry, *Nucl. Phys.* **B207**, 96 (1982).
- [16] C. R. Nappi and B. A. Ovrut, Supersymmetric extension of the $SU(3) \times SU(2) \times U(1)$ model, *Phys. Lett.* **113B**, 175 (1982).
- [17] L. Randall and R. Sundrum, Out of this world supersymmetry breaking, *Nucl. Phys.* **B557**, 79 (1999).
- [18] G. F. Giudice, M. A. Luty, H. Murayama, and R. Rattazzi, Gaugino mass without singlets, *J. High Energy Phys.* **12** (1998) 027.
- [19] The LEP SUSY Working Group and the ALEPH, DELPHI, L3 and OPAL experiments, Report No. LEPSU-SYWG/01-03.1, 04-01.1, <http://lepsusy.web.cern.ch/lepsusy/Welcome.html>.
- [20] ALEPH Collaboration, Search for scalar leptons in e^+e^- collisions at centre-of-mass energies up to 209 GeV, *Phys. Lett. B* **526**, 206 (2002).
- [21] ALEPH Collaboration, Absolute mass lower limit for the lightest neutralino of the MSSM from e^+e^- data at \sqrt{s} up to 209 GeV, *Phys. Lett. B* **583**, 247 (2004).
- [22] DELPHI Collaboration, Searches for supersymmetric particles in e^+e^- collisions up to 208 GeV and interpretation of the results within the MSSM, *Eur. Phys. J. C* **31**, 421 (2003).
- [23] L3 Collaboration, Search for scalar quarks and scalar leptons at LEP, *Phys. Lett. B* **580**, 37 (2004).
- [24] OPAL Collaboration, Search for anomalous production of di-lepton events with missing transverse momentum in e^+e^- collisions at $\sqrt{s} = 183\text{--}209$ GeV, *Eur. Phys. J. C* **32**, 453 (2004).
- [25] ATLAS Collaboration, Search for the electroweak production of supersymmetric particles in $\sqrt{s} = 8$ TeV pp collisions with the ATLAS detector, *Phys. Rev. D* **93**, 052002 (2016).
- [26] CMS Collaboration, Search for electroweak production of charginos in final states with two τ leptons in pp collisions at $\sqrt{s} = 8$ TeV, *J. High Energy Phys.* **04** (2017) 018.
- [27] CMS Collaboration, Search for direct pair production of supersymmetric partners to the τ lepton in proton-proton collisions at $\sqrt{s} = 13$ TeV, [arXiv:1907.13179](https://arxiv.org/abs/1907.13179).
- [28] ATLAS Collaboration, The ATLAS experiment at the CERN large hadron collider, *J. Instrum.* **3**, S08003 (2008).
- [29] ATLAS Collaboration, ATLAS insertable B -layer technical design report, Report No. ATLAS-TDR-19, 2010, <https://cds.cern.ch/record/1291633>; Addendum: Report No. ATLAS-TDR-19-ADD-1, 2012, <https://cds.cern.ch/record/1451888>.
- [30] B. Abbott *et al.*, Production and integration of the ATLAS Insertable B-Layer, *J. Instrum.* **13**, T05008 (2018).
- [31] ATLAS Collaboration, Performance of the ATLAS trigger system in 2015, *Eur. Phys. J. C* **77**, 317 (2017).
- [32] ATLAS Collaboration, Luminosity determination in pp collisions at $\sqrt{s} = 13$ TeV using the ATLAS detector at the LHC, Report No. ATLAS-CONF-2019-021, 2019, <https://cds.cern.ch/record/2677054>.
- [33] G. Avoni *et al.*, The new LUCID-2 detector for luminosity measurement and monitoring in ATLAS, *J. Instrum.* **13**, P07017 (2018).
- [34] ATLAS Collaboration, The ATLAS simulation infrastructure, *Eur. Phys. J. C* **70**, 823 (2010).
- [35] S. Agostinelli *et al.*, GEANT4—a simulation toolkit, *Nucl. Instrum. Methods Phys. Res., Sect. A* **506**, 250 (2003).
- [36] T. Sjöstrand, S. Mrenna, and P. Z. Skands, A brief introduction to PYTHIA 8.1, *Comput. Phys. Commun.* **178**, 852 (2008).
- [37] ATLAS Collaboration, The Pythia 8 A3 tune description of ATLAS minimum bias and inelastic measurements incorporating the Donnachie–Landshoff diffractive model, Report No. ATL-PHYS-PUB-2016-017, 2016, <https://cds.cern.ch/record/2206965>.
- [38] A. D. Martin, W. Stirling, R. S. Thorne, and G. Watt, Parton distributions for the LHC, *Eur. Phys. J. C* **63**, 189 (2009).
- [39] T. Gleisberg, S. Höche, F. Krauss, M. Schönherr, S. Schumann, F. Siegert, and J. Winter, Event generation with SHERPA 1.1, *J. High Energy Phys.* **02** (2009) 007.
- [40] S. Höche, F. Krauss, M. Schönherr, and F. Siegert, QCD matrix elements + parton showers: The NLO case, *J. High Energy Phys.* **04** (2013) 027.
- [41] T. Gleisberg and S. Höche, Comix, a new matrix element generator, *J. High Energy Phys.* **12** (2008) 039.
- [42] F. Cascioli, P. Maierhofer, and S. Pozzorini, Scattering Amplitudes with Open Loops, *Phys. Rev. Lett.* **108**, 111601 (2012).
- [43] A. Denner, S. Dittmaier, and L. Hofer, Collier: A fortran-based complex one-loop library in extended regularizations, *Comput. Phys. Commun.* **212**, 220 (2017).
- [44] S. Schumann and F. Krauss, A Parton shower algorithm based on Catani–Seymour dipole factorisation, *J. High Energy Phys.* **03** (2008) 038.

- [45] R. D. Ball *et al.*, Parton distributions for the LHC Run II, *J. High Energy Phys.* **04** (2015) 040.
- [46] S. Catani, L. Cieri, G. Ferrera, D. de Florian, and M. Grazzini, Vector Boson Production at Hadron Colliders: A Fully Exclusive QCD Calculation at Next-to-Next-to-Leading Order, *Phys. Rev. Lett.* **103**, 082001 (2009).
- [47] S. Höche, F. Krauss, M. Schonherr, and F. Siegert, A critical appraisal of NLO + PS matching methods, *J. High Energy Phys.* **09** (2012) 049.
- [48] S. Catani, F. Krauss, R. Kuhn, and B. R. Webber, QCD matrix elements + parton showers, *J. High Energy Phys.* **11** (2001) 063.
- [49] S. Höche, F. Krauss, S. Schumann, and F. Siegert, QCD matrix elements and truncated showers, *J. High Energy Phys.* **05** (2009) 053.
- [50] S. Frixione, P. Nason, and G. Ridolfi, A positive-weight next-to-leading-order Monte Carlo for heavy flavour hadroproduction, *J. High Energy Phys.* **09** (2007) 126.
- [51] P. Nason, A new method for combining NLO QCD with shower Monte Carlo algorithms, *J. High Energy Phys.* **11** (2004) 040.
- [52] S. Frixione, P. Nason, and C. Oleari, Matching NLO QCD computations with Parton Shower simulations: The POWHEG method, *J. High Energy Phys.* **11** (2007) 070.
- [53] S. Alioli, P. Nason, C. Oleari, and E. Re, A general framework for implementing NLO calculations in shower Monte Carlo programs: The POWHEG BOX, *J. High Energy Phys.* **06** (2010) 043.
- [54] R. D. Ball *et al.*, Parton distributions with LHC data, *Nucl. Phys.* **B867**, 244 (2013).
- [55] ATLAS Collaboration, ATLAS Pythia 8 tunes to 7 TeV data, Report No. ATL-PHYS-PUB-2014-021, 2014, <https://cds.cern.ch/record/1966419>.
- [56] M. Beneke, P. Falgari, S. Klein, and C. Schwinn, Hadronic top-quark pair production with NNLL threshold resummation, *Nucl. Phys.* **B855**, 695 (2012).
- [57] M. Cacciari, M. Czakon, M. Mangano, A. Mitov, and P. Nason, Top-pair production at hadron colliders with next-to-next-to-leading logarithmic soft-gluon resummation, *Phys. Lett. B* **710**, 612 (2012).
- [58] P. Bärnreuther, M. Czakon, and A. Mitov, Percent-Level-Precision Physics at the Tevatron: Next-to-Next-to-Leading Order QCD Corrections to $q\bar{q} \rightarrow t\bar{t} + X$, *Phys. Rev. Lett.* **109**, 132001 (2012).
- [59] M. Czakon and A. Mitov, NNLO corrections to top-pair production at hadron colliders: The all-fermionic scattering channels, *J. High Energy Phys.* **12** (2012) 054.
- [60] M. Czakon and A. Mitov, NNLO corrections to top pair production at hadron colliders: The quark-gluon reaction, *J. High Energy Phys.* **01** (2013) 080.
- [61] M. Czakon, P. Fiedler, and A. Mitov, Total Top-Quark Pair-Production Cross Section at Hadron Colliders Through $O(\alpha_s^4)$, *Phys. Rev. Lett.* **110**, 252004 (2013).
- [62] M. Czakon and A. Mitov, Top++: A program for the calculation of the top-pair cross-section at hadron colliders, *Comput. Phys. Commun.* **185**, 2930 (2014).
- [63] M. Aliev, H. Lacker, U. Langenfeld, S. Moch, P. Uwer, and M. Wiedermann, HATHOR—HADronic Top and Heavy quarks crOSS section calculator, *Comput. Phys. Commun.* **182**, 1034 (2011).
- [64] P. Kant, O. M. Kind, T. Kintscher, T. Lohse, T. Martini, S. Mölbitz, P. Rieck, and P. Uwer, HatHor for single top-quark production: Updated predictions and uncertainty estimates for single top-quark production in hadronic collisions, *Comput. Phys. Commun.* **191**, 74 (2015).
- [65] J. Alwall, R. Frederix, S. Frixione, V. Hirschi, F. Maltoni, O. Mattelaer, H.-S. Shao, T. Stelzer, P. Torrielli, and M. Zaro, The automated computation of tree-level and next-to-leading order differential cross sections, and their matching to parton shower simulations, *J. High Energy Phys.* **07** (2014) 079.
- [66] A. Lazopoulos, T. McElmurry, K. Melnikov, and F. Petriello, Next-to-leading order QCD corrections to $t\bar{t}Z$ production at the LHC, *Phys. Lett. B* **666**, 62 (2008).
- [67] J. M. Campbell and R. K. Ellis, $t\bar{t}W^{++}$ production and decay at NLO, *J. High Energy Phys.* **07** (2012) 052.
- [68] D. de Florian *et al.*, Handbook of LHC higgs cross sections: 4. Deciphering the nature of the Higgs sector, [arXiv:1610.07922](https://arxiv.org/abs/1610.07922).
- [69] D. J. Lange, The EvtGen particle decay simulation package, *Nucl. Instrum. Methods Phys. Res., Sect. A* **462**, 152 (2001).
- [70] L. Lönnblad and S. Prestel, Matching tree-level matrix elements with interleaved showers, *J. High Energy Phys.* **03** (2012) 019.
- [71] B. Fuks, M. Klasen, D. R. Lamprea, and M. Rothering, Precision predictions for electroweak superpartner production at hadron colliders with Resummino, *Eur. Phys. J. C* **73**, 2480 (2013).
- [72] W. Beenakker, M. Klasen, M. Krämer, T. Plehn, M. Spira, and P. M. Zerwas, Production of Charginos, Neutralinos, and Stopped Squarks at Hadron Colliders, *Phys. Rev. Lett.* **83**, 3780 (1999).
- [73] G. Bozzi, B. Fuks, and M. Klasen, Threshold resummation for slepton-pair production at hadron colliders, *Nucl. Phys.* **B777**, 157 (2007).
- [74] B. Fuks, M. Klasen, D. R. Lamprea, and M. Rothering, Revisiting slepton pair production at the Large Hadron Collider, *J. High Energy Phys.* **01** (2014) 168.
- [75] J. Fiaschi and M. Klasen, Slepton pair production at the LHC in NLO + NLL with resummation-improved parton densities, *J. High Energy Phys.* **03** (2018) 094.
- [76] ATLAS Collaboration, Vertex Reconstruction Performance of the ATLAS Detector at $\sqrt{s} = 13$ TeV, Report No. ATL-PHYS-PUB-2015-026, 2015, <https://cds.cern.ch/record/2037717>.
- [77] ATLAS Collaboration, Topological cell clustering in the ATLAS calorimeters and its performance in LHC Run 1, *Eur. Phys. J. C* **77**, 490 (2017).
- [78] M. Cacciari, G. P. Salam, and G. Soyez, The anti- k_T jet clustering algorithm, *J. High Energy Phys.* **04** (2008) 063.
- [79] M. Cacciari, G. P. Salam, and G. Soyez, FastJet user manual, *Eur. Phys. J. C* **72**, 1896 (2012).
- [80] ATLAS Collaboration, Jet energy scale measurements and their systematic uncertainties in proton-proton collisions at $\sqrt{s} = 13$ TeV with the ATLAS detector, *Phys. Rev. D* **96**, 072002 (2017).
- [81] M. Cacciari and G. P. Salam, Pileup subtraction using jet areas, *Phys. Lett. B* **659**, 119 (2008).

- [82] ATLAS Collaboration, Tagging and suppression of pileup jets with the ATLAS detector, Report No. ATLASCONF-2014-018, 2014, <https://cds.cern.ch/record/1700870>.
- [83] ATLAS Collaboration, Measurements of b -jet tagging efficiency with the ATLAS detector using $t\bar{t}$ events at $\sqrt{s} = 13$ TeV, *J. High Energy Phys.* **08** (2018) 089.
- [84] ATLAS Collaboration, ATLAS b -jet identification performance and efficiency measurement with $t\bar{t}$ events in pp collisions at $\sqrt{s} = 13$ TeV, *Eur. Phys. J. C* **79**, 970 (2019).
- [85] ATLAS Collaboration, Measurement of b -tagging efficiency of c -jets in $t\bar{t}$ events using a likelihood approach with the ATLAS detector, Report No. ATLAS-CONF-2018-001, 2018, <https://cds.cern.ch/record/2306649>.
- [86] ATLAS Collaboration, Calibration of light-flavour b -jet mistagging rates using ATLAS proton–proton collision data at $\sqrt{s} = 13$ TeV, Report No. ATLAS-CONF-2018-006, 2018, <https://cds.cern.ch/record/2314418>.
- [87] ATLAS Collaboration, Electron and photon performance measurements with the ATLAS detector using the 2015–2017 LHC proton–proton collision data, *J. Instrum.* **14**, P12006 (2019).
- [88] ATLAS Collaboration, Muon reconstruction performance of the ATLAS detector in proton–proton collision data at $\sqrt{s} = 13$ TeV, *Eur. Phys. J. C* **76**, 292 (2016).
- [89] ATLAS Collaboration, Measurement of the tau lepton reconstruction and identification performance in the ATLAS experiment using pp collisions at $\sqrt{s} = 13$ TeV, Report No. ATLAS-CONF-2017-029, 2017, <https://cds.cern.ch/record/2261772>.
- [90] ATLAS Collaboration, Identification and energy calibration of hadronically decaying tau leptons with the ATLAS experiment in pp collisions at $\sqrt{s} = 8$ TeV, *Eur. Phys. J. C* **75**, 303 (2015).
- [91] ATLAS Collaboration, Performance of missing transverse momentum reconstruction with the ATLAS detector using proton–proton collisions at $\sqrt{s} = 13$ TeV, *Eur. Phys. J. C* **78**, 903 (2018).
- [92] ATLAS Collaboration, The ATLAS tau trigger in Run 2, Report No. ATLAS-CONF-2017-061, 2017, <https://cds.cern.ch/record/2274201>.
- [93] C. G. Lester and D. J. Summers, Measuring masses of semi-invisibly decaying particles pair produced at hadron colliders, *Phys. Lett. B* **463**, 99 (1999).
- [94] A. Barr, C. Lester, and P. Stephens, A variable for measuring masses at hadron colliders when missing energy is expected; mT2: The truth behind the glamour, *J. Phys. G* **29**, 2343 (2003).
- [95] D. Tovey, On measuring the masses of pair-produced semi-invisibly decaying particles at hadron colliders, *J. High Energy Phys.* **04** (2008) 034.
- [96] ATLAS Collaboration, Measurement of the Inelastic Proton–Proton Cross Section at $\sqrt{s} = 13$ TeV with the ATLAS Detector at the LHC, *Phys. Rev. Lett.* **117**, 182002 (2016).
- [97] J. Butterworth *et al.*, PDF4LHC recommendations for LHC Run II, *J. Phys. G* **43**, 023001 (2016).
- [98] E. Bothmann, M. Schönherr, and S. Schumann, Reweighting QCD matrix-element and parton shower calculations, *Eur. Phys. J. C* **76**, 590 (2016).
- [99] M. Baak, G. J. Besjes, D. Côté, A. Koutsman, J. Lorenz, and D. Short, HistFitter software framework for statistical data analysis, *Eur. Phys. J. C* **75**, 153 (2015).
- [100] G. Cowan, K. Cranmer, E. Gross, and O. Vitells, Asymptotic formulae for likelihood-based tests of new physics, *Eur. Phys. J. C* **71**, 1554 (2011); Erratum, *Eur. Phys. J. C* **73**, 2501 (2013);
- [101] A. L. Read, Presentation of search results: The CLs technique, *J. Phys. G* **28**, 2693 (2002).
- [102] CMS Collaboration, Searches for electroweak production of charginos, neutralinos, and sleptons decaying to leptons and W, Z, and Higgs bosons in pp collisions at 8 TeV, *Eur. Phys. J. C* **74**, 3036 (2014).
- [103] CMS Collaboration, Search for supersymmetry in events with a τ lepton pair and missing transverse momentum in proton–proton collisions at $\sqrt{s} = 13$ TeV, *J. High Energy Phys.* **11** (2018) 151.
- [104] ATLAS Collaboration, ATLAS computing acknowledgements, Report No. ATL-GEN-PUB-2016-002, <https://cds.cern.ch/record/2202407>.

G. Aad,¹⁰¹ B. Abbott,¹²⁸ D. C. Abbott,¹⁰² A. Abed Abud,^{70a,70b} K. Abeling,⁵³ D. K. Abhayasinghe,⁹³ S. H. Abidi,¹⁶⁷ O. S. AbouZeid,⁴⁰ N. L. Abraham,¹⁵⁶ H. Abramowicz,¹⁶¹ H. Abreu,¹⁶⁰ Y. Abulaiti,⁶ B. S. Acharya,^{66a,66b,b} B. Achkar,⁵³ S. Adachi,¹⁶³ L. Adam,⁹⁹ C. Adam Bourdarios,⁵ L. Adamczyk,^{83a} L. Adamek,¹⁶⁷ J. Adelman,¹²⁰ M. Adersberger,¹¹³ A. Adiguzel,^{12c,c} S. Adorni,⁵⁴ T. Adye,¹⁴⁴ A. A. Affolder,¹⁴⁶ Y. Afik,¹⁶⁰ C. Agapopoulou,¹³² M. N. Agaras,³⁸ A. Aggarwal,¹¹⁸ C. Agheorghiesei,^{27c} J. A. Aguilar-Saavedra,^{140f,140a,d} F. Ahmadov,⁷⁹ W. S. Ahmed,¹⁰³ X. Ai,¹⁸ G. Aielli,^{73a,73b} S. Akatsuka,⁸⁵ T. P. A. Åkesson,⁹⁶ E. Akilli,⁵⁴ A. V. Akimov,¹¹⁰ K. Al Khoury,¹³² G. L. Alberghi,^{23b,23a} J. Albert,¹⁷⁶ M. J. Alconada Verzin,¹⁶¹ S. Alderweireldt,³⁶ M. Aleksa,³⁶ I. N. Aleksandrov,⁷⁹ C. Alexa,^{27b} D. Alexandre,¹⁹ T. Alexopoulos,¹⁰ A. Alfonsi,¹¹⁹ F. Alfonsi,^{23b,23a} M. Alhroob,¹²⁸ B. Ali,¹⁴² G. Alimonti,^{68a} J. Alison,³⁷ S. P. Alkire,¹⁴⁸ C. Allaire,¹³² B. M. M. Allbrooke,¹⁵⁶ B. W. Allen,¹³¹ P. P. Allport,²¹ A. Aloisio,^{69a,69b} A. Alonso,⁴⁰ F. Alonso,⁸⁸ C. Alpigiani,¹⁴⁸ A. A. Alshehri,⁵⁷ M. Alvarez Estevez,⁹⁸ D. Álvarez Piqueras,¹⁷⁴ M. G. Alvigi,^{69a,69b} Y. Amaral Coutinho,^{80b} A. Ambler,¹⁰³ L. Ambroz,¹³⁵ C. Amelung,²⁶ D. Amidei,¹⁰⁵ S. P. Amor Dos Santos,^{140a} S. Amoroso,⁴⁶ C. S. Amrouche,⁵⁴ F. An,⁷⁸ C. Anastopoulos,¹⁴⁹ N. Andari,¹⁴⁵ T. Andeen,¹¹ C. F. Anders,^{61b} J. K. Anders,²⁰

A. Andreazza,^{68a,68b} V. Andrei,^{61a} C. R. Anelli,¹⁷⁶ S. Angelidakis,³⁸ A. Angerami,³⁹ A. V. Anisenkov,^{121b,121a} A. Annovi,^{71a} C. Antel,^{61a} M. T. Anthony,¹⁴⁹ M. Antonelli,⁵¹ D. J. A. Antrim,¹⁷¹ F. Anulli,^{72a} M. Aoki,⁸¹ J. A. Aparisi Pozo,¹⁷⁴ L. Aperio Bella,^{15a} G. Arabidze,¹⁰⁶ J. P. Araque,^{140a} V. Araujo Ferraz,^{80b} R. Araujo Pereira,^{80b} C. Arcangeletti,⁵¹ A. T. H. Arce,⁴⁹ F. A. Arduh,⁸⁸ J.-F. Arguin,¹⁰⁹ S. Argyropoulos,⁷⁷ J.-H. Arling,⁴⁶ A. J. Armbruster,³⁶ A. Armstrong,¹⁷¹ O. Arnaz,¹⁶⁷ H. Arnold,¹¹⁹ Z. P. Arrubarrena Tame,¹¹³ A. Artamonov,^{123a} G. Artoni,¹³⁵ S. Artz,⁹⁹ S. Asai,¹⁶³ N. Asbah,⁵⁹ E. M. Asimakopoulou,¹⁷² L. Asquith,¹⁵⁶ J. Assahsah,^{35d} K. Assamagan,²⁹ R. Astalos,^{28a} R. J. Atkin,^{33a} M. Atkinson,¹⁷³ N. B. Atlay,¹⁹ H. Atmani,¹³² K. Augsten,¹⁴² G. Avolio,³⁶ R. Avramidou,^{60a} M. K. Ayoub,^{15a} A. M. Azoulay,^{168b} G. Azuelos,^{109,e} H. Bachacou,¹⁴⁵ K. Bachas,^{67a,67b} M. Backes,¹³⁵ F. Backman,^{45a,45b} P. Bagnaia,^{72a,72b} M. Bahmani,⁸⁴ H. Bahrasemani,¹⁵² A. J. Bailey,¹⁷⁴ V. R. Bailey,¹⁷³ J. T. Baines,¹⁴⁴ M. Bajic,⁴⁰ C. Bakalis,¹⁰ O. K. Baker,¹⁸³ P. J. Bakker,¹¹⁹ D. Bakshi Gupta,⁸ S. Balaji,¹⁵⁷ E. M. Baldin,^{121b,121a} P. Balek,¹⁸⁰ F. Balli,¹⁴⁵ W. K. Balunas,¹³⁵ J. Balz,⁹⁹ E. Banas,⁸⁴ A. Bandyopadhyay,²⁴ Sw. Banerjee,^{181,f} A. A. E. Bannoura,¹⁸² L. Barak,¹⁶¹ W. M. Barbe,³⁸ E. L. Barberio,¹⁰⁴ D. Barberis,^{55b,55a} M. Barbero,¹⁰¹ G. Barbour,⁹⁴ T. Barillari,¹¹⁴ M.-S. Barisits,³⁶ J. Barkeloo,¹³¹ T. Barklow,¹⁵³ R. Barnea,¹⁶⁰ S. L. Barnes,^{60c} B. M. Barnett,¹⁴⁴ R. M. Barnett,¹⁸ Z. Barnovska-Blenessy,^{60a} A. Baroncelli,^{60a} G. Barone,²⁹ A. J. Barr,¹³⁵ L. Barranco Navarro,^{45a,45b} F. Barreiro,⁹⁸ J. Barreiro Guimarães da Costa,^{15a} S. Barsov,¹³⁸ R. Bartoldus,¹⁵³ G. Bartolini,¹⁰¹ A. E. Barton,⁸⁹ P. Bartos,^{28a} A. Basalaeu,⁴⁶ A. Bassalat,^{132,g} M. J. Basso,¹⁶⁷ R. L. Bates,⁵⁷ S. Batlamous,^{35e} J. R. Batley,³² B. Batool,¹⁵¹ M. Battaglia,¹⁴⁶ M. Baue,^{72a,72b} F. Bauer,¹⁴⁵ K. T. Bauer,¹⁷¹ H. S. Bawa,^{31,h} J. B. Beacham,⁴⁹ T. Beau,¹³⁶ P. H. Beauchemin,¹⁷⁰ F. Becherer,⁵² P. Bechtel,²⁴ H. C. Beck,⁵³ H. P. Beck,^{20,i} K. Becker,⁵² M. Becker,⁹⁹ C. Becot,⁴⁶ A. Beddall,^{12d} A. J. Beddall,^{12a} V. A. Bednyakov,⁷⁹ M. Bedognetti,¹¹⁹ C. P. Bee,¹⁵⁵ T. A. Beermann,⁷⁶ M. Begalli,^{80b} M. Begel,²⁹ A. Behera,¹⁵⁵ J. K. Behr,⁴⁶ F. Beisiegel,²⁴ A. S. Bell,⁹⁴ G. Bella,¹⁶¹ L. Bellagamba,^{23b} A. Bellerive,³⁴ P. Bellos,⁹ K. Beloborodov,^{121b,121a} K. Belotskiy,¹¹¹ N. L. Belyaev,¹¹¹ D. Benckekroun,^{35a} N. Benekos,¹⁰ Y. Benhammou,¹⁶¹ D. P. Benjamin,⁶ M. Benoit,⁵⁴ J. R. Bensinger,²⁶ S. Bentvelsen,¹¹⁹ L. Beresford,¹³⁵ M. Beretta,⁵¹ D. Berge,⁴⁶ E. Bergeas Kuutmann,¹⁷² N. Berger,⁵ B. Bergmann,¹⁴² L. J. Bergsten,²⁶ J. Beringer,¹⁸ S. Berlendis,⁷ N. R. Bernard,¹⁰² G. Bernardi,¹³⁶ C. Bernius,¹⁵³ F. U. Bernlochner,²⁴ T. Berry,⁹³ P. Berta,⁹⁹ C. Bertella,^{15a} I. A. Bertram,⁸⁹ O. Bessidskaia Bylund,¹⁸² N. Besson,¹⁴⁵ A. Bethani,¹⁰⁰ S. Bethke,¹¹⁴ A. Betti,²⁴ A. J. Bevan,⁹² J. Beyer,¹¹⁴ D. S. Bhattacharya,¹⁷⁷ R. Bi,¹³⁹ R. M. Bianchi,¹³⁹ O. Biebel,¹¹³ D. Biedermann,¹⁹ R. Bielski,³⁶ K. Bierwagen,⁹⁹ N. V. Biesuz,^{71a,71b} M. Biglietti,^{74a} T. R. V. Billoud,¹⁰⁹ M. Bindi,⁵³ A. Bingul,^{12d} C. Bini,^{72a,72b} S. Biondi,^{23b,23a} M. Birman,¹⁸⁰ T. Bisanz,⁵³ J. P. Biswal,¹⁶¹ D. Biswas,^{181,f} A. Bitadze,¹⁰⁰ C. Bittrich,⁴⁸ K. Björke,¹³⁴ K. M. Black,²⁵ T. Blazek,^{28a} I. Bloch,⁴⁶ C. Blocker,²⁶ A. Blue,⁵⁷ U. Blumenschein,⁹² G. J. Bobbink,¹¹⁹ V. S. Bobrovnikov,^{121b,121a} S. S. Bocchetta,⁹⁶ A. Bocci,⁴⁹ D. Boerner,⁴⁶ D. Bogavac,¹⁴ A. G. Bogdanchikov,^{121b,121a} C. Bohm,^{45a} V. Boisvert,⁹³ P. Boka,^{53,172} T. Bold,^{83a} A. S. Boldyrev,¹¹² A. E. Bolz,^{61b} M. Bomben,¹³⁶ M. Bona,⁹² J. S. Bonilla,¹³¹ M. Boonekamp,¹⁴⁵ H. M. Borecka-Bielska,⁹⁰ A. Borisov,¹²² G. Borissov,⁸⁹ J. Bortfeldt,³⁶ D. Bortoletto,¹³⁵ D. Boscherini,^{23b} M. Bosman,¹⁴ J. D. Bossio Sola,¹⁰³ K. Bouaouda,^{35a} J. Boudreau,¹³⁹ E. V. Bouhova-Thacker,⁸⁹ D. Boumediene,³⁸ S. K. Boutle,⁵⁷ A. Boveia,¹²⁶ J. Boyd,³⁶ D. Boyle,^{33b,j} I. R. Boyko,⁷⁹ A. J. Bozson,⁹³ J. Bracinik,²¹ N. Brahimi,¹⁰¹ G. Brandt,¹⁸² O. Brandt,³² F. Braren,⁴⁶ B. Brau,¹⁰² J. E. Brau,¹³¹ W. D. Breaden Madden,⁵⁷ K. Brendlinger,⁴⁶ L. Brenner,⁴⁶ R. Brenner,¹⁷² S. Bressler,¹⁸⁰ B. Brickwedde,⁹⁹ D. L. Briglin,²¹ D. Britton,⁵⁷ D. Britzger,¹¹⁴ I. Brock,²⁴ R. Brock,¹⁰⁶ G. Brooijmans,³⁹ W. K. Brooks,^{147c} E. Brost,¹²⁰ J. H. Broughton,²¹ P. A. Bruckman de Renstrom,⁸⁴ D. Bruncko,^{28b} A. Bruni,^{23b} G. Bruni,^{23b} L. S. Bruni,¹¹⁹ S. Bruno,^{73a,73b} B. H. Brunt,³² M. Bruschi,^{23b} N. Bruscino,¹³⁹ P. Bryant,³⁷ L. Bryngemark,⁹⁶ T. Buanes,¹⁷ Q. Buat,³⁶ P. Buchholz,¹⁵¹ A. G. Buckley,⁵⁷ I. A. Budagov,⁷⁹ M. K. Bugge,¹³⁴ F. Bühner,⁵² O. Bulekov,¹¹¹ T. J. Burch,¹²⁰ S. Burdin,⁹⁰ C. D. Burgard,¹¹⁹ A. M. Burger,¹²⁹ B. Burghgrave,⁸ J. T. P. Burr,⁴⁶ C. D. Burton,¹¹ J. C. Burzynski,¹⁰² V. Büscher,⁹⁹ E. Buschmann,⁵³ P. J. Bussey,⁵⁷ J. M. Butler,²⁵ C. M. Buttar,⁵⁷ J. M. Butterworth,⁹⁴ P. Butti,³⁶ W. Buttinger,³⁶ A. Buzatu,¹⁵⁸ A. R. Buzykaev,^{121b,121a} G. Cabras,^{23b,23a} S. Cabrera Urbán,¹⁷⁴ D. Caforio,⁵⁶ H. Cai,¹⁷³ V. M. M. Cairo,¹⁵³ O. Cakir,^{4a} N. Calace,³⁶ P. Calafiura,¹⁸ A. Calandri,¹⁰¹ G. Calderini,¹³⁶ P. Calfayan,⁶⁵ G. Callea,⁵⁷ L. P. Caloba,^{80b} S. Calvente Lopez,⁹⁸ D. Calvet,³⁸ S. Calvet,³⁸ T. P. Calvet,¹⁵⁵ M. Calvetti,^{71a,71b} R. Camacho Toro,¹³⁶ S. Camarda,³⁶ D. Camarero Munoz,⁹⁸ P. Camarri,^{73a,73b} D. Cameron,¹³⁴ R. Caminal Armadans,¹⁰² C. Camincher,³⁶ S. Campana,³⁶ M. Campanelli,⁹⁴ A. Camplani,⁴⁰ A. Campoverde,¹⁵¹ V. Canale,^{69a,69b} A. Canesse,¹⁰³ M. Cano Bret,^{60c} J. Cantero,¹²⁹ T. Cao,¹⁶¹ Y. Cao,¹⁷³ M. D. M. Capeans Garrido,³⁶ M. Capua,^{41b,41a} R. Cardarelli,^{73a} F. Cardillo,¹⁴⁹ G. Carducci,^{41b,41a} I. Carli,¹⁴³ T. Carli,³⁶ G. Carlino,^{69a} B. T. Carlson,¹³⁹ L. Carminati,^{68a,68b} R. M. D. Carney,^{45a,45b} S. Caron,¹¹⁸ E. Carquin,^{147c} S. Carrá,⁴⁶ J. W. S. Carter,¹⁶⁷ M. P. Casado,^{14,k} A. F. Casha,¹⁶⁷ D. W. Casper,¹⁷¹ R. Castelijns,¹¹⁹ F. L. Castillo,¹⁷⁴ V. Castillo Gimenez,¹⁷⁴ N. F. Castro,^{140a,140e} A. Catinaccio,³⁶ J. R. Catmore,¹³⁴ A. Cattai,³⁶ J. Caudron,²⁴ V. Cavaliere,²⁹ E. Cavallaro,¹⁴

L. Fiorini,¹⁷⁴ F. Fischer,¹¹³ W. C. Fisher,¹⁰⁶ I. Fleck,¹⁵¹ P. Fleischmann,¹⁰⁵ R. R. M. Fletcher,¹³⁷ T. Flick,¹⁸² B. M. Flierl,¹¹³ L. Flores,¹³⁷ L. R. Flores Castillo,^{63a} F. M. Follega,^{75a,75b} N. Fomin,¹⁷ J. H. Foo,¹⁶⁷ G. T. Forcolin,^{75a,75b} A. Formica,¹⁴⁵ F. A. Förster,¹⁴ A. C. Forti,¹⁰⁰ A. G. Foster,²¹ M. G. Foti,¹³⁵ D. Fournier,¹³² H. Fox,⁸⁹ P. Francavilla,^{71a,71b} S. Francescato,^{72a,72b} M. Franchini,^{23b,23a} S. Franchino,^{61a} D. Francis,³⁶ L. Franconi,²⁰ M. Franklin,⁵⁹ A. N. Fray,⁹² P. M. Freeman,²¹ B. Freund,¹⁰⁹ W. S. Freund,^{80b} E. M. Freundlich,⁴⁷ D. C. Frizzell,¹²⁸ D. Froidevaux,³⁶ J. A. Frost,¹³⁵ C. Fukunaga,¹⁶⁴ E. Fullana Torregrosa,¹⁷⁴ E. Fumagalli,^{55b,55a} T. Fusayasu,¹¹⁵ J. Fuster,¹⁷⁴ A. Gabrielli,^{23b,23a} A. Gabrielli,¹⁸ G. P. Gach,^{83a} S. Gadatsch,⁵⁴ P. Gadow,¹¹⁴ G. Gagliardi,^{55b,55a} L. G. Gagnon,¹⁰⁹ C. Galea,^{27b} B. Galhardo,^{140a} G. E. Gallardo,¹³⁵ E. J. Gallas,¹³⁵ B. J. Gallop,¹⁴⁴ G. Galster,⁴⁰ R. Gamboa Goni,⁹² K. K. Gan,¹²⁶ S. Ganguly,¹⁸⁰ J. Gao,^{60a} Y. Gao,⁵⁰ Y. S. Gao,^{31,h} C. García,¹⁷⁴ J. E. García Navarro,¹⁷⁴ J. A. García Pascual,^{15a} C. Garcia-Argos,⁵² M. Garcia-Sciveres,¹⁸ R. W. Gardner,³⁷ N. Garelli,¹⁵³ S. Gargiulo,⁵² V. Garonne,¹³⁴ A. Gaudiello,^{55b,55a} G. Gaudio,^{70a} I. L. Gavrilenko,¹¹⁰ A. Gavriluk,¹²³ C. Gay,¹⁷⁵ G. Gaycken,⁴⁶ E. N. Gazis,¹⁰ A. A. Geanta,^{27b} C. M. Gee,¹⁴⁶ C. N. P. Gee,¹⁴⁴ J. Geisen,⁵³ M. Geisen,⁹⁹ M. P. Geisler,^{61a} C. Gemme,^{55b} M. H. Genest,⁵⁸ C. Geng,¹⁰⁵ S. Gentile,^{72a,72b} S. George,⁹³ T. Geralis,⁴⁴ L. O. Gerlach,⁵³ P. Gessinger-Befurt,⁹⁹ G. Gessner,⁴⁷ S. Ghasemi,¹⁵¹ M. Ghasemi Bostanabad,¹⁷⁶ A. Ghosh,¹³² A. Ghosh,⁷⁷ B. Giacobbe,^{23b} S. Giagu,^{72a,72b} N. Giangiacomi,^{23b,23a} P. Giannetti,^{71a} A. Giannini,^{69a,69b} G. Giannini,¹⁴ S. M. Gibson,⁹³ M. Gignac,¹⁴⁶ D. Gillberg,³⁴ G. Gilles,¹⁸² D. M. Gingrich,^{3,e} M. P. Giordani,^{66a,66c} F. M. Giorgi,^{23b} P. F. Giraud,¹⁴⁵ G. Giudliarelli,^{66a,66c} D. Giugni,^{68a} F. Giuli,^{73a,73b} S. Gkaitatzis,¹⁶² I. Gkialas,^{9,v} E. L. Gkoukousis,¹⁴ P. Gkoutoumis,¹⁰ L. K. Gladilin,¹¹² C. Glasman,⁹⁸ J. Glatzer,¹⁴ P. C. F. Glaysheer,⁴⁶ A. Glazov,⁴⁶ G. R. Gledhill,¹³¹ M. Goblirsch-Kolb,²⁶ D. Godin,¹⁰⁹ S. Goldfarb,¹⁰⁴ T. Golling,⁵⁴ D. Golubkov,¹²² A. Gomes,^{140a,140b} R. Goncalves Gama,⁵³ R. Gonçalves,^{140a,140b} G. Gonella,⁵² L. Gonella,²¹ A. Gongadze,⁷⁹ F. Gonnella,²¹ J. L. Gonski,⁵⁹ S. González de la Hoz,¹⁷⁴ S. Gonzalez-Sevilla,⁵⁴ G. R. Gonzalvo Rodriguez,¹⁷⁴ L. Goossens,³⁶ P. A. Gorbounov,¹²³ H. A. Gordon,²⁹ B. Gorini,³⁶ E. Gorini,^{67a,67b} A. Gorišek,⁹¹ A. T. Goshaw,⁴⁹ M. I. Gostkin,⁷⁹ C. A. Gottardo,¹¹⁸ M. Goughri,^{35b} D. Goudami,^{35c} A. G. Goussiou,¹⁴⁸ N. Govender,^{33b} C. Goy,⁵ E. Gozani,¹⁶⁰ I. Grabowska-Bold,^{83a} E. C. Graham,⁹⁰ J. Gramling,¹⁷¹ E. Gramstad,¹³⁴ S. Grancagnolo,¹⁹ M. Grandi,¹⁵⁶ V. Gratchev,¹³⁸ P. M. Gravila,^{27f} F. G. Gravili,^{67a,67b} C. Gray,⁵⁷ H. M. Gray,¹⁸ C. Grefe,²⁴ K. Gregersen,⁹⁶ I. M. Gregor,⁴⁶ P. Grenier,¹⁵³ K. Grevtsov,⁴⁶ C. Grieco,¹⁴ N. A. Grieser,¹²⁸ J. Griffiths,⁸ A. A. Grillo,¹⁴⁶ K. Grimm,^{31,w} S. Grinstein,^{14,x} J.-F. Grivaz,¹³² S. Groh,⁹⁹ E. Gross,¹⁸⁰ J. Grosse-Knetter,⁵³ Z. J. Grout,⁹⁴ C. Grud,¹⁰⁵ A. Grummer,¹¹⁷ L. Guan,¹⁰⁵ W. Guan,¹⁸¹ J. Guenther,³⁶ A. Guerguichon,¹³² J. G. R. Guerrero Rojas,¹⁷⁴ F. Guescini,¹¹⁴ D. Guest,¹⁷¹ R. Gugel,⁹⁹ T. Guillemin,⁵ S. Guindon,³⁶ U. Gul,⁵⁷ J. Guo,^{60c} W. Guo,¹⁰⁵ Y. Guo,^{60a,y} Z. Guo,¹⁰¹ R. Gupta,⁴⁶ S. Gurbuz,^{12c} G. Gustavino,¹²⁸ M. Guth,⁵² P. Gutierrez,¹²⁸ C. Gutsche,⁹⁴ C. Guyot,¹⁴⁵ C. Gwenlan,¹³⁵ C. B. Gwilliam,⁹⁰ A. Haas,¹²⁴ C. Haber,¹⁸ H. K. Hadavand,⁸ N. Haddad,^{35e} A. Hadeef,^{60a} S. Hageböck,³⁶ M. Haleem,¹⁷⁷ J. Haley,¹²⁹ G. Halladjian,¹⁰⁶ G. D. Hallowell,¹⁰¹ K. Hamacher,¹⁸² P. Hamal,¹³⁰ K. Hamano,¹⁷⁶ H. Hamdaoui,^{35e} G. N. Hamity,¹⁴⁹ K. Han,^{60a,z} L. Han,^{60a} S. Han,^{15a} Y. F. Han,¹⁶⁷ K. Hanagaki,^{81,aa} M. Hance,¹⁴⁶ D. M. Handl,¹¹³ B. Haney,¹³⁷ R. Hankache,¹³⁶ E. Hansen,⁹⁶ J. B. Hansen,⁴⁰ J. D. Hansen,⁴⁰ M. C. Hansen,²⁴ P. H. Hansen,⁴⁰ E. C. Hanson,¹⁰⁰ K. Hara,¹⁶⁹ T. Harenberg,¹⁸² S. Harkusha,¹⁰⁷ P. F. Harrison,¹⁷⁸ N. M. Hartmann,¹¹³ Y. Hasegawa,¹⁵⁰ A. Hasib,⁵⁰ S. Hassani,¹⁴⁵ S. Haug,²⁰ R. Hauser,¹⁰⁶ L. B. Havener,³⁹ M. Havranek,¹⁴² C. M. Hawkes,²¹ R. J. Hawkings,³⁶ D. Hayden,¹⁰⁶ C. Hayes,¹⁵⁵ R. L. Hayes,¹⁷⁵ C. P. Hays,¹³⁵ J. M. Hays,⁹² H. S. Hayward,⁹⁰ S. J. Haywood,¹⁴⁴ F. He,^{60a} M. P. Heath,⁵⁰ V. Hedberg,⁹⁶ L. Heelan,⁸ S. Heer,²⁴ K. K. Heidegger,⁵² W. D. Heidorn,⁷⁸ J. Heilman,³⁴ S. Heim,⁴⁶ T. Heim,¹⁸ B. Heinemann,^{46,bb} J. J. Heinrich,¹³¹ L. Heinrich,³⁶ C. Heinz,⁵⁶ J. Hejbal,¹⁴¹ L. Helary,^{61b} A. Held,¹⁷⁵ S. Hellesund,¹³⁴ C. M. Helling,¹⁴⁶ S. Hellman,^{45a,45b} C. Helsens,³⁶ R. C. W. Henderson,⁸⁹ Y. Heng,¹⁸¹ S. Henkelmann,¹⁷⁵ A. M. Henriques Correia,³⁶ G. H. Herbert,¹⁹ H. Herde,²⁶ V. Herget,¹⁷⁷ Y. Hernández Jiménez,^{33d} H. Herr,⁹⁹ M. G. Herrmann,¹¹³ T. Herrmann,⁴⁸ G. Herten,⁵² R. Hertenberger,¹¹³ L. Hervas,³⁶ T. C. Herwig,¹³⁷ G. G. Hesketh,⁹⁴ N. P. Hessey,^{168a} A. Higashida,¹⁶³ S. Higashino,⁸¹ E. Higón-Rodríguez,¹⁷⁴ K. Hildebrand,³⁷ E. Hill,¹⁷⁶ J. C. Hill,³² K. K. Hill,²⁹ K. H. Hiller,⁴⁶ S. J. Hillier,²¹ M. Hils,⁴⁸ I. Hinchliffe,¹⁸ F. Hinterkeuser,²⁴ M. Hirose,¹³³ S. Hirose,⁵² D. Hirschbuehl,¹⁸² B. Hiti,⁹¹ O. Hladik,¹⁴¹ D. R. Hlaluku,^{33d} X. Hoad,⁵⁰ J. Hobbs,¹⁵⁵ N. Hod,¹⁸⁰ M. C. Hodgkinson,¹⁴⁹ A. Hoecker,³⁶ F. Hoenig,¹¹³ D. Hohn,⁵² D. Hohov,¹³² T. R. Holmes,³⁷ M. Holzbock,¹¹³ L. B. A. H. Hommels,³² S. Honda,¹⁶⁹ T. M. Hong,¹³⁹ A. Hönle,¹¹⁴ B. H. Hooberman,¹⁷³ W. H. Hopkins,⁶ Y. Horii,¹¹⁶ P. Horn,⁴⁸ L. A. Horyn,³⁷ S. Hou,¹⁵⁸ A. Hoummada,^{35a} J. Howarth,¹⁰⁰ J. Hoya,⁸⁸ M. Hrabovsky,¹³⁰ J. Hrdinka,⁷⁶ I. Hristova,¹⁹ J. Hrivnac,¹³² A. Hrynevich,¹⁰⁸ T. Hryn'ova,⁵ P. J. Hsu,⁶⁴ S.-C. Hsu,¹⁴⁸ Q. Hu,²⁹ S. Hu,^{60c} D. P. Huang,⁹⁴ Y. Huang,^{60a} Y. Huang,^{15a} Z. Hubacek,¹⁴² F. Hubaut,¹⁰¹ M. Huebner,²⁴ F. Huegging,²⁴ T. B. Huffman,¹³⁵ M. Huhtinen,³⁶ R. F. H. Hunter,³⁴ P. Huo,¹⁵⁵ A. M. Hupe,³⁴ N. Huseynov,^{79,cc} J. Huston,¹⁰⁶ J. Huth,⁵⁹ R. Hyneman,¹⁰⁵ S. Hyrych,^{28a} G. Iacobucci,⁵⁴ G. Iakovidis,²⁹ I. Ibragimov,¹⁵¹

- L. Iconomidou-Fayard,¹³² Z. Idrissi,^{35e} P. Iengo,³⁶ R. Ignazzi,⁴⁰ O. Igonkina,^{119,a,dd} R. Iguchi,¹⁶³ T. Iizawa,⁵⁴ Y. Ikegami,⁸¹ M. Ikeno,⁸¹ D. Iliadis,¹⁶² N. Ilic,^{118,167,q} F. Iltzsche,⁴⁸ G. Introzzi,^{70a,70b} M. Iodice,^{74a} K. Iordanidou,^{168a} V. Ippolito,^{72a,72b} M. F. Isacson,¹⁷² M. Ishino,¹⁶³ W. Islam,¹²⁹ C. Issever,¹³⁵ S. Istina,¹⁶⁰ F. Ito,¹⁶⁹ J. M. Iturbe Ponce,^{63a} R. Iuppa,^{75a,75b} A. Ivina,¹⁸⁰ H. Iwasaki,⁸¹ J. M. Izen,⁴³ V. Izzo,^{69a} P. Jacka,¹⁴¹ P. Jackson,¹ R. M. Jacobs,²⁴ B. P. Jaeger,¹⁵² V. Jain,² G. Jäkel,¹⁸² K. B. Jakobi,⁹⁹ K. Jakobs,⁵² S. Jakobsen,⁷⁶ T. Jakoubek,¹⁴¹ J. Jamieson,⁵⁷ K. W. Janas,^{83a} R. Jansky,⁵⁴ J. Janssen,²⁴ M. Janus,⁵³ P. A. Janus,^{83a} G. Jarlskog,⁹⁶ N. Javadov,^{79,cc} T. Javůrek,³⁶ M. Javurkova,⁵² F. Jeanneau,¹⁴⁵ L. Jeanty,¹³¹ J. Jejelava,^{159a,ee} A. Jelinskas,¹⁷⁸ P. Jenni,^{52,ff} J. Jeong,⁴⁶ N. Jeong,⁴⁶ S. Jézéquel,⁵ H. Ji,¹⁸¹ J. Jia,¹⁵⁵ H. Jiang,⁷⁸ Y. Jiang,^{60a} Z. Jiang,^{153,gg} S. Jiggins,⁵² F. A. Jimenez Morales,³⁸ J. Jimenez Pena,¹¹⁴ S. Jin,^{15c} A. Jinaru,^{27b} O. Jinnouchi,¹⁶⁵ H. Jivan,^{33d} P. Johansson,¹⁴⁹ K. A. Johns,⁷ C. A. Johnson,⁶⁵ K. Jon-And,^{45a,45b} R. W. L. Jones,⁸⁹ S. D. Jones,¹⁵⁶ S. Jones,⁷ T. J. Jones,⁹⁰ J. Jongmanns,^{61a} P. M. Jorge,^{140a} J. Jovicevic,³⁶ X. Ju,¹⁸ J. J. Junggeburth,¹¹⁴ A. Juste Rozas,^{14,x} A. Kaczmarek,⁸⁴ M. Kado,^{72a,72b} H. Kagan,¹²⁶ M. Kagan,¹⁵³ C. Kahra,⁹⁹ T. Kaji,¹⁷⁹ E. Kajomovitz,¹⁶⁰ C. W. Kalderon,⁹⁶ A. Kaluza,⁹⁹ A. Kamenshchikov,¹²² M. Kaneda,¹⁶³ L. Kanjir,⁹¹ Y. Kano,¹⁶³ V. A. Kantserov,¹¹¹ J. Kanzaki,⁸¹ L. S. Kaplan,¹⁸¹ D. Kar,^{33d} K. Karava,¹³⁵ M. J. Kareem,^{168b} S. N. Karpov,⁷⁹ Z. M. Karpova,⁷⁹ V. Kartvelishvili,⁸⁹ A. N. Karyukhin,¹²² L. Kashif,¹⁸¹ R. D. Kass,¹²⁶ A. Kastanas,^{45a,45b} C. Kato,^{60d,60c} J. Katzy,⁴⁶ K. Kawade,¹⁵⁰ K. Kawagoe,⁸⁷ T. Kawaguchi,¹¹⁶ T. Kawamoto,¹⁶³ G. Kawamura,⁵³ E. F. Kay,¹⁷⁶ V. F. Kazanin,^{121b,121a} R. Keeler,¹⁷⁶ R. Kehoe,⁴² J. S. Keller,³⁴ E. Kellermann,⁹⁶ D. Kelsey,¹⁵⁶ J. J. Kempster,²¹ J. Kendrick,²¹ O. Kepka,¹⁴¹ S. Kersten,¹⁸² B. P. Kerševan,⁹¹ S. Ketabchi Haghighat,¹⁶⁷ M. Khader,¹⁷³ F. Khalil-Zada,¹³ M. Khandoga,¹⁴⁵ A. Khanov,¹²⁹ A. G. Kharlamov,^{121b,121a} T. Kharlamova,^{121b,121a} E. E. Khoda,¹⁷⁵ A. Khodinov,¹⁶⁶ T. J. Khoo,⁵⁴ E. Khramov,⁷⁹ J. Khubua,^{159b} S. Kido,⁸² M. Kiehn,⁵⁴ C. R. Kilby,⁹³ Y. K. Kim,³⁷ N. Kimura,⁹⁴ O. M. Kind,¹⁹ B. T. King,^{90,a} D. Kirchmeier,⁴⁸ J. Kirk,¹⁴⁴ A. E. Kiryunin,¹¹⁴ T. Kishimoto,¹⁶³ D. P. Kisliuk,¹⁶⁷ V. Kitali,⁴⁶ O. Kivernyk,⁵ T. Klapdor-Kleingrothaus,⁵² M. Klassen,^{61a} M. H. Klein,¹⁰⁵ M. Klein,⁹⁰ U. Klein,⁹⁰ K. Kleinknecht,⁹⁹ P. Klimek,¹²⁰ A. Klimentov,²⁹ T. Klingl,²⁴ T. Klioutchnikova,³⁶ F. F. Klitzner,¹¹³ P. Kluit,¹¹⁹ S. Kluth,¹¹⁴ E. Kneringer,⁷⁶ E. B. F. G. Knoops,¹⁰¹ A. Knue,⁵² D. Kobayashi,⁸⁷ T. Kobayashi,¹⁶³ M. Kobel,⁴⁸ M. Kocian,¹⁵³ P. Kodys,¹⁴³ P. T. Koenig,²⁴ T. Koffas,³⁴ N. M. Köhler,³⁶ T. Koi,¹⁵³ M. Kolb,^{61b} I. Koletsou,⁵ T. Komarek,¹³⁰ T. Kondo,⁸¹ N. Kondrashova,^{60c} K. Köneke,⁵² A. C. König,¹¹⁸ T. Kono,¹²⁵ R. Konoplich,^{124,hh} V. Konstantinides,⁹⁴ N. Konstantinidis,⁹⁴ B. Konya,⁹⁶ R. Kopeliansky,⁶⁵ S. Koperny,^{83a} K. Korcyl,⁸⁴ K. Kordas,¹⁶² G. Koren,¹⁶¹ A. Korn,⁹⁴ I. Korolkov,¹⁴ E. V. Korolkova,¹⁴⁹ N. Korotkova,¹¹² O. Kortner,¹¹⁴ S. Kortner,¹¹⁴ T. Kosek,¹⁴³ V. V. Kostyukhin,^{166,166} A. Kotwal,⁴⁹ A. Koulouris,¹⁰ A. Kourkoulis-Charalampidi,^{70a,70b} C. Kourkoulis,⁹ E. Kourlitis,¹⁴⁹ V. Kouskoura,²⁹ A. B. Kowalewska,⁸⁴ R. Kowalewski,¹⁷⁶ C. Kozakai,¹⁶³ W. Kozanecki,¹⁴⁵ A. S. Kozhin,¹²² V. A. Kramarenko,¹¹² G. Kramberger,⁹¹ D. Krasnopevtsev,^{60a} M. W. Krasny,¹³⁶ A. Krasznahorkay,³⁶ D. Krauss,¹¹⁴ J. A. Kremer,^{83a} J. Kretschmar,⁹⁰ P. Krieger,¹⁶⁷ F. Krieter,¹¹³ A. Krishnan,^{61b} K. Krizka,¹⁸ K. Kroeninger,⁴⁷ H. Kroha,¹¹⁴ J. Kroll,¹⁴¹ J. Kroll,¹³⁷ J. Krstic,¹⁶ U. Kruchonak,⁷⁹ H. Krüger,²⁴ N. Krumnack,⁷⁸ M. C. Kruse,⁴⁹ J. A. Krzysiak,⁸⁴ T. Kubota,¹⁰⁴ O. Kuchinskaia,¹⁶⁶ S. Kuday,^{4b} J. T. Kuechler,⁴⁶ S. Kuehn,³⁶ A. Kugel,^{61a} T. Kuhl,⁴⁶ V. Kukhtin,⁷⁹ R. Kukla,¹⁰¹ Y. Kulchitsky,^{107,ii} S. Kuleshov,^{147c} Y. P. Kulinich,¹⁷³ M. Kuna,⁵⁸ T. Kunigo,⁸⁵ A. Kupco,¹⁴¹ T. Kupfer,⁴⁷ O. Kuprash,⁵² H. Kurashige,⁸² L. L. Kurchaninov,^{168a} Y. A. Kurochkin,¹⁰⁷ A. Kurova,¹¹¹ M. G. Kurth,^{15a,15d} E. S. Kuwertz,³⁶ M. Kuze,¹⁶⁵ A. K. Kvam,¹⁴⁸ J. Kvita,¹³⁰ T. Kwan,¹⁰³ A. La Rosa,¹¹⁴ L. La Rotonda,^{41b,41a} F. La Ruffa,^{41b,41a} C. Lacasta,¹⁷⁴ F. Lacava,^{72a,72b} D. P. J. Lack,¹⁰⁰ H. Lacker,¹⁹ D. Lacour,¹³⁶ E. Ladygin,⁷⁹ R. Lafaye,⁵ B. Laforge,¹³⁶ T. Lagouri,^{33d} S. Lai,⁵³ S. Lammers,⁶⁵ W. Lampl,⁷ C. Lampoudis,¹⁶² E. Lançon,²⁹ U. Landgraf,⁵² M. P. J. Landon,⁹² M. C. Lanfermann,⁵⁴ V. S. Lang,⁴⁶ J. C. Lange,⁵³ R. J. Langenberg,³⁶ A. J. Lankford,¹⁷¹ F. Lanni,²⁹ K. Lantzsche,²⁴ A. Lanza,^{70a} A. Lapertosa,^{55b,55a} S. Laplace,¹³⁶ J. F. Laporte,¹⁴⁵ T. Lari,^{68a} F. Lasagni Manghi,^{23b,23a} M. Lassnig,³⁶ T. S. Lau,^{63a} A. Laudrain,¹³² A. Laurier,³⁴ M. Lavorgna,^{69a,69b} S. D. Lawlor,⁹³ M. Lazzaroni,^{68a,68b} B. Le,¹⁰⁴ E. Le Guirriec,¹⁰¹ M. LeBlanc,⁷ T. LeCompte,⁶ F. Ledroit-Guillon,⁵⁸ A. C. A. Lee,⁹⁴ C. A. Lee,²⁹ G. R. Lee,¹⁷ L. Lee,⁵⁹ S. C. Lee,¹⁵⁸ S. J. Lee,³⁴ B. Lefebvre,^{168a} M. Lefebvre,¹⁷⁶ F. Legger,¹¹³ C. Leggett,¹⁸ K. Lehmann,¹⁵² N. Lehmann,¹⁸² G. Lehmann Miotto,³⁶ W. A. Leight,⁴⁶ A. Leisos,^{162,ji} M. A. L. Leite,^{80d} C. E. Leitgeb,¹¹³ R. Leitner,¹⁴³ D. Lellouch,^{180,a} K. J. C. Leney,⁴² T. Lenz,²⁴ B. Lenzi,³⁶ R. Leone,⁷ S. Leone,^{71a} C. Leonidopoulos,⁵⁰ A. Leopold,¹³⁶ G. Lerner,¹⁵⁶ C. Leroy,¹⁰⁹ R. Les,¹⁶⁷ C. G. Lester,³² M. Levchenko,¹³⁸ J. Levêque,⁵ D. Levin,¹⁰⁵ L. J. Levinson,¹⁸⁰ D. J. Lewis,²¹ B. Li,^{15b} B. Li,¹⁰⁵ C.-Q. Li,^{60a} F. Li,^{60c} H. Li,^{60a} H. Li,^{60b} J. Li,^{60c} K. Li,¹⁵³ L. Li,^{60c} M. Li,^{15a,15d} Q. Li,^{15a,15d} Q. Y. Li,^{60a} S. Li,^{60d,60c} X. Li,⁴⁶ Y. Li,⁴⁶ Z. Li,^{60b} Z. Liang,^{15a} B. Liberti,^{73a} A. Liblong,¹⁶⁷ K. Lie,^{63c} C. Y. Lin,³² K. Lin,¹⁰⁶ T. H. Lin,⁹⁹ R. A. Linck,⁶⁵ J. H. Lindon,²¹ A. L. Lioni,⁵⁴ E. Lipeles,¹³⁷ A. Lipniacka,¹⁷ M. Lisovyi,^{61b} T. M. Liss,^{173,kk} A. Lister,¹⁷⁵ A. M. Litke,¹⁴⁶ J. D. Little,⁸ B. Liu,⁷⁸ B. L. Liu,⁶ H. B. Liu,²⁹ H. Liu,¹⁰⁵ J. B. Liu,^{60a} J. K. K. Liu,¹³⁵ K. Liu,¹³⁶ M. Liu,^{60a} P. Liu,¹⁸ Y. Liu,^{15a,15d} Y. L. Liu,¹⁰⁵ Y. W. Liu,^{60a}

M. Livan,^{70a,70b} A. Lleres,⁵⁸ J. Llorente Merino,¹⁵² S. L. Lloyd,⁹² C. Y. Lo,^{63b} F. Lo Sterzo,⁴² E. M. Lobodzinska,⁴⁶ P. Loch,⁷ S. Loffredo,^{73a,73b} T. Lohse,¹⁹ K. Lohwasser,¹⁴⁹ M. Lokajicek,¹⁴¹ J. D. Long,¹⁷³ R. E. Long,⁸⁹ L. Longo,³⁶ K. A. Looper,¹²⁶ J. A. Lopez,^{147c} I. Lopez Paz,¹⁰⁰ A. Lopez Solis,¹⁴⁹ J. Lorenz,¹¹³ N. Lorenzo Martinez,⁵ M. Losada,²² P. J. Lösel,¹¹³ A. Lösle,⁵² X. Lou,⁴⁶ X. Lou,^{15a} A. Lounis,¹³² J. Love,⁶ P. A. Love,⁸⁹ J. J. Lozano Bahilo,¹⁷⁴ M. Lu,^{60a} Y. J. Lu,⁶⁴ H. J. Lubatti,¹⁴⁸ C. Luci,^{72a,72b} A. Lucotte,⁵⁸ C. Luedtke,⁵² F. Luehring,⁶⁵ I. Luise,¹³⁶ L. Luminari,^{72a} B. Lund-Jensen,¹⁵⁴ M. S. Lutz,¹⁰² D. Lynn,²⁹ R. Lysak,¹⁴¹ E. Lytken,⁹⁶ F. Lyu,^{15a} V. Lyubushkin,⁷⁹ T. Lyubushkina,⁷⁹ H. Ma,²⁹ L. L. Ma,^{60b} Y. Ma,^{60b} G. Maccarrone,⁵¹ A. Macchiolo,¹¹⁴ C. M. Macdonald,¹⁴⁹ J. Machado Miguens,¹³⁷ D. Madaffari,¹⁷⁴ R. Madar,³⁸ W. F. Mader,⁴⁸ N. Madysa,⁴⁸ J. Maeda,⁸² S. Maeland,¹⁷ T. Maeno,²⁹ M. Maerker,⁴⁸ A. S. Maevskiy,¹¹² V. Magerl,⁵² N. Magini,⁷⁸ D. J. Mahon,³⁹ C. Maidantchik,^{80b} T. Maier,¹¹³ A. Maio,^{140a,140b,140d} K. Maj,^{83a} O. Majersky,^{28a} S. Majewski,¹³¹ Y. Makida,⁸¹ N. Makovec,¹³² B. Malaescu,¹³⁶ Pa. Malecki,⁸⁴ V. P. Maleev,¹³⁸ F. Malek,⁵⁸ U. Mallik,⁷⁷ D. Malon,⁶ C. Malone,³² S. Maltezos,¹⁰ S. Malyukov,⁷⁹ J. Mamuzic,¹⁷⁴ G. Mancini,⁵¹ I. Mandić,⁹¹ L. Manhaes de Andrade Filho,^{80a} I. M. Maniatis,¹⁶² J. Manjarres Ramos,⁴⁸ K. H. Mankinen,⁹⁶ A. Mann,¹¹³ A. Manousos,⁷⁶ B. Mansoulie,¹⁴⁵ I. Manthos,¹⁶² S. Manzoni,¹¹⁹ A. Marantis,¹⁶² G. Marceca,³⁰ L. Marchese,¹³⁵ G. Marchiori,¹³⁶ M. Marcisovsky,¹⁴¹ C. Marcon,⁹⁶ C. A. Marin Tobon,³⁶ M. Marjanovic,¹²⁸ Z. Marshall,¹⁸ M. U. F. Martensson,¹⁷² S. Marti-Garcia,¹⁷⁴ C. B. Martin,¹²⁶ T. A. Martin,¹⁷⁸ V. J. Martin,⁵⁰ B. Martin dit Latour,¹⁷ L. Martinelli,^{74a,74b} M. Martinez,^{14,x} V. I. Martinez Outschoorn,¹⁰² S. Martin-Haugh,¹⁴⁴ V. S. Martoiu,^{27b} A. C. Martyniuk,⁹⁴ A. Marzin,³⁶ S. R. Maschek,¹¹⁴ L. Masetti,⁹⁹ T. Mashimo,¹⁶³ R. Mashinistov,¹¹⁰ J. Masik,¹⁰⁰ A. L. Maslennikov,^{121b,121a} L. Massa,^{73a,73b} P. Massarotti,^{69a,69b} P. Mastrandrea,^{71a,71b} A. Mastroberardino,^{41b,41a} T. Masubuchi,¹⁶³ D. Matakias,¹⁰ A. Matic,¹¹³ P. Mättig,²⁴ J. Maurer,^{27b} B. Maček,⁹¹ D. A. Maximov,^{121b,121a} R. Mazini,¹⁵⁸ I. Maznas,¹⁶² S. M. Mazza,¹⁴⁶ S. P. Mc Kee,¹⁰⁵ T. G. McCarthy,¹¹⁴ W. P. McCormack,¹⁸ E. F. McDonald,¹⁰⁴ J. A. Mcfayden,³⁶ G. Mchedlidze,^{159b} M. A. McKay,⁴² K. D. McLean,¹⁷⁶ S. J. McMahon,¹⁴⁴ P. C. McNamara,¹⁰⁴ C. J. McNicol,¹⁷⁸ R. A. McPherson,^{176,q} J. E. Mdhululi,^{33d} Z. A. Meadows,¹⁰² S. Meehan,³⁶ T. Megy,⁵² S. Mehlhase,¹¹³ A. Mehta,⁹⁰ T. Meideck,⁵⁸ B. Meirose,⁴³ D. Melini,¹⁷⁴ B. R. Mellado Garcia,^{33d} J. D. Mellenthin,⁵³ M. Melo,^{28a} F. Meloni,⁴⁶ A. Melzer,²⁴ S. B. Menary,¹⁰⁰ E. D. Mendes Gouveia,^{140a,140e} L. Meng,³⁶ X. T. Meng,¹⁰⁵ S. Menke,¹¹⁴ E. Meoni,^{41b,41a} S. Mergelmeyer,¹⁹ S. A. M. Merkt,¹³⁹ C. Merlassino,²⁰ P. Mermod,⁵⁴ L. Merola,^{69a,69b} C. Meroni,^{68a} O. Meshkov,^{112,110} J. K. R. Meshreki,¹⁵¹ A. Messina,^{72a,72b} J. Metcalfe,⁶ A. S. Mete,¹⁷¹ C. Meyer,⁶⁵ J. Meyer,¹⁶⁰ J.-P. Meyer,¹⁴⁵ H. Meyer Zu Theenhausen,^{61a} F. Miano,¹⁵⁶ M. Michetti,¹⁹ R. P. Middleton,¹⁴⁴ L. Mijović,⁵⁰ G. Mikenberg,¹⁸⁰ M. Mikestikova,¹⁴¹ M. Mikuž,⁹¹ H. Mildner,¹⁴⁹ M. Milesi,¹⁰⁴ A. Milic,¹⁶⁷ D. A. Millar,⁹² D. W. Miller,³⁷ A. Milov,¹⁸⁰ D. A. Milstead,^{45a,45b} R. A. Mina,^{153,gg} A. A. Minaenko,¹²² M. Miñano Moya,¹⁷⁴ I. A. Minashvili,^{159b} A. I. Mincer,¹²⁴ B. Mindur,^{83a} M. Mineev,⁷⁹ Y. Minegishi,¹⁶³ L. M. Mir,¹⁴ A. Mirtó,^{67a,67b} K. P. Mistry,¹³⁷ T. Mitani,¹⁷⁹ J. Mitrevski,¹¹³ V. A. Mitsou,¹⁷⁴ M. Mittal,^{60c} O. Miu,¹⁶⁷ A. Miucci,²⁰ P. S. Miyagawa,¹⁴⁹ A. Mizukami,⁸¹ J. U. Mjörnmark,⁹⁶ T. Mkrtchyan,¹⁸⁴ M. Mlynarikova,¹⁴³ T. Moa,^{45a,45b} K. Mochizuki,¹⁰⁹ P. Mogg,⁵² S. Mohapatra,³⁹ R. Moles-Valls,²⁴ M. C. Mondragon,¹⁰⁶ K. Mönig,⁴⁶ J. Monk,⁴⁰ E. Monnier,¹⁰¹ A. Montalbano,¹⁵² J. Montejo Berlingen,³⁶ M. Montella,⁹⁴ F. Monticelli,⁸⁸ S. Monzani,^{68a} N. Morange,¹³² D. Moreno,²² M. Moreno Llácer,³⁶ C. Moreno Martinez,¹⁴ P. Morettini,^{55b} M. Morgenstern,¹¹⁹ S. Morgenstern,⁴⁸ D. Mori,¹⁵² M. Morii,⁵⁹ M. Morinaga,¹⁷⁹ V. Morisbak,¹³⁴ A. K. Morley,³⁶ G. Mornacchi,³⁶ A. P. Morris,⁹⁴ L. Morvaj,¹⁵⁵ P. Moschovakos,³⁶ B. Moser,¹¹⁹ M. Mosidze,^{159b} T. Moskalets,¹⁴⁵ H. J. Moss,¹⁴⁹ J. Moss,^{31,II} E. J. W. Moyse,¹⁰² S. Muanza,¹⁰¹ J. Mueller,¹³⁹ R. S. P. Mueller,¹¹³ D. Muenstermann,⁸⁹ G. A. Mullier,⁹⁶ J. L. Munoz Martinez,¹⁴ F. J. Munoz Sanchez,¹⁰⁰ P. Murin,^{28b} W. J. Murray,^{178,144} A. Murrone,^{68a,68b} M. Muškinja,¹⁸ C. Mwewa,^{33a} A. G. Myagkov,^{122,mm} J. Myers,¹³¹ M. Myska,¹⁴² B. P. Nachman,¹⁸ O. Nackenhorst,⁴⁷ A. Nag Nag,⁴⁸ K. Nagai,¹³⁵ K. Nagano,⁸¹ Y. Nagasaka,⁶² M. Nagel,⁵² J. L. Nagle,²⁹ E. Nagy,¹⁰¹ A. M. Nairz,³⁶ Y. Nakahama,¹¹⁶ K. Nakamura,⁸¹ T. Nakamura,¹⁶³ I. Nakano,¹²⁷ H. Nanjo,¹³³ F. Napolitano,^{61a} R. F. Naranjo Garcia,⁴⁶ R. Narayan,⁴² I. Naryshkin,¹³⁸ T. Naumann,⁴⁶ G. Navarro,²² H. A. Neal,^{105,a} P. Y. Nechaeva,¹¹⁰ F. Nechansky,⁴⁶ T. J. Neep,²¹ A. Negri,^{70a,70b} M. Negrini,^{23b} C. Nellist,⁵³ M. E. Nelson,¹³⁵ S. Nemecek,¹⁴¹ P. Nemethy,¹²⁴ M. Nessi,^{36,nn} M. S. Neubauer,¹⁷³ M. Neumann,¹⁸² P. R. Newman,²¹ Y. S. Ng,¹⁹ Y. W. Y. Ng,¹⁷¹ B. Ngair,^{35e} H. D. N. Nguyen,¹⁰¹ T. Nguyen Manh,¹⁰⁹ E. Nibigira,³⁸ R. B. Nickerson,¹³⁵ R. Nicolaidou,¹⁴⁵ D. S. Nielsen,⁴⁰ J. Nielsen,¹⁴⁶ N. Nikiporou,¹¹ V. Nikolaenko,^{122,mm} I. Nikolic-Audit,¹³⁶ K. Nikolopoulos,²¹ P. Nilsson,²⁹ H. R. Nindhito,⁵⁴ Y. Ninomiya,⁸¹ A. Nisati,^{72a} N. Nishu,^{60c} R. Nisius,¹¹⁴ I. Nitsche,⁴⁷ T. Nitta,¹⁷⁹ T. Nobe,¹⁶³ Y. Noguchi,⁸⁵ I. Nomidis,¹³⁶ M. A. Nomura,²⁹ M. Nordberg,³⁶ N. Norjoharuddeen,¹³⁵ T. Novak,⁹¹ O. Novgorodova,⁴⁸ R. Novotny,¹⁴² L. Nozka,¹³⁰ K. Ntekas,¹⁷¹ E. Nurse,⁹⁴ F. G. Oakham,^{34,e} H. Oberlack,¹¹⁴ J. Ocariz,¹³⁶ A. Ochi,⁸² I. Ochoa,³⁹ J. P. Ochoa-Ricoux,^{147a} K. O'Connor,²⁶ S. Oda,⁸⁷ S. Odaka,⁸¹ S. Oerdek,⁵³ A. Ogrodnik,^{83a} A. Oh,¹⁰⁰ S. H. Oh,⁴⁹ C. C. Ohm,¹⁵⁴ H. Oide,¹⁶⁵ M. L. Ojeda,¹⁶⁷

- H. Okawa,¹⁶⁹ Y. Okazaki,⁸⁵ Y. Okumura,¹⁶³ T. Okuyama,⁸¹ A. Olariu,^{27b} L. F. Oleiro Seabra,^{140a} S. A. Olivares Pino,^{147a} D. Oliveira Damazio,²⁹ J. L. Oliver,¹ M. J. R. Olsson,¹⁷¹ A. Olszewski,⁸⁴ J. Olszowska,⁸⁴ D. C. O'Neil,¹⁵² A. P. O'Neill,¹³⁵ A. Onofre,^{140a,140e} P. U. E. Onyisi,¹¹ H. Oppen,¹³⁴ M. J. Oreglia,³⁷ G. E. Orellana,⁸⁸ D. Orestano,^{74a,74b} N. Orlando,¹⁴ R. S. Orr,¹⁶⁷ V. O'Shea,⁵⁷ R. Ospanov,^{60a} G. Otero y Garzon,³⁰ H. Otono,⁸⁷ P. S. Ott,^{61a} M. Ouchrif,^{35d} J. Ouellette,²⁹ F. Ould-Saada,¹³⁴ A. Ouraou,¹⁴⁵ Q. Ouyang,^{15a} M. Owen,⁵⁷ R. E. Owen,²¹ V. E. Ozcan,^{12c} N. Ozturk,⁸ J. Pacalt,¹³⁰ H. A. Pacey,³² K. Pachal,⁴⁹ A. Pacheco Pages,¹⁴ C. Padilla Aranda,¹⁴ S. Pagan Griso,¹⁸ M. Paganini,¹⁸³ G. Palacino,⁶⁵ S. Palazzo,⁵⁰ S. Palestini,³⁶ M. Palka,^{83b} D. Pallin,³⁸ I. Panagoulas,¹⁰ C. E. Pandini,³⁶ J. G. Panduro Vazquez,⁹³ P. Pani,⁴⁶ G. Panizzo,^{66a,66c} L. Paolozzi,⁵⁴ C. Papadatos,¹⁰⁹ K. Papageorgiou,^{9,v} S. Parajuli,⁴³ A. Paramonov,⁶ D. Paredes Hernandez,^{63b} S. R. Paredes Saenz,¹³⁵ B. Parida,¹⁶⁶ T. H. Park,¹⁶⁷ A. J. Parker,³¹ M. A. Parker,³² F. Parodi,^{55b,55a} E. W. Parrish,¹²⁰ J. A. Parsons,³⁹ U. Parzefall,⁵² L. Pascual Dominguez,¹³⁶ V. R. Pascuzzi,¹⁶⁷ J. M. P. Pasner,¹⁴⁶ E. Pasqualucci,^{72a} S. Passaggio,^{55b} F. Pastore,⁹³ P. Pasuwan,^{45a,45b} S. Patariaia,⁹⁹ J. R. Pater,¹⁰⁰ A. Pathak,^{181,f} T. Pauly,³⁶ B. Pearson,¹¹⁴ M. Pedersen,¹³⁴ L. Pedraza Diaz,¹¹⁸ R. Pedro,^{140a} T. Peiffer,⁵³ S. V. Peleganchuk,^{121b,121a} O. Penc,¹⁴¹ H. Peng,^{60a} B. S. Peralva,^{80a} M. M. Perego,¹³² A. P. Pereira Peixoto,^{140a} D. V. Perepelitsa,²⁹ F. Peri,¹⁹ L. Perini,^{68a,68b} H. Pernegger,³⁶ S. Perrella,^{69a,69b} K. Peters,⁴⁶ R. F. Y. Peters,¹⁰⁰ B. A. Petersen,³⁶ T. C. Petersen,⁴⁰ E. Petit,¹⁰¹ A. Petridis,¹ C. Petridou,¹⁶² P. Petroff,¹³² M. Petrov,¹³⁵ F. Petrucci,^{74a,74b} M. Pettee,¹⁸³ N. E. Pettersson,¹⁰² K. Petukhova,¹⁴³ A. Peyaud,¹⁴⁵ R. Pezoa,^{147c} L. Pezzotti,^{70a,70b} T. Pham,¹⁰⁴ F. H. Phillips,¹⁰⁶ P. W. Phillips,¹⁴⁴ M. W. Phipps,¹⁷³ G. Piacquadio,¹⁵⁵ E. Pianori,¹⁸ A. Picazio,¹⁰² R. H. Pickles,¹⁰⁰ R. Piegaiia,³⁰ D. Pietreanu,^{27b} J. E. Pilcher,³⁷ A. D. Pilkington,¹⁰⁰ M. Pinamonti,^{73a,73b} J. L. Pinfold,³ M. Pitt,¹⁶¹ L. Pizzimento,^{73a,73b} M.-A. Pleier,²⁹ V. Pleskot,¹⁴³ E. Plotnikova,⁷⁹ P. Podberezko,^{121b,121a} R. Poettgen,⁹⁶ R. Poggi,⁵⁴ L. Poggioli,¹³² I. Pogrebnnyak,¹⁰⁶ D. Pohl,²⁴ I. Pokharel,⁵³ G. Polesello,^{70a} A. Poley,¹⁸ A. Policicchio,^{72a,72b} R. Polifka,¹⁴³ A. Polini,^{23b} C. S. Pollard,⁴⁶ V. Polychronakos,²⁹ D. Ponomarenko,¹¹¹ L. Pontecorvo,³⁶ S. Popa,^{27a} G. A. Popeneciu,^{27d} L. Portales,⁵ D. M. Portillo Quintero,⁵⁸ S. Pospisil,¹⁴² K. Potamianos,⁴⁶ I. N. Potrap,⁷⁹ C. J. Potter,³² H. Potti,¹¹ T. Poulsen,⁹⁶ J. Poveda,³⁶ T. D. Powell,¹⁴⁹ G. Pownall,⁴⁶ M. E. Pozo Astigarraga,³⁶ P. Pralavorio,¹⁰¹ S. Prell,⁷⁸ D. Price,¹⁰⁰ M. Primavera,^{67a} S. Prince,¹⁰³ M. L. Proffitt,¹⁴⁸ N. Proklova,¹¹¹ K. Prokofiev,^{63c} F. Prokoshin,⁷⁹ S. Protopopescu,²⁹ J. Proudfoot,⁶ M. Przybycien,^{83a} D. Pudzha,¹³⁸ A. Puri,¹⁷³ P. Puzo,¹³² J. Qian,¹⁰⁵ Y. Qin,¹⁰⁰ A. Quadt,⁵³ M. Queitsch-Maitland,⁴⁶ A. Qureshi,¹ M. Racko,^{28a} P. Rados,¹⁰⁴ F. Ragusa,^{68a,68b} G. Rahal,⁹⁷ J. A. Raine,⁵⁴ S. Rajagopalan,²⁹ A. Ramirez Morales,⁹² K. Ran,^{15a,15d} T. Rashid,¹³² S. Raspopov,⁵ D. M. Rauch,⁴⁶ F. Rauscher,¹¹³ S. Rave,⁹⁹ B. Ravina,¹⁴⁹ I. Ravinovich,¹⁸⁰ J. H. Rawling,¹⁰⁰ M. Raymond,³⁶ A. L. Read,¹³⁴ N. P. Readioff,⁵⁸ M. Reale,^{67a,67b} D. M. Rebuffi,^{70a,70b} A. Redelbach,¹⁷⁷ G. Redlinger,²⁹ K. Reeves,⁴³ L. Rehnisch,¹⁹ J. Reichert,¹³⁷ D. Reikher,¹⁶¹ A. Reiss,⁹⁹ A. Rej,¹⁵¹ C. Rembser,³⁶ M. Renda,^{27b} M. Rescigno,^{72a} S. Resconi,^{68a} E. D. Resseguie,¹³⁷ S. Rettie,¹⁷⁵ E. Reynolds,²¹ O. L. Rezanova,^{121b,121a} P. Reznicek,¹⁴³ E. Ricci,^{75a,75b} R. Richter,¹¹⁴ S. Richter,⁴⁶ E. Richter-Was,^{83b} O. Ricken,²⁴ M. Ridel,¹³⁶ P. Rieck,¹¹⁴ C. J. Riegel,¹⁸² O. Rifki,⁴⁶ M. Rijssenbeek,¹⁵⁵ A. Rimoldi,^{70a,70b} M. Rimoldi,⁴⁶ L. Rinaldi,^{23b} G. Ripellino,¹⁵⁴ I. Riu,¹⁴ J. C. Rivera Vergara,¹⁷⁶ F. Rizatdinova,¹²⁹ E. Rizvi,⁹² C. Rizzi,³⁶ R. T. Roberts,¹⁰⁰ S. H. Robertson,^{103,q} M. Robin,⁴⁶ D. Robinson,³² J. E. M. Robinson,⁴⁶ C. M. Robles Gajardo,^{147c} A. Robson,⁵⁷ A. Rocchi,^{73a,73b} E. Rocco,⁹⁹ C. Roda,^{71a,71b} S. Rodriguez Bosca,¹⁷⁴ A. Rodriguez Perez,¹⁴ D. Rodriguez Rodriguez,¹⁷⁴ A. M. Rodríguez Vera,^{168b} S. Roe,³⁶ O. Røhne,¹³⁴ R. Röhrig,¹¹⁴ C. P. A. Roland,⁶⁵ J. Roloff,⁵⁹ A. Romaniouk,¹¹¹ M. Romano,^{23b,23a} N. Rompotis,⁹⁰ M. Ronzani,¹²⁴ L. Roos,¹³⁶ S. Rosati,^{72a} K. Rosbach,⁵² G. Rosin,¹⁰² B. J. Rosser,¹³⁷ E. Rossi,⁴⁶ E. Rossi,^{74a,74b} E. Rossi,^{69a,69b} L. P. Rossi,^{55b} L. Rossini,^{68a,68b} R. Rosten,¹⁴ M. Rotaru,^{27b} J. Rothberg,¹⁴⁸ D. Rousseau,¹³² G. Rovelli,^{70a,70b} A. Roy,¹¹ D. Roy,^{33d} A. Rozanov,¹⁰¹ Y. Rozen,¹⁶⁰ X. Ruan,^{33d} F. Rubbo,¹⁵³ F. Rühr,⁵² A. Ruiz-Martinez,¹⁷⁴ A. Rummler,³⁶ Z. Rurikova,⁵² N. A. Rusakovich,⁷⁹ H. L. Russell,¹⁰³ L. Rustige,^{38,47} J. P. Rutherford,⁷ E. M. Rüttinger,¹⁴⁹ M. Rybar,³⁹ G. Rybkin,¹³² E. B. Rye,¹³⁴ A. Ryzhov,¹²² P. Sabatini,⁵³ G. Sabato,¹¹⁹ S. Sacerdoti,¹³² H. F-W. Sadrozinski,¹⁴⁶ R. Sadykov,⁷⁹ F. Safai Tehrani,^{72a} B. Safarzadeh Samani,¹⁵⁶ P. Saha,¹²⁰ S. Saha,¹⁰³ M. Sahinsoy,^{61a} A. Sahu,¹⁸² M. Saimpert,⁴⁶ M. Saito,¹⁶³ T. Saito,¹⁶³ H. Sakamoto,¹⁶³ A. Sakharov,^{124,hh} D. Salamani,⁵⁴ G. Salamanna,^{74a,74b} J. E. Salazar Loyola,^{147c} P. H. Sales De Bruin,¹⁷² A. Salnikov,¹⁵³ J. Salt,¹⁷⁴ D. Salvatore,^{41b,41a} F. Salvatore,¹⁵⁶ A. Salvucci,^{63a,63b,63c} A. Salzburger,³⁶ J. Samarati,³⁶ D. Sammel,⁵² D. Sampsonidis,¹⁶² D. Sampsonidou,¹⁶² J. Sánchez,¹⁷⁴ A. Sanchez Pineda,^{66a,66c} H. Sandaker,¹³⁴ C. O. Sander,⁴⁶ I. G. Sanderswood,⁸⁹ M. Sandhoff,¹⁸² C. Sandoval,²² D. P. C. Sankey,¹⁴⁴ M. Sannino,^{55b,55a} Y. Sano,¹¹⁶ A. Sansoni,⁵¹ C. Santoni,³⁸ H. Santos,^{140a,140b} S. N. Santpur,¹⁸ A. Santra,¹⁷⁴ A. Saponov,⁷⁹ J. G. Saraiva,^{140a,140d} O. Sasaki,⁸¹ K. Sato,¹⁶⁹ F. Sauerburger,⁵² E. Sauvan,⁵ P. Savard,^{167,e} N. Savic,¹¹⁴ R. Sawada,¹⁶³ C. Sawyer,¹⁴⁴ L. Sawyer,^{95,oo} C. Sbarra,^{23b} A. Sbrizzi,^{23a} T. Scanlon,⁹⁴ J. Schaarschmidt,¹⁴⁸ P. Schacht,¹¹⁴ B. M. Schachtner,¹¹³ D. Schaefer,³⁷ L. Schaefer,¹³⁷ J. Schaeffer,⁹⁹ S. Schaepe,³⁶

U. Schäfer,⁹⁹ A. C. Schaffer,¹³² D. Schaile,¹¹³ R. D. Schamberger,¹⁵⁵ N. Scharmberg,¹⁰⁰ V. A. Schegelsky,¹³⁸ D. Scheirich,¹⁴³ F. Schenck,¹⁹ M. Schernau,¹⁷¹ C. Schiavi,^{55b,55a} S. Schier,¹⁴⁶ L. K. Schildgen,²⁴ Z. M. Schillaci,²⁶ E. J. Schioppa,³⁶ M. Schioppa,^{41b,41a} K. E. Schleicher,⁵² S. Schlenker,³⁶ K. R. Schmidt-Sommerfeld,¹¹⁴ K. Schmieden,³⁶ C. Schmitt,⁹⁹ S. Schmitt,⁴⁶ S. Schmitz,⁹⁹ J. C. Schmoeckel,⁴⁶ U. Schnoor,⁵² L. Schoeffel,¹⁴⁵ A. Schoening,^{61b} P. G. Scholer,⁵² E. Schopf,¹³⁵ M. Schott,⁹⁹ J. F. P. Schouwenger,¹¹⁸ J. Schovancova,³⁶ S. Schramm,⁵⁴ F. Schroeder,¹⁸² A. Schulte,⁹⁹ H.-C. Schultz-Coulon,^{61a} M. Schumacher,⁵² B. A. Schumm,¹⁴⁶ Ph. Schune,¹⁴⁵ A. Schwartzman,¹⁵³ T. A. Schwarz,¹⁰⁵ Ph. Schwemling,¹⁴⁵ R. Schwienhorst,¹⁰⁶ A. Sciandra,¹⁴⁶ G. Sciolla,²⁶ M. Scodeggio,⁴⁶ M. Scornajenghi,^{41b,41a} F. Scuri,^{71a} F. Scutti,¹⁰⁴ L. M. Scyboz,¹¹⁴ C. D. Sebastiani,^{72a,72b} P. Seema,¹⁹ S. C. Seidel,¹¹⁷ A. Seiden,¹⁴⁶ B. D. Seidlitz,²⁹ T. Seiss,³⁷ J. M. Seixas,^{80b} G. Sekhniaidze,^{69a} K. Sekhon,¹⁰⁵ S. J. Sekula,⁴² N. Semprini-Cesari,^{23b,23a} S. Sen,⁴⁹ S. Senkin,³⁸ C. Serfon,⁷⁶ L. Serin,¹³² L. Serkin,^{66a,66b} M. Sessa,^{60a} H. Severini,¹²⁸ T. Šfiligoj,⁹¹ F. Sforza,^{55b,55a} A. Sfyrila,⁵⁴ E. Shabalina,⁵³ J. D. Shahinian,¹⁴⁶ N. W. Shaikh,^{45a,45b} D. Shaked Renous,¹⁸⁰ L. Y. Shan,^{15a} R. Shang,¹⁷³ J. T. Shank,²⁵ M. Shapiro,¹⁸ A. Sharma,¹³⁵ A. S. Sharma,¹ P. B. Shatalov,¹²³ K. Shaw,¹⁵⁶ S. M. Shaw,¹⁰⁰ A. Shcherbakova,¹³⁸ M. Shehade,¹⁸⁰ Y. Shen,¹²⁸ N. Sherafati,³⁴ A. D. Sherman,²⁵ P. Sherwood,⁹⁴ L. Shi,^{158,pp} S. Shimizu,⁸¹ C. O. Shimmin,¹⁸³ Y. Shimogama,¹⁷⁹ M. Shimojima,¹¹⁵ I. P. J. Shipsey,¹³⁵ S. Shirabe,⁸⁷ M. Shiyakova,^{79,qq} J. Shlomi,¹⁸⁰ A. Shmeleva,¹¹⁰ M. J. Shochet,³⁷ J. Shojaii,¹⁰⁴ D. R. Shope,¹²⁸ S. Shrestha,¹²⁶ E. M. Shrif,^{33d} E. Shulga,¹⁸⁰ P. Sicho,¹⁴¹ A. M. Sickles,¹⁷³ P. E. Sidebo,¹⁵⁴ E. Sideras Haddad,^{33d} O. Sidiropoulou,³⁶ A. Sidoti,^{23b,23a} F. Siegert,⁴⁸ Dj. Sijacki,¹⁶ M. Silva Jr.,¹⁸¹ M. V. Silva Oliveira,^{80a} S. B. Silverstein,^{45a} S. Simion,¹³² E. Simioni,⁹⁹ R. Simonello,⁹⁹ S. Simsek,^{12b} P. Sinervo,¹⁶⁷ V. Sinetckii,^{112,110} N. B. Sinev,¹³¹ M. Sioli,^{23b,23a} I. Siral,¹⁰⁵ S. Yu. Sivoklov,¹¹² J. Sjölin,^{45a,45b} E. Skorda,⁹⁶ P. Skubic,¹²⁸ M. Slawinska,⁸⁴ K. Sliwa,¹⁷⁰ R. Slovak,¹⁴³ V. Smakhtin,¹⁸⁰ B. H. Smart,¹⁴⁴ J. Smiesko,^{28a} N. Smirnov,¹¹¹ S. Yu. Smirnov,¹¹¹ Y. Smirnov,¹¹¹ L. N. Smirnova,^{112,rr} O. Smirnova,⁹⁶ J. W. Smith,⁵³ M. Smizanska,⁸⁹ K. Smolek,¹⁴² A. Smykiewicz,⁸⁴ A. A. Snesev,¹¹⁰ H. L. Snoek,¹¹⁹ I. M. Snyder,¹³¹ S. Snyder,²⁹ R. Sobie,^{176,q} A. Soffer,¹⁶¹ A. Sogaard,⁵⁰ F. Sohns,⁵³ C. A. Solans Sanchez,³⁶ E. Yu. Soldatov,¹¹¹ U. Soldevila,¹⁷⁴ A. A. Solodkov,¹²² A. Soloshenko,⁷⁹ O. V. Solovyanov,¹²² V. Solovyev,¹³⁸ P. Sommer,¹⁴⁹ H. Son,¹⁷⁰ W. Song,¹⁴⁴ W. Y. Song,^{168b} A. Sopczak,¹⁴² F. Sopkova,^{28b} C. L. Sotiropoulou,^{71a,71b} S. Sottocornola,^{70a,70b} R. Soualah,^{66a,66c,ss} A. M. Soukharev,^{121b,121a} D. South,⁴⁶ S. Spagnolo,^{67a,67b} M. Spalla,¹¹⁴ M. Spangenberg,¹⁷⁸ F. Spanò,⁹³ D. Sperlich,⁵² T. M. Spieker,^{61a} R. Spighi,^{23b} G. Spigo,³⁶ M. Spina,¹⁵⁶ D. P. Spiteri,⁵⁷ M. Spusta,¹⁴³ A. Stabile,^{68a,68b} B. L. Stamas,¹²⁰ R. Stamen,^{61a} M. Stamenkovic,¹¹⁹ E. Stanecka,⁸⁴ B. Stanislaus,¹³⁵ M. M. Stanitzki,⁴⁶ M. Stankaityte,¹³⁵ B. Stapf,¹¹⁹ E. A. Starchenko,¹²² G. H. Stark,¹⁴⁶ J. Stark,⁵⁸ S. H. Stark,⁴⁰ P. Staroba,¹⁴¹ P. Starovoitov,^{61a} S. Stärz,¹⁰³ R. Staszewski,⁸⁴ G. Stavropoulos,⁴⁴ M. Stegler,⁴⁶ P. Steinberg,²⁹ A. L. Steinhebel,¹³¹ B. Stelzer,¹⁵² H. J. Stelzer,¹³⁹ O. Stelzer-Chilton,^{168a} H. Stenzel,⁵⁶ T. J. Stevenson,¹⁵⁶ G. A. Stewart,³⁶ M. C. Stockton,³⁶ G. Stoicea,^{27b} M. Stolarski,^{140a} S. Stonjek,¹¹⁴ A. Straessner,⁴⁸ J. Strandberg,¹⁵⁴ S. Strandberg,^{45a,45b} M. Strauss,¹²⁸ P. Strizenec,^{28b} R. Ströhmer,¹⁷⁷ D. M. Strom,¹³¹ R. Stroynowski,⁴² A. Strubig,⁵⁰ S. A. Stucci,²⁹ B. Stugu,¹⁷ J. Stupak,¹²⁸ N. A. Styles,⁴⁶ D. Su,¹⁵³ S. Suchek,^{61a} V. V. Sulin,¹¹⁰ M. J. Sullivan,⁹⁰ D. M. S. Sultan,⁵⁴ S. Sultansoy,^{4c} T. Sumida,⁸⁵ S. Sun,¹⁰⁵ X. Sun,³ K. Suruliz,¹⁵⁶ C. J. E. Suster,¹⁵⁷ M. R. Sutton,¹⁵⁶ S. Suzuki,⁸¹ M. Svatos,¹⁴¹ M. Swiatlowski,³⁷ S. P. Swift,² T. Swirski,¹⁷⁷ A. Sydorenko,⁹⁹ I. Sykora,^{28a} M. Sykora,¹⁴³ T. Sykora,¹⁴³ D. Ta,⁹⁹ K. Tackmann,^{46,tt} J. Taenzer,¹⁶¹ A. Taffard,¹⁷¹ R. Tahirout,^{168a} H. Takai,²⁹ R. Takashima,⁸⁶ K. Takeda,⁸² T. Takeshita,¹⁵⁰ E. P. Takeva,⁵⁰ Y. Takubo,⁸¹ M. Talby,¹⁰¹ A. A. Talyshev,^{121b,121a} N. M. Tamir,¹⁶¹ J. Tanaka,¹⁶³ M. Tanaka,¹⁶⁵ R. Tanaka,¹³² S. Tapia Araya,¹⁷³ S. Tapprogge,⁹⁹ A. Tarek Abouelfadl Mohamed,¹³⁶ S. Tarem,¹⁶⁰ K. Tariq,^{60b} G. Tarna,^{27b,uu} G. F. Tartarelli,^{68a} P. Tas,¹⁴³ M. Tasevsky,¹⁴¹ T. Tashiro,⁸⁵ E. Tassi,^{41b,41a} A. Tavares Delgado,^{140a,140b} Y. Tayalati,^{35e} A. J. Taylor,⁵⁰ G. N. Taylor,¹⁰⁴ W. Taylor,^{168b} A. S. Tee,⁸⁹ R. Teixeira De Lima,¹⁵³ P. Teixeira-Dias,⁹³ H. Ten Kate,³⁶ J. J. Teoh,¹¹⁹ S. Terada,⁸¹ K. Terashi,¹⁶³ J. Terron,⁹⁸ S. Terzo,¹⁴ M. Testa,⁵¹ R. J. Teuscher,^{167,q} S. J. Thais,¹⁸³ T. Theveneaux-Pelzer,⁴⁶ F. Thiele,⁴⁰ D. W. Thomas,⁹³ J. O. Thomas,⁴² J. P. Thomas,²¹ A. S. Thompson,⁵⁷ P. D. Thompson,²¹ L. A. Thomsen,¹⁸³ E. Thomson,¹³⁷ E. J. Thorpe,⁹² Y. Tian,³⁹ R. E. Ticse Torres,⁵³ V. O. Tikhomirov,^{110,vv} Yu. A. Tikhonov,^{121b,121a} S. Timoshenko,¹¹¹ P. Tipton,¹⁸³ S. Tisserant,¹⁰¹ K. Todome,^{23b,23a} S. Todorova-Nova,⁵ S. Todt,⁴⁸ J. Tojo,⁸⁷ S. Tokár,^{28a} K. Tokushuku,⁸¹ E. Tolley,¹²⁶ K. G. Tomiwa,^{33d} M. Tomoto,¹¹⁶ L. Tompkins,^{153,gg} B. Tong,⁵⁹ P. Tornambe,¹⁰² E. Torrence,¹³¹ H. Torres,⁴⁸ E. Torró Pastor,¹⁴⁸ C. Tosceri,¹³⁵ J. Toth,^{101,ww} D. R. Tovey,¹⁴⁹ A. Traet,¹⁷ C. J. Treado,¹²⁴ T. Trefzger,¹⁷⁷ F. Tresoldi,¹⁵⁶ A. Tricoli,²⁹ I. M. Trigger,^{168a} S. Trincas-Duvold,¹³⁶ W. Trischuk,¹⁶⁷ B. Trocmé,⁵⁸ A. Trofymov,¹⁴⁵ C. Troncon,^{68a} M. Trovatelli,¹⁷⁶ F. Trovato,¹⁵⁶ L. Truong,^{33b} M. Trzebinski,⁸⁴ A. Trzupek,⁸⁴ F. Tsai,⁴⁶ J. C.-L. Tseng,¹³⁵ P. V. Tsiareshka,^{107,ii} A. Tsirigotis,¹⁶² N. Tsirintanis,⁹ V. Tsiskaridze,¹⁵⁵ E. G. Tskhadadze,^{159a} M. Tsopoulou,¹⁶² I. I. Tsukerman,¹²³ V. Tsulaia,¹⁸ S. Tsuno,⁸¹ D. Tsybychev,¹⁵⁵ Y. Tu,^{63b} A. Tudorache,^{27b} V. Tudorache,^{27b} T. T. Tulbure,^{27a} A. N. Tuna,⁵⁹ S. Turchikhin,⁷⁹

D. Turgeman,¹⁸⁰ I. Turk Cakir,^{4b,xx} R. J. Turner,²¹ R. T. Turra,^{68a} P. M. Tuts,³⁹ S. Tzamarias,¹⁶² E. Tzovara,⁹⁹ G. Ucchielli,⁴⁷ K. Uchida,¹⁶³ I. Ueda,⁸¹ M. Ughetto,^{45a,45b} F. Ukegawa,¹⁶⁹ G. Unal,³⁶ A. Undrus,²⁹ G. Unel,¹⁷¹ F. C. Ungaro,¹⁰⁴ Y. Unno,⁸¹ K. Uno,¹⁶³ J. Urban,^{28b} P. Urquijo,¹⁰⁴ G. Usai,⁸ Z. Uysal,^{12d} L. Vacavant,¹⁰¹ V. Vacek,¹⁴² B. Vachon,¹⁰³ K. O. H. Vadla,¹³⁴ A. Vaidya,⁹⁴ C. Valderanis,¹¹³ E. Valdes Santurio,^{45a,45b} M. Valente,⁵⁴ S. Valentineti,^{23b,23a} A. Valero,¹⁷⁴ L. Valéry,⁴⁶ R. A. Vallance,²¹ A. Vallier,³⁶ J. A. Valls Ferrer,¹⁷⁴ T. R. Van Daalen,¹⁴ P. Van Gemmeren,⁶ I. Van Vulpen,¹¹⁹ M. Vanadia,^{73a,73b} W. Vandelli,³⁶ A. Vaniachine,¹⁶⁶ D. Vannicola,^{72a,72b} R. Vari,^{72a} E. W. Varnes,⁷ C. Varni,^{55b,55a} T. Varol,¹⁵⁸ D. Varouchas,¹³² K. E. Varvell,¹⁵⁷ M. E. Vasile,^{27b} G. A. Vasquez,¹⁷⁶ J. G. Vasquez,¹⁸³ F. Vazeille,³⁸ D. Vazquez Furelos,¹⁴ T. Vazquez Schroeder,³⁶ J. Veatch,⁵³ V. Vecchio,^{74a,74b} M. J. Veen,¹¹⁹ L. M. Veloce,¹⁶⁷ F. Veloso,^{140a,140c} S. Veneziano,^{72a} A. Ventura,^{67a,67b} N. Venturi,³⁶ A. Verbytskyi,¹¹⁴ V. Vercesi,^{70a} M. Verducci,^{71a,71b} C. M. Vergel Infante,⁷⁸ C. Vergis,²⁴ W. Verkerke,¹¹⁹ A. T. Vermeulen,¹¹⁹ J. C. Vermeulen,¹¹⁹ M. C. Vetterli,^{152,e} N. Viaux Maira,^{147c} M. Vicente Barreto Pinto,⁵⁴ T. Vickey,¹⁴⁹ O. E. Vickey Boeriu,¹⁴⁹ G. H. A. Viehhauser,¹³⁵ L. Vigani,^{61b} M. Villa,^{23b,23a} M. Villaplana Perez,^{68a,68b} E. Vilucchi,⁵¹ M. G. Vincter,³⁴ G. S. Virdee,²¹ A. Vishwakarma,⁴⁶ C. Vittori,^{23b,23a} I. Vivarelli,¹⁵⁶ M. Vogel,¹⁸² P. Vokac,¹⁴² S. E. von Buddenbrock,^{33d} E. Von Toerne,²⁴ V. Vorobel,¹⁴³ K. Vorobev,¹¹¹ M. Vos,¹⁷⁴ J. H. Vosseveld,⁹⁰ M. Vozak,¹⁰⁰ N. Vranjes,¹⁶ M. Vranjes Milosavljevic,¹⁶ V. Vrba,¹⁴² M. Vreeswijk,¹¹⁹ R. Vuillermet,³⁶ I. Vukotic,³⁷ P. Wagner,²⁴ W. Wagner,¹⁸² J. Wagner-Kuhr,¹¹³ S. Wahdan,¹⁸² H. Wahlberg,⁸⁸ V. M. Walbrecht,¹¹⁴ J. Walder,⁸⁹ R. Walker,¹¹³ S. D. Walker,⁹³ W. Walkowiak,¹⁵¹ V. Wallangen,^{45a,45b} A. M. Wang,⁵⁹ C. Wang,^{60c} C. Wang,^{60b} F. Wang,¹⁸¹ H. Wang,¹⁸ H. Wang,³ J. Wang,¹⁵⁷ J. Wang,^{61b} P. Wang,⁴² Q. Wang,¹²⁸ R.-J. Wang,⁹⁹ R. Wang,^{60a} R. Wang,⁶ S. M. Wang,¹⁵⁸ W. T. Wang,^{60a} W. Wang,^{15c,yy} W. X. Wang,^{60a,yy} Y. Wang,^{60a,zz} Z. Wang,^{60c} C. Wanotayaroj,⁴⁶ A. Warburton,¹⁰³ C. P. Ward,³² D. R. Wardrope,⁹⁴ N. Warrack,⁵⁷ A. Washbrook,⁵⁰ A. T. Watson,²¹ M. F. Watson,²¹ G. Watts,¹⁴⁸ B. M. Waugh,⁹⁴ A. F. Webb,¹¹ S. Webb,⁹⁹ C. Weber,¹⁸³ M. S. Weber,²⁰ S. A. Weber,³⁴ S. M. Weber,^{61a} A. R. Weidberg,¹³⁵ J. Weingarten,⁴⁷ M. Weirich,⁹⁹ C. Weiser,⁵² P. S. Wells,³⁶ T. Wenaus,²⁹ T. Wengler,³⁶ S. Wenig,³⁶ N. Wermes,²⁴ M. D. Werner,⁷⁸ M. Wessels,^{61a} T. D. Weston,²⁰ K. Whalen,¹³¹ N. L. Whallon,¹⁴⁸ A. M. Wharton,⁸⁹ A. S. White,¹⁰⁵ A. White,⁸ M. J. White,¹ D. Whiteson,¹⁷¹ B. W. Whitmore,⁸⁹ W. Wiedenmann,¹⁸¹ M. WIELERS,¹⁴⁴ N. Wieseotte,⁹⁹ C. Wiglesworth,⁴⁰ L. A. M. Wiik-Fuchs,⁵² F. Wilk,¹⁰⁰ H. G. Wilkens,³⁶ L. J. Wilkins,⁹³ H. H. Williams,¹³⁷ S. Williams,³² C. Willis,¹⁰⁶ S. Willocq,¹⁰² J. A. Wilson,²¹ I. Wingerter-Seez,⁵ E. Winkels,¹⁵⁶ F. Winklmeier,¹³¹ O. J. Winston,¹⁵⁶ B. T. Winter,⁵² M. Wittgen,¹⁵³ M. Wobisch,⁹⁵ A. Wolf,⁹⁹ T. M. H. Wolf,¹¹⁹ R. Wolff,¹⁰¹ R. W. Wölker,¹³⁵ J. Wollrath,⁵² M. W. Wolter,⁸⁴ H. Wolters,^{140a,140c} V. W. S. Wong,¹⁷⁵ N. L. Woods,¹⁴⁶ S. D. Worm,²¹ B. K. Wosiek,⁸⁴ K. W. Woźniak,⁸⁴ K. Wraight,⁵⁷ S. L. Wu,¹⁸¹ X. Wu,⁵⁴ Y. Wu,^{60a} T. R. Wyatt,¹⁰⁰ B. M. Wynne,⁵⁰ S. Xella,⁴⁰ Z. Xi,¹⁰⁵ L. Xia,¹⁷⁸ X. Xiao,¹⁰⁵ I. Xiotidis,¹⁵⁶ D. Xu,^{15a} H. Xu,^{60a,uu} L. Xu,²⁹ T. Xu,¹⁴⁵ W. Xu,¹⁰⁵ Z. Xu,^{60b} Z. Xu,¹⁵³ B. Yabsley,¹⁵⁷ S. Yacoob,^{33a} K. Yajima,¹³³ D. P. Yallup,⁹⁴ D. Yamaguchi,¹⁶⁵ Y. Yamaguchi,¹⁶⁵ A. Yamamoto,⁸¹ M. Yamatani,¹⁶³ T. Yamazaki,¹⁶³ Y. Yamazaki,⁸² Z. Yan,²⁵ H. J. Yang,^{60c,60d} H. T. Yang,¹⁸ S. Yang,⁷⁷ X. Yang,^{60b,58} Y. Yang,¹⁶³ W.-M. Yao,¹⁸ Y. C. Yap,⁴⁶ Y. Yasu,⁸¹ E. Yatsenko,^{60c,60d} J. Ye,⁴² S. Ye,²⁹ I. Yeletsikh,⁷⁹ M. R. Yexley,⁸⁹ E. Yigitbasi,²⁵ K. Yorita,¹⁷⁹ K. Yoshihara,¹³⁷ C. J. S. Young,³⁶ C. Young,¹⁵³ J. Yu,⁷⁸ R. Yuan,^{60b,aaa} X. Yue,^{61a} S. P. Y. Yuen,²⁴ M. Zaazoua,^{35e} B. Zabinski,⁸⁴ G. Zacharis,¹⁰ E. Zaffaroni,⁵⁴ J. Zahreddine,¹³⁶ A. M. Zaitsev,^{122,mmm} T. Zakareishvili,^{159b} N. Zakharchuk,³⁴ S. Zambito,⁵⁹ D. Zanzi,³⁶ D. R. Zaripovas,⁵⁷ S. V. Zeißner,⁴⁷ C. Zeitnitz,¹⁸² G. Zemaityte,¹³⁵ J. C. Zeng,¹⁷³ O. Zenin,¹²² T. Ženiš,^{28a} D. Zerwas,¹³² M. Zgubič,¹³⁵ D. F. Zhang,^{15b} G. Zhang,^{15b} H. Zhang,^{15c} J. Zhang,⁶ L. Zhang,^{15c} L. Zhang,^{60a} M. Zhang,¹⁷³ R. Zhang,²⁴ X. Zhang,^{60b} Y. Zhang,^{15a,15d} Z. Zhang,^{63a} Z. Zhang,¹³² P. Zhao,⁴⁹ Y. Zhao,^{60b} Z. Zhao,^{60a} A. Zhemchugov,⁷⁹ Z. Zheng,¹⁰⁵ D. Zhong,¹⁷³ B. Zhou,¹⁰⁵ C. Zhou,¹⁸¹ M. S. Zhou,^{15a,15d} M. Zhou,¹⁵⁵ N. Zhou,^{60c} Y. Zhou,⁷ C. G. Zhu,^{60b} C. Zhu,^{15a,15d} H. L. Zhu,^{60a} H. Zhu,^{15a} J. Zhu,¹⁰⁵ Y. Zhu,^{60a} X. Zhuang,^{15a} K. Zhukov,¹¹⁰ V. Zhulanov,^{121b,121a} D. Ziemska,⁶⁵ N. I. Zimine,⁷⁹ S. Zimmermann,⁵² Z. Zinonos,¹¹⁴ M. Ziolkowski,¹⁵¹ L. Živković,¹⁶ G. Zobernig,¹⁸¹ A. Zoccoli,^{23b,23a} K. Zoch,⁵³ T. G. Zorbas,¹⁴⁹ R. Zou,³⁷ and L. Zwalinski³⁶

(ATLAS Collaboration)

¹*Department of Physics, University of Adelaide, Adelaide, Australia*²*Physics Department, SUNY Albany, Albany, New York, USA*³*Department of Physics, University of Alberta, Edmonton AB, Canada*^{4a}*Department of Physics, Ankara University, Ankara, Turkey*^{4b}*Istanbul Aydin University, Istanbul, Turkey*^{4c}*Division of Physics, TOBB University of Economics and Technology, Ankara, Turkey*

- ⁵LAPP, Université Grenoble Alpes, Université Savoie Mont Blanc, CNRS/IN2P3, Annecy, France
- ⁶High Energy Physics Division, Argonne National Laboratory, Argonne, Illinois, USA
- ⁷Department of Physics, University of Arizona, Tucson, Arizona, USA
- ⁸Department of Physics, University of Texas at Arlington, Arlington, Texas, USA
- ⁹Physics Department, National and Kapodistrian University of Athens, Athens, Greece
- ¹⁰Physics Department, National Technical University of Athens, Zografou, Greece
- ¹¹Department of Physics, University of Texas at Austin, Austin, Texas, USA
- ^{12a}Bahcesehir University, Faculty of Engineering and Natural Sciences, Istanbul, Turkey
- ^{12b}Istanbul Bilgi University, Faculty of Engineering and Natural Sciences, Istanbul, Turkey
- ^{12c}Department of Physics, Bogazici University, Istanbul, Turkey
- ^{12d}Department of Physics Engineering, Gaziantep University, Gaziantep, Turkey
- ¹³Institute of Physics, Azerbaijan Academy of Sciences, Baku, Azerbaijan
- ¹⁴Institut de Física d'Altes Energies (IFAE), Barcelona Institute of Science and Technology, Barcelona, Spain
- ^{15a}Institute of High Energy Physics, Chinese Academy of Sciences, Beijing, China
- ^{15b}Physics Department, Tsinghua University, Beijing, China
- ^{15c}Department of Physics, Nanjing University, Nanjing, China
- ^{15d}University of Chinese Academy of Science (UCAS), Beijing, China
- ¹⁶Institute of Physics, University of Belgrade, Belgrade, Serbia
- ¹⁷Department for Physics and Technology, University of Bergen, Bergen, Norway
- ¹⁸Physics Division, Lawrence Berkeley National Laboratory and University of California, Berkeley, California, USA
- ¹⁹Institut für Physik, Humboldt Universität zu Berlin, Berlin, Germany
- ²⁰Albert Einstein Center for Fundamental Physics and Laboratory for High Energy Physics, University of Bern, Bern, Switzerland
- ²¹School of Physics and Astronomy, University of Birmingham, Birmingham, United Kingdom
- ²²Facultad de Ciencias y Centro de Investigaciones, Universidad Antonio Nariño, Bogota, Colombia
- ^{23a}INFN Bologna and Università di Bologna, Dipartimento di Fisica, Bologna, Italy
- ^{23b}INFN Sezione di Bologna, Bologna, Italy
- ²⁴Physikalisches Institut, Universität Bonn, Bonn, Germany
- ²⁵Department of Physics, Boston University, Boston, Massachusetts, USA
- ²⁶Department of Physics, Brandeis University, Waltham, Massachusetts, USA
- ^{27a}Transilvania University of Brasov, Brasov, Romania
- ^{27b}Horia Hulubei National Institute of Physics and Nuclear Engineering, Bucharest, Romania
- ^{27c}Department of Physics, Alexandru Ioan Cuza University of Iasi, Iasi, Romania
- ^{27d}National Institute for Research and Development of Isotopic and Molecular Technologies, Physics Department, Cluj-Napoca, Romania
- ^{27e}University Politehnica Bucharest, Bucharest, Romania
- ^{27f}West University in Timisoara, Timisoara, Romania
- ^{28a}Faculty of Mathematics, Physics and Informatics, Comenius University, Bratislava, Slovak Republic
- ^{28b}Department of Subnuclear Physics, Institute of Experimental Physics of the Slovak Academy of Sciences, Kosice, Slovak Republic
- ²⁹Physics Department, Brookhaven National Laboratory, Upton, New York, USA
- ³⁰Departamento de Física, Universidad de Buenos Aires, Buenos Aires, Argentina
- ³¹California State University, California, USA
- ³²Cavendish Laboratory, University of Cambridge, Cambridge, United Kingdom
- ^{33a}Department of Physics, University of Cape Town, Cape Town, South Africa
- ^{33b}Department of Mechanical Engineering Science, University of Johannesburg, Johannesburg, South Africa
- ^{33c}University of South Africa, Department of Physics, Pretoria, South Africa
- ^{33d}School of Physics, University of the Witwatersrand, Johannesburg, South Africa
- ³⁴Department of Physics, Carleton University, Ottawa, Ontario, Canada
- ^{35a}Faculté des Sciences Ain Chock, Réseau Universitaire de Physique des Hautes Energies—Université Hassan II, Casablanca, Morocco
- ^{35b}Faculté des Sciences, Université Ibn-Tofail, Kénitra, Morocco
- ^{35c}Faculté des Sciences Semlalia, Université Cadi Ayyad, LPHEA-Marrakech, Morocco
- ^{35d}Faculté des Sciences, Université Mohamed Premier and LTPM, Oujda, Morocco
- ^{35e}Faculté des sciences, Université Mohammed V, Rabat, Morocco
- ³⁶CERN, Geneva, Switzerland
- ³⁷Enrico Fermi Institute, University of Chicago, Chicago, Illinois, USA

- ³⁸LPC, Université Clermont Auvergne, CNRS/IN2P3, Clermont-Ferrand, France
³⁹Nevis Laboratory, Columbia University, Irvington, New York, USA
⁴⁰Niels Bohr Institute, University of Copenhagen, Copenhagen, Denmark
^{41a}Dipartimento di Fisica, Università della Calabria, Rende, Italy
^{41b}INFN Gruppo Collegato di Cosenza, Laboratori Nazionali di Frascati, Italy
⁴²Physics Department, Southern Methodist University, Dallas, Texas, USA
⁴³Physics Department, University of Texas at Dallas, Richardson, Texas, USA
⁴⁴National Centre for Scientific Research “Demokritos”, Agia Paraskevi, Greece
^{45a}Department of Physics, Stockholm University, Stockholm, Sweden
^{45b}Oskar Klein Centre, Stockholm, Sweden
⁴⁶Deutsches Elektronen-Synchrotron DESY, Hamburg and Zeuthen, Germany
⁴⁷Lehrstuhl für Experimentelle Physik IV, Technische Universität Dortmund, Dortmund, Germany
⁴⁸Institut für Kern- und Teilchenphysik, Technische Universität Dresden, Dresden, Germany
⁴⁹Department of Physics, Duke University, Durham, North Carolina, USA
⁵⁰SUPA—School of Physics and Astronomy, University of Edinburgh, Edinburgh, United Kingdom
⁵¹INFN e Laboratori Nazionali di Frascati, Frascati, Italy
⁵²Physikalisches Institut, Albert-Ludwigs-Universität Freiburg, Freiburg, Germany
⁵³II. Physikalisches Institut, Georg-August-Universität Göttingen, Göttingen, Germany
⁵⁴Département de Physique Nucléaire et Corpusculaire, Université de Genève, Genève, Switzerland
^{55a}Dipartimento di Fisica, Università di Genova, Genova, Italy
^{55b}INFN Sezione di Genova, Genova, Italy
⁵⁶II. Physikalisches Institut, Justus-Liebig-Universität Giessen, Giessen, Germany
⁵⁷SUPA—School of Physics and Astronomy, University of Glasgow, Glasgow, United Kingdom
⁵⁸LPSC, Université Grenoble Alpes, CNRS/IN2P3, Grenoble INP, Grenoble, France
⁵⁹Laboratory for Particle Physics and Cosmology, Harvard University, Cambridge, Massachusetts, USA
^{60a}Department of Modern Physics and State Key Laboratory of Particle Detection and Electronics, University of Science and Technology of China, Hefei, China
^{60b}Institute of Frontier and Interdisciplinary Science and Key Laboratory of Particle Physics and Particle Irradiation (MOE), Shandong University, Qingdao, China
^{60c}School of Physics and Astronomy, Shanghai Jiao Tong University, KLPPAC-MoE, SKLPPC, Shanghai, China
^{60d}Tsung-Dao Lee Institute, Shanghai, China
^{61a}Kirchhoff-Institut für Physik, Ruprecht-Karls-Universität Heidelberg, Heidelberg, Germany
^{61b}Physikalisches Institut, Ruprecht-Karls-Universität Heidelberg, Heidelberg, Germany
⁶²Faculty of Applied Information Science, Hiroshima Institute of Technology, Hiroshima, Japan
^{63a}Department of Physics, Chinese University of Hong Kong, Shatin, N.T., Hong Kong, China
^{63b}Department of Physics, University of Hong Kong, Hong Kong, China
^{63c}Department of Physics and Institute for Advanced Study, Hong Kong University of Science and Technology, Clear Water Bay, Kowloon, Hong Kong, China
⁶⁴Department of Physics, National Tsing Hua University, Hsinchu, Taiwan
⁶⁵Department of Physics, Indiana University, Bloomington, Indiana, USA
^{66a}INFN Gruppo Collegato di Udine, Sezione di Trieste, Udine, Italy
^{66b}ICTP, Trieste, Italy
^{66c}Dipartimento Politecnico di Ingegneria e Architettura, Università di Udine, Udine, Italy
^{67a}INFN Sezione di Lecce, Italy
^{67b}Dipartimento di Matematica e Fisica, Università del Salento, Lecce, Italy
^{68a}INFN Sezione di Milano, Milano, Italy
^{68b}Dipartimento di Fisica, Università di Milano, Milano, Italy
^{69a}INFN Sezione di Napoli, Napoli, Italy
^{69b}Dipartimento di Fisica, Università di Napoli, Napoli, Italy
^{70a}INFN Sezione di Pavia, Pavia, Italy
^{70b}Dipartimento di Fisica, Università di Pavia, Pavia, Italy
^{71a}INFN Sezione di Pisa, Pisa, Italy
^{71b}Dipartimento di Fisica E. Fermi, Università di Pisa, Pisa, Italy
^{72a}INFN Sezione di Roma, Roma, Italy
^{72b}Dipartimento di Fisica, Sapienza Università di Roma, Roma, Italy
^{73a}INFN Sezione di Roma Tor Vergata, Roma, Italy
^{73b}Dipartimento di Fisica, Università di Roma Tor Vergata, Roma, Italy
^{74a}INFN Sezione di Roma Tre, Roma, Italy
^{74b}Dipartimento di Matematica e Fisica, Università Roma Tre, Roma, Italy

- ^{75a}INFN-TIFPA, Trento, Italy
- ^{75b}Università degli Studi di Trento, Trento, Italy
- ⁷⁶Institut für Astro- und Teilchenphysik, Leopold-Franzens-Universität, Innsbruck, Austria
- ⁷⁷University of Iowa, Iowa City, Iowa, USA
- ⁷⁸Department of Physics and Astronomy, Iowa State University, Ames, Iowa, USA
- ⁷⁹Joint Institute for Nuclear Research, Dubna, Russia
- ^{80a}Departamento de Engenharia Elétrica, Universidade Federal de Juiz de Fora (UFJF), Juiz de Fora, Brazil
- ^{80b}Universidade Federal do Rio De Janeiro COPPE/EE/IF, Rio de Janeiro, Brazil
- ^{80c}Universidade Federal de São João del Rei (UFSJ), São João del Rei, Brazil
- ^{80d}Instituto de Física, Universidade de São Paulo, São Paulo, Brazil
- ⁸¹KEK, High Energy Accelerator Research Organization, Tsukuba, Japan
- ⁸²Graduate School of Science, Kobe University, Kobe, Japan
- ^{83a}AGH University of Science and Technology, Faculty of Physics and Applied Computer Science, Krakow, Poland
- ^{83b}Marian Smoluchowski Institute of Physics, Jagiellonian University, Krakow, Poland
- ⁸⁴Institute of Nuclear Physics Polish Academy of Sciences, Krakow, Poland
- ⁸⁵Faculty of Science, Kyoto University, Kyoto, Japan
- ⁸⁶Kyoto University of Education, Kyoto, Japan
- ⁸⁷Research Center for Advanced Particle Physics and Department of Physics, Kyushu University, Fukuoka, Japan
- ⁸⁸Instituto de Física La Plata, Universidad Nacional de La Plata and CONICET, La Plata, Argentina
- ⁸⁹Physics Department, Lancaster University, Lancaster, United Kingdom
- ⁹⁰Oliver Lodge Laboratory, University of Liverpool, Liverpool, United Kingdom
- ⁹¹Department of Experimental Particle Physics, Jožef Stefan Institute and Department of Physics, University of Ljubljana, Ljubljana, Slovenia
- ⁹²School of Physics and Astronomy, Queen Mary University of London, London, United Kingdom
- ⁹³Department of Physics, Royal Holloway University of London, Egham, United Kingdom
- ⁹⁴Department of Physics and Astronomy, University College London, London, United Kingdom
- ⁹⁵Louisiana Tech University, Ruston, Louisiana, USA
- ⁹⁶Fysiska institutionen, Lunds universitet, Lund, Sweden
- ⁹⁷Centre de Calcul de l'Institut National de Physique Nucléaire et de Physique des Particules (IN2P3), Villeurbanne, France
- ⁹⁸Departamento de Física Teórica C-15 and CIAFF, Universidad Autónoma de Madrid, Madrid, Spain
- ⁹⁹Institut für Physik, Universität Mainz, Mainz, Germany
- ¹⁰⁰School of Physics and Astronomy, University of Manchester, Manchester, United Kingdom
- ¹⁰¹CPPM, Aix-Marseille Université, CNRS/IN2P3, Marseille, France
- ¹⁰²Department of Physics, University of Massachusetts, Amherst, Massachusetts, USA
- ¹⁰³Department of Physics, McGill University, Montreal, Quebec, Canada
- ¹⁰⁴School of Physics, University of Melbourne, Victoria, Australia
- ¹⁰⁵Department of Physics, University of Michigan, Ann Arbor, Michigan, USA
- ¹⁰⁶Department of Physics and Astronomy, Michigan State University, East Lansing, Michigan, USA
- ¹⁰⁷B.I. Stepanov Institute of Physics, National Academy of Sciences of Belarus, Minsk, Belarus
- ¹⁰⁸Research Institute for Nuclear Problems of Byelorussian State University, Minsk, Belarus
- ¹⁰⁹Group of Particle Physics, University of Montreal, Montreal, Quebec, Canada
- ¹¹⁰P.N. Lebedev Physical Institute of the Russian Academy of Sciences, Moscow, Russia
- ¹¹¹National Research Nuclear University MEPhI, Moscow, Russia
- ¹¹²D.V. Skobel'syn Institute of Nuclear Physics, M.V. Lomonosov Moscow State University, Moscow, Russia
- ¹¹³Fakultät für Physik, Ludwig-Maximilians-Universität München, München, Germany
- ¹¹⁴Max-Planck-Institut für Physik (Werner-Heisenberg-Institut), München, Germany
- ¹¹⁵Nagasaki Institute of Applied Science, Nagasaki, Japan
- ¹¹⁶Graduate School of Science and Kobayashi-Maskawa Institute, Nagoya University, Nagoya, Japan
- ¹¹⁷Department of Physics and Astronomy, University of New Mexico, Albuquerque, New Mexico, USA
- ¹¹⁸Institute for Mathematics, Astrophysics and Particle Physics, Radboud University Nijmegen/Nikhef, Nijmegen, Netherlands
- ¹¹⁹Nikhef National Institute for Subatomic Physics and University of Amsterdam, Amsterdam, Netherlands
- ¹²⁰Department of Physics, Northern Illinois University, DeKalb, Illinois, USA
- ^{121a}Budker Institute of Nuclear Physics and NSU, SB RAS, Novosibirsk, Russia
- ^{121b}Novosibirsk State University Novosibirsk, Russia

- ¹²²*Institute for High Energy Physics of the National Research Centre Kurchatov Institute, Protvino, Russia*
- ¹²³*Institute for Theoretical and Experimental Physics named by A.I. Alikhanov of National Research Centre “Kurchatov Institute”, Moscow, Russia*
- ¹²⁴*Department of Physics, New York University, New York, New York, USA*
- ¹²⁵*Ochanomizu University, Otsuka, Bunkyo-ku, Tokyo, Japan*
- ¹²⁶*The Ohio State University, Columbus, Ohio, USA*
- ¹²⁷*Faculty of Science, Okayama University, Okayama, Japan*
- ¹²⁸*Homer L. Dodge Department of Physics and Astronomy, University of Oklahoma, Norman, Oklahoma, USA*
- ¹²⁹*Department of Physics, Oklahoma State University, Stillwater, Oklahoma, USA*
- ¹³⁰*Palacký University, RCPTM, Joint Laboratory of Optics, Olomouc, Czech Republic*
- ¹³¹*Center for High Energy Physics, University of Oregon, Eugene, Oregon, USA*
- ¹³²*LAL, Université Paris-Sud, CNRS/IN2P3, Université Paris-Saclay, Orsay, France*
- ¹³³*Graduate School of Science, Osaka University, Osaka, Japan*
- ¹³⁴*Department of Physics, University of Oslo, Oslo, Norway*
- ¹³⁵*Department of Physics, Oxford University, Oxford, United Kingdom*
- ¹³⁶*LPNHE, Sorbonne Université, Université de Paris, CNRS/IN2P3, Paris, France*
- ¹³⁷*Department of Physics, University of Pennsylvania, Philadelphia, Pennsylvania, USA*
- ¹³⁸*Konstantinov Nuclear Physics Institute of National Research Centre “Kurchatov Institute”, PNPI, St. Petersburg, Russia*
- ¹³⁹*Department of Physics and Astronomy, University of Pittsburgh, Pittsburgh, Pennsylvania, USA*
- ^{140a}*Laboratório de Instrumentação e Física Experimental de Partículas—LIP, Lisboa, Portugal*
- ^{140b}*Departamento de Física, Faculdade de Ciências, Universidade de Lisboa, Lisboa, Portugal*
- ^{140c}*Departamento de Física, Universidade de Coimbra, Coimbra, Portugal*
- ^{140d}*Centro de Física Nuclear da Universidade de Lisboa, Lisboa, Portugal*
- ^{140e}*Departamento de Física, Universidade do Minho, Braga, Portugal*
- ^{140f}*Departamento de Física Teórica y del Cosmos, Universidad de Granada, Granada (Spain), Spain*
- ^{140g}*Dep Física and CEFITEC of Faculdade de Ciências e Tecnologia, Universidade Nova de Lisboa, Caparica, Portugal*
- ^{140h}*Instituto Superior Técnico, Universidade de Lisboa, Lisboa, Portugal*
- ¹⁴¹*Institute of Physics of the Czech Academy of Sciences, Prague, Czech Republic*
- ¹⁴²*Czech Technical University in Prague, Prague, Czech Republic*
- ¹⁴³*Charles University, Faculty of Mathematics and Physics, Prague, Czech Republic*
- ¹⁴⁴*Particle Physics Department, Rutherford Appleton Laboratory, Didcot, United Kingdom*
- ¹⁴⁵*IRFU, CEA, Université Paris-Saclay, Gif-sur-Yvette, France*
- ¹⁴⁶*Santa Cruz Institute for Particle Physics, University of California Santa Cruz, Santa Cruz, California, USA*
- ^{147a}*Departamento de Física, Pontificia Universidad Católica de Chile, Santiago, Chile*
- ^{147b}*Universidad Andres Bello, Department of Physics, Santiago, Chile*
- ^{147c}*Departamento de Física, Universidad Técnica Federico Santa María, Valparaíso, Chile*
- ¹⁴⁸*Department of Physics, University of Washington, Seattle, Washington, USA*
- ¹⁴⁹*Department of Physics and Astronomy, University of Sheffield, Sheffield, United Kingdom*
- ¹⁵⁰*Department of Physics, Shinshu University, Nagano, Japan*
- ¹⁵¹*Department Physik, Universität Siegen, Siegen, Germany*
- ¹⁵²*Department of Physics, Simon Fraser University, Burnaby, British Columbia, Canada*
- ¹⁵³*SLAC National Accelerator Laboratory, Stanford, California, USA*
- ¹⁵⁴*Physics Department, Royal Institute of Technology, Stockholm, Sweden*
- ¹⁵⁵*Departments of Physics and Astronomy, Stony Brook University, Stony Brook, New York, USA*
- ¹⁵⁶*Department of Physics and Astronomy, University of Sussex, Brighton, United Kingdom*
- ¹⁵⁷*School of Physics, University of Sydney, Sydney, Australia*
- ¹⁵⁸*Institute of Physics, Academia Sinica, Taipei, Taiwan*
- ^{159a}*E. Andronikashvili Institute of Physics, Iv. Javakhishvili Tbilisi State University, Tbilisi, Georgia*
- ^{159b}*High Energy Physics Institute, Tbilisi State University, Tbilisi, Georgia*
- ¹⁶⁰*Department of Physics, Technion, Israel Institute of Technology, Haifa, Israel*
- ¹⁶¹*Raymond and Beverly Sackler School of Physics and Astronomy, Tel Aviv University, Tel Aviv, Israel*
- ¹⁶²*Department of Physics, Aristotle University of Thessaloniki, Thessaloniki, Greece*
- ¹⁶³*International Center for Elementary Particle Physics and Department of Physics, University of Tokyo, Tokyo, Japan*
- ¹⁶⁴*Graduate School of Science and Technology, Tokyo Metropolitan University, Tokyo, Japan*
- ¹⁶⁵*Department of Physics, Tokyo Institute of Technology, Tokyo, Japan*

- ¹⁶⁶*Tomsk State University, Tomsk, Russia*
¹⁶⁷*Department of Physics, University of Toronto, Toronto, Ontario, Canada*
^{168a}*TRIUMF, Vancouver, British Columbia, Canada*
^{168b}*Department of Physics and Astronomy, York University, Toronto, Ontario, Canada*
¹⁶⁹*Division of Physics and Tomonaga Center for the History of the Universe,
Faculty of Pure and Applied Sciences, University of Tsukuba, Tsukuba, Japan*
¹⁷⁰*Department of Physics and Astronomy, Tufts University, Medford, Massachusetts, USA*
¹⁷¹*Department of Physics and Astronomy, University of California Irvine, Irvine, California, USA*
¹⁷²*Department of Physics and Astronomy, University of Uppsala, Uppsala, Sweden*
¹⁷³*Department of Physics, University of Illinois, Urbana, Illinois, USA*
¹⁷⁴*Instituto de Física Corpuscular (IFIC), Centro Mixto Universidad de Valencia—CSIC, Valencia, Spain*
¹⁷⁵*Department of Physics, University of British Columbia, Vancouver, British Columbia, Canada*
¹⁷⁶*Department of Physics and Astronomy, University of Victoria, Victoria, British Columbia, Canada*
¹⁷⁷*Fakultät für Physik und Astronomie, Julius-Maximilians-Universität Würzburg, Würzburg, Germany*
¹⁷⁸*Department of Physics, University of Warwick, Coventry, United Kingdom*
¹⁷⁹*Waseda University, Tokyo, Japan*
¹⁸⁰*Department of Particle Physics, Weizmann Institute of Science, Rehovot, Israel*
¹⁸¹*Department of Physics, University of Wisconsin, Madison, Wisconsin, USA*
¹⁸²*Fakultät für Mathematik und Naturwissenschaften, Fachgruppe Physik,
Bergische Universität Wuppertal, Wuppertal, Germany*
¹⁸³*Department of Physics, Yale University, New Haven, Connecticut, USA*
¹⁸⁴*Yerevan Physics Institute, Yerevan, Armenia*

^aDeceased.

^bAlso at Department of Physics, King's College London, London, United Kingdom.

^cAlso at Istanbul University, Dept. of Physics, Istanbul, Turkey.

^dAlso at Instituto de Física Teórica, IFT-UAM/CSIC, Madrid, Spain.

^eAlso at TRIUMF, Vancouver BC, Canada.

^fAlso at Department of Physics and Astronomy, University of Louisville, Louisville, Kentucky, USA.

^gAlso at Physics Department, An-Najah National University, Nablus, Palestine.

^hAlso at Department of Physics, California State University, Fresno, USA.

ⁱAlso at Department of Physics, University of Fribourg, Fribourg, Switzerland.

^jAlso at Physics Dept, University of South Africa, Pretoria, South Africa.

^kAlso at Departament de Física de la Universitat Autònoma de Barcelona, Barcelona, Spain.

^lAlso at Tomsk State University, Tomsk, and Moscow Institute of Physics and Technology State University, Dolgoprudny, Russia.

^mAlso at The Collaborative Innovation Center of Quantum Matter (CICQM), Beijing, China.

ⁿAlso at Department of Physics, Ben Gurion University of the Negev, Beer Sheva, Israel.

^oAlso at Departamento de Física, Instituto Superior Técnico, Universidade de Lisboa, Lisboa, Portugal.

^pAlso at Università di Napoli Parthenope, Napoli, Italy.

^qAlso at Institute of Particle Physics (IPP), Vancouver, Canada.

^rAlso at Department of Physics, University of Adelaide, Adelaide, Australia.

^sAlso at Dipartimento di Matematica, Informatica e Fisica, Università di Udine, Udine, Italy.

^tAlso at Department of Physics, St. Petersburg State Polytechnical University, St. Petersburg, Russia.

^uAlso at Borough of Manhattan Community College, City University of New York, New York, New York, USA.

^vAlso at Department of Financial and Management Engineering, University of the Aegean, Chios, Greece.

^wAlso at Department of Physics, California State University, East Bay, USA.

^xAlso at Institutio Catalana de Recerca i Estudis Avancats, ICREA, Barcelona, Spain.

^yAlso at Department of Physics, University of Michigan, Ann Arbor, Michigan, USA.

^zAlso at LAL, Université Paris-Sud, CNRS/IN2P3, Université Paris-Saclay, Orsay, France.

^{aa}Also at Graduate School of Science, Osaka University, Osaka, Japan.

^{bb}Also at Physikalisches Institut, Albert-Ludwigs-Universität Freiburg, Freiburg, Germany.

^{cc}Also at Institute of Physics, Azerbaijan Academy of Sciences, Baku, Azerbaijan.

^{dd}Also at Institute for Mathematics, Astrophysics and Particle Physics, Radboud University Nijmegen/Nikhef, Nijmegen, Netherlands.

^{ee}Also at Institute of Theoretical Physics, Ilia State University, Tbilisi, Georgia.

^{ff}Also at CERN, Geneva, Switzerland.

^{gg}Also at Department of Physics, Stanford University, Stanford, California, USA.

^{hh}Also at Manhattan College, New York, New York, USA.

ⁱⁱAlso at Joint Institute for Nuclear Research, Dubna, Russia.

^{jj}Also at Hellenic Open University, Patras, Greece.

^{kk}Also at The City College of New York, New York, New York, USA.

^{ll}Also at Department of Physics, California State University, Sacramento, USA.

^{mm}Also at Moscow Institute of Physics and Technology State University, Dolgoprudny, Russia.

ⁿⁿAlso at Département de Physique Nucléaire et Corpusculaire, Université de Genève, Genève, Switzerland.

^{oo}Also at Louisiana Tech University, Ruston, Louisiana, USA.

^{pp}Also at School of Physics, Sun Yat-sen University, Guangzhou, China.

^{qq}Also at Institute for Nuclear Research and Nuclear Energy (INRNE) of the Bulgarian Academy of Sciences, Sofia, Bulgaria.

^{rr}Also at Faculty of Physics, M.V. Lomonosov Moscow State University, Moscow, Russia.

^{ss}Also at Department of Applied Physics and Astronomy, University of Sharjah, Sharjah, United Arab Emirates.

^{tt}Also at Institut für Experimentalphysik, Universität Hamburg, Hamburg, Germany.

^{uu}Also at CPPM, Aix-Marseille Université, CNRS/IN2P3, Marseille, France.

^{vv}Also at National Research Nuclear University MEPhI, Moscow, Russia.

^{ww}Also at Institute for Particle and Nuclear Physics, Wigner Research Centre for Physics, Budapest, Hungary.

^{xx}Also at Giresun University, Faculty of Engineering, Giresun, Turkey.

^{yy}Also at Institute of Physics, Academia Sinica, Taipei, Taiwan.

^{zz}Also at LPNHE, Sorbonne Université, Université de Paris, CNRS/IN2P3, Paris, France.

^{aaa}Also at Department of Physics and Astronomy, Michigan State University, East Lansing, Michigan, USA.